PERFORMANCE AND OPTIMIZATION OF AN UNDERFLOOR AIR DISTRIBUTION SYSTEM IN AN EDUCATIONAL BUILDING IN A HOT AND HUMID CLIMATE

A Thesis

by

VASILIY KHMELENKO

Submitted to the Office of Graduate and Professional Studies of
Texas A&M University
in partial fulfillment of the requirements for the degree of

MASTER OF SCIENCE

Chair of Committee,	David E. Claridge
Committee Members,	Charles Culp
	Juan-Carlos Baltazar
Head of Department,	Andreas Polycarpou

May 2015

Major Subject: Mechanical Engineering

ABSTRACT

Today there is a proliferation of different HVAC system configurations. Design and performance of each HVAC system are dependent on climate and the intended use of the building. Energy recovery ventilation is becoming more common in new buildings and is one of the more popular retrofit options in hot and humid climates. Currently there is a lack of optimization strategies that involve the underfloor air systems combined with Energy Recovery Ventilation (ERV) especially in hot and humid climate.

This thesis examines the performance and optimization of underfloor air distribution systems (UFAD) in hot and humid climates. This thesis also compares the UFAD system performance to a typical overhead air handler unit (AHU) system found in Texas. The performance comparison is done with EnergyPlus modeling software. Separate sets of models are created to examine performance of at different operational parameters. The minimum air flow rates are modeled at 0.1 cfm/ft2, 0.2 cfm/ft2, 0.3 cfm/ft2, 0.4 cfm/ft2 for both UFAD and overhead (OH) systems. The supply air temperatures were modeled at 55 °F, 60°F, and 63 °F. Outside air strategies include simple economizer, energy recovery ventilation (ERV), as well as a combination of both economizer and ERV.

The study found that at low minimum (0.1 cfm/ft2) flow rates an overhead system will slightly outperform a UFAD system (OH 2.6% cheaper to operate than UFAD) while at 0.3 cfm/ft2 a UFAD system is more efficient (UFAD 14.8% cheaper to operate). The outside air strategies have the same energy savings effect on both systems.

The UFAD system has a higher peak cooling load and a lower peak heating load compared to the overhead system.

This thesis also covers the stratification and supply air temperature measurements within two offices inside the Mitchell Physics building, located on the Texas A&M campus. The stratification measurements showed that on average the stratification was lower than expected for such systems with office 411 having average stratification of 1.8 °F and office 423 average stratification of 1.5 °F. Temperature measurements at the diffuser level showed some reheat, especially during unoccupied periods such as early mornings, late evenings and weekends, even when the outside temperature was above the interior thermostat set point. System level total supply air flow rate showed little variation with a minimum of 0.47 cfm/ft2 and a maximum of 0.59 cfm/ft2. The analysis of energy recovery wheel operation concluded that the low exhaust air flow of only 0.2 of the outside air is responsible for the low temperature difference observed in the outside air stream through the ERV.

ACKNOWLEDGEMENTS

I would like to thank my superman supervisor and committee chair, Dr. Claridge for his incredible patience, guidance and support. Also, I would like to thank Dr. Culp for his interest in the work below and for stimulating discussions; and Dr. Baltazar, for always being acutely nice and supportive whenever I have come for advice or help.

My friends and colleagues, the department faculty and staff — thank you so much for making my time at Texas A&M University a great experience.

I also want to extend my gratitude to the Energy Systems Laboratory, which provided the possibility to perform the research. Finally, thanks to my mother and father for their love and support I have always received.

TABLE OF CONTENTS

LIST OF FIGURES

Page

LIST OF TABLES

CHAPTER I

INTRODUCTION AND LITERATURE REVIEW

1.1. Introduction

In 2010 the buildings sector consumed 39 quads of energy. Building energy consumption represents 41% of total energy consumption in the United States. In the United States and around the world building energy consumption is expected to rise due to growth of population and increasing demand for comfortable indoor environments.

Out of all the building energy in United States, 46% of the consumption is from commercial buildings. On average, half of the energy used in the buildings is used for heating, ventilation and air conditioning (HVAC) systems; however this proportion is higher in the hot and humid climates. The Energy Systems Laboratory at Texas A&M University has shown average savings of 20%; during their work with the Texas LoanSTAR program using the Continuous Commissioning® process (Claridge et al. 2000). Another study focusing on 224 new and existing commercial buildings across the country demonstrated savings of 15% of whole building energy use from commissioning by 18 different commissioning providers (Mills et al. 2005).

The new generation of green buildings that are designed with sustainability in mind can have complex systems that are harder to operate than those in traditional buildings. This extra complexity can require significant analysis of the operation of the HVAC system for further optimization.

This thesis will use empirical measurements of HVAC system parameters and energy simulation to develop an energy optimization strategy for the Mitchell Physics

Building located on the Texas A&M University campus in College Station, Texas, which has a hot and humid climate. The Mitchell Physics Building uses various technologies to improve the comfort and energy performance. The system that sets this building apart from the rest is underfloor air distribution, which is currently unusual for this climate; however recently such systems are gaining more traction. Another feature of this building is the sensible and latent energy recovery ventilation system. This building also has an excellent building automation system, which is capable of logging hundreds of HVAC operation points.

1.2. Literature Review

Underfloor air distribution systems (UFADs) became more popular in North America during the 1990's and are continuing to grow in popularity. The UFAD systems use the pressurized under-floor airway to supply conditioned air to the occupied zone through floor diffusers. The potential advantages of UFAD systems have been identified as: (1) improved ventilation effectiveness, (2) improved air quality and thermal comfort in the occupant zone, (3) improved energy efficiency in suitable climates, (4) flexible layouts, and (5) reduced life cycle costs. (Alajmi, et al., 2011, Lee, et al., 2013) However, these potential advantages of UFAD system can only be achieved in practice by: (1) better understanding of system operation and performance, (2) proper installation and use of the system, and (3) proper underlying design. (Montanya, et al., 2009)

The energy usage advantages of UFAD systems come from the air being supplied from the floor. During the cooling mode, natural convection helps to move the air towards the return plenum located at the ceiling as it warms, creating room air stratification. Webster (Webster, 2002) conducted a study to determine effects of airflow, supply air temperature, and blinds on room air stratification. The results showed that lowering flow rate increases stratification, and supply air temperature does not change the stratification profile, however it does translate the profile to higher or lower temperatures. Fisk (Fisk, et al., 2004) conducted a field study in a medium-size office building, measuring air change effectiveness, pollutant removal efficiency, air stratification, and occupant satisfaction. The air stratification was measured to be 2°F-4°F, which potentially reduces cooling energy consumption by approximately 10%. In this study, the pollutant removal efficiency for carbon dioxide was 13% higher than expected in space with well-mixed air. The occupant thermal comfort satisfaction was well above average. Measured air change effectiveness was not significantly different compared to overhead distribution systems. It was found that the stratified air inside the room changes the dynamics of the heat transfer mechanisms both within the room and between the floors. A study was conducted to investigate primary pathways of heat transfer within the UFAD system. Two unique pathways for UFAD systems are (1) heat extraction via return air exiting the room at ceiling level and (2) heat entering the underfloor supply plenum through the slab and raised floor panels. The study concludes that 40% of total cooling load is transferred via heat entering the supply plenum while 60% is via heat extraction through the return. (Bauman, et al., 2006)

The interaction between the heat gains and the concrete slab in a raised floor system changes the thermal behavior of the building. A study of cooling load profile for an office building concluded that the peak cooling load in a system with raised floor is from 7 to 40% larger than in a system without raised floors. The most significant parameters affecting peak load are the zone orientation, i.e. the exposure to direct solar radiation, and the presence of floor carpeting. (Schiavon, et al., 2010) UFAD systems may experience draught during the heating mode. The draught is caused by natural convection along the cold window surface, causing discomfort. One solution to this is to block the draught by a warm jet coming from the terminal close to the window.

The impact of supply air temperature (SAT) on underfloor air distribution is an important parameter for energy efficient operation of the UFAD system. Multiple studies have been conducted to optimize the AHU SAT for different climates. When the AHU is operating in cooling mode, resetting the AHU SAT creates a tradeoff between the fan and cooling energy consumption. The optimal operation temperature varies from climate to climate. One study targeting California concluded that the optimal SAT set point for Sacramento was 15.6 °C (60°F) while, in San Francisco the optimal SAT set point was 17.2 °C (63°F). (Webster, Lee et al. 2012) Another study conducted similar analysis on a prototype building in Incheon, Korea. In this study a prototype building was simulated under three different AHU SAT, which were 13°C (55.4°F), 15°C (59°F), and 17°C (62.6°F). The study concluded that increasing AHU SAT increases both fan energy and heating energy of the building. The increase in heating energy was due to use of a central AHU heating coil.

CHAPTER II ENERGY MODELING

2.1 EnergyPlus Modeling Methodology

Modeling the UFAD system requires special attention to underfloor plenum performance and room air stratification. The DOE 2.1e or DOE 2.2 program variations (such as eQUEST and EnergyPro) calculate the space cooling loads by summing up all heat losses and heat gains within a space, without taking into account how the loads are influenced by airflow patterns and the buoyancy of warm air. This means that most simulation programs assume that the air inside conditioned space has uniform temperature.

In the actual building, the buoyancy force drives the hot air to rise, producing warmer temperatures near the ceiling and cooler temperatures near the floor. In the overhead air distribution system the warmer air at the top is pushed down to promote mixing of conditioned space. The uniform temperature assumption is acceptable for overhead air distribution systems, because overhead diffusers are designed to uniformly mix the air within the room.

In the case of an underfloor air distribution system, the air is supplied from the bottom, preserving the warm air temperature near the ceiling. The advantage of this thermal stratification is that the hot air can be removed directly by the return air duct, instead of cooling it to the room temperature set point. This removal of hot air due to stratification reduces the cooling loads relative to the overhead system.

EnergyPlus has the capability to model different room air model types. The default room air type is well-mixed, which assumes uniform temperature. The available room air models include user defined temperature patterns, multiple displacement ventilation models as well as UFAD interior and UFAD exterior room air model types. The interior and exterior UFAD room air models were used for the respective zones in this simulation.

RoomAirSettings:UnderFloorAirDistributionInterior (DOE 2013) is a room air component model for heat transfer and a vertical temperature profile for interior zones of the UFAD system. The loads of the interior zones are assumed to be from internal sources, with some of them generating thermal plumes. This room air model uses two nodes for first order approximation of non-uniform temperature profile. The two nodes represent two regions, each assumed to have uniform temperature. One node represents the lower occupied zone, while the other represents the upper well mixed zone. The heat transfer from one region to another is facilitated by the hot plumes generated by people, and some equipment. The height of the occupied zone is determined by the flow rate of cold air into the zone, and by the plume heat transfer rate into the upper zone. It is important to note that the height and the temperatures of the nodes will vary throughout the simulation giving a good first order approximation of UFAD stratification energy performance and comfort.

RoomAirSettings:UnderFloorAirDistributionExterior (DOE 2013) is similar to the interior UFAD model in that it models room temperature as two nodes representing the occupied and upper mixed regions. The exterior model also takes the convective heat transfer from the envelope into account thus requiring a different algorithm from the interior model to calculate the height and temperatures of the nodes.

Two sets of EnergyPlus models were created as a part of the thesis. One set of models simulates the overhead system and the other set simulates the UFAD system. Both sets of models are using ANSI/ASHRAE/IES Standard 90.1-2007 Building envelope requirements for climate zone 2 (A,B). The prototype buildings have a square shape with 100’ (30.48m) sides. The building has 3 stories, with 40% window to wall ratio strip windows. Each floor has 5 zones, including a single interior zone and 4 exterior zones. The exterior zones have 12’ (3.66m) depth. The climate data from Easterwood Field, College Station TX was used for the simulation.

The overhead system EnergyPlus model geometry has a 12’ 6” well mixed height and a 1’ 6” return plenum. The UFAD model geometry has a 1’ 6” supply plenum and 11’ total room height and a 1’ 6” return plenum. The reason for this particular geometry is because the Mitchell Physics Building has an 11’ room height as well as two plenums. The room height of the overhead system is unusually large in order to keep the envelope surfaces consistent. **Figure 1** shows the overview of the prototype building with UFAD system. The UFAD system model has 2 plenum spaces for each floor.

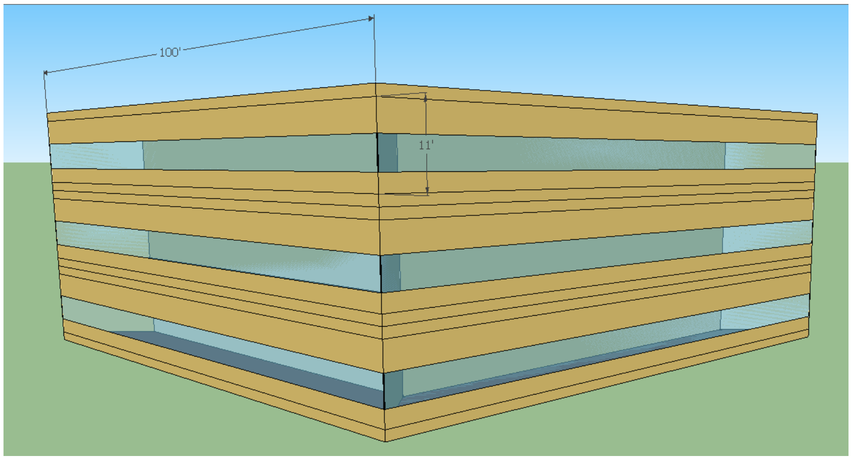

Figure 1. Overview of prototype building with UFAD system.

Figure 2 shows the overview of the prototype OH building. Each floor in the model has a single return plenum, and no supply plenum. The extra height of the plenum is added to the occupied space.

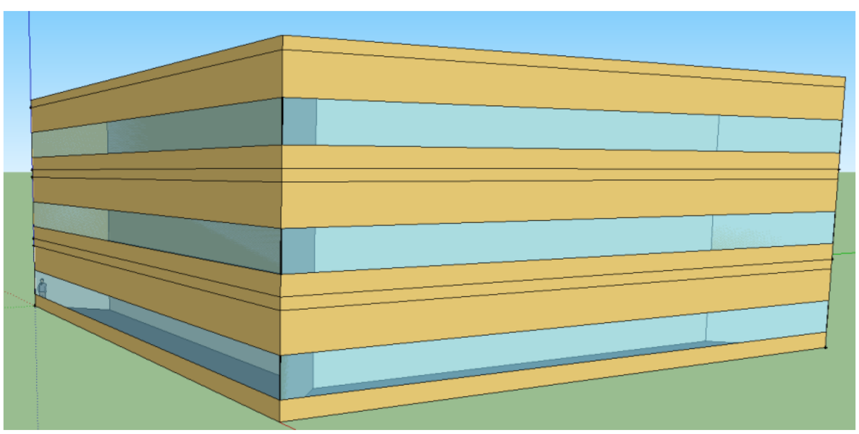

Figure 2. Overview of prototype building with overhead system

Figure 3 shows the floor plan of the model. Both UFAD ond OH models have the same floor plan. Each floor within the building also has an identical floor plan. The perimeter zones are 12 ft. deep.

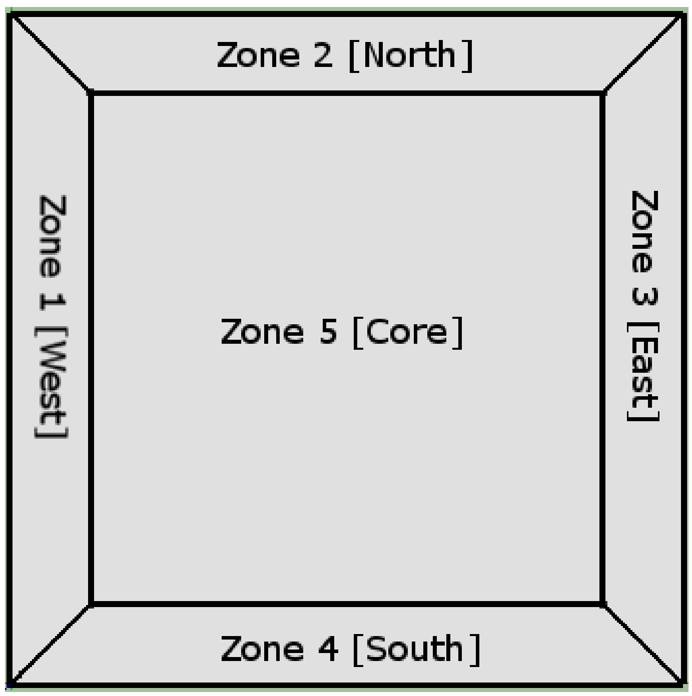

Figure 3. Floor plan of prototype buildings

The wall areas are summarized in the **Table 1** (metric) and **Table 2** (imperial). The wall and window areas are identical between the UFAD and OH models.

Table 1. Wall and window summary for both OH and UFAD models in metric units

Walls	Total	North	East	South	West
Gross Wall Area [m^2]	1561	390	390	390	390
Above Ground Wall Area [m^2]	1561	390	390	390	390
Window Opening Area [m^2]	491	123	123	123	123
Gross Window-Wall Ratio [%]	31	31	31	31	31
Above Ground Window-Wall Ratio [%]	31	31	31	31	31
Roof[m^2]	929				

Table 2. Wall and window summary for both OH and UFAD models in imperial units

Walls	Total	North	East	South	West
Gross Wall Area [ft^2]	16800	4200	4200	4200.0	4200.0
Above Ground Wall Area [ft^2]	16800	4200	4200	4200.0	4200.0
Window Opening Area [ft^2]	5280	1320	1320	1320	1320
Gross Window-Wall Ratio [%]	31	31	31	31	31
Above Ground Window-Wall Ratio [%]	31	31	31	31	31
Roof[ft^2]	10000				

The four exterior zones are summarized in

Table 3 and **Table 4**. The reason there are two tables is because the gross wall area and volume of the zones are larger in the OH model. The lighting, plug, and people loads in the tables are peak loads.

Table 3. Zone summary OH model in metric units

	Area m^2	Volume m^3	Gross Wall Area m^2	Window Area m^2	Lighting W/m^2	People m^2/person	Plug and Process W/m^2
East Thermal Zone	98	374	116	41	10.7	17.7	7.6
North Thermal Zone	98	374	116	41	10.7	17.7	7.6
South Thermal Zone	98	374	116	41	10.7	17.7	7.6
West Thermal Zone	98	374	116	41	10.7	17.7	7.6
Interior Thermal Zone	537	2044	0	0	10.7	17.7	7.6

The occupancy, equipment, and lighting profiles were downloaded from the OpenStudio building component library. The schedule set is the 189.1 -2009 large office schedule set for climate zones 1-3. The actual profiles originated from the ANSI/ASHRAE/IES Standard 90.1 prototype building models that can be found on the DOE website http://www.energycodes.gov/commercial-prototype-building-models.

The occupancy profile is graphed in **Figure 4**, equipment profile in **Figure 5**, and lighting profiles in **Figure 6**.

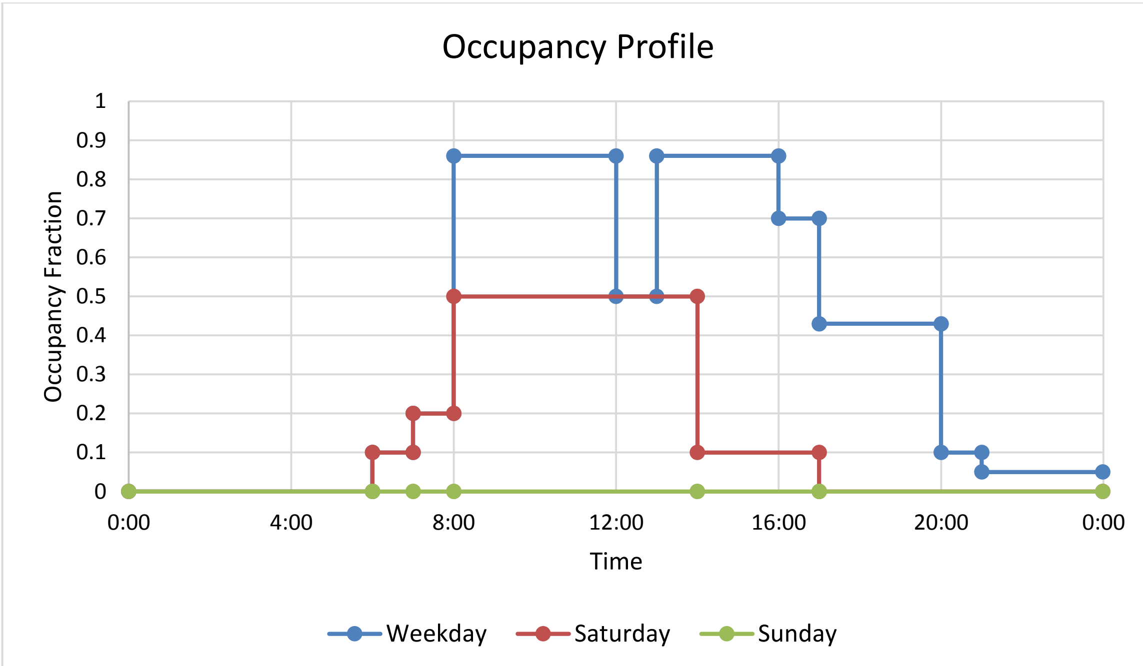

Figure 4. Occupancy profiles of both building models

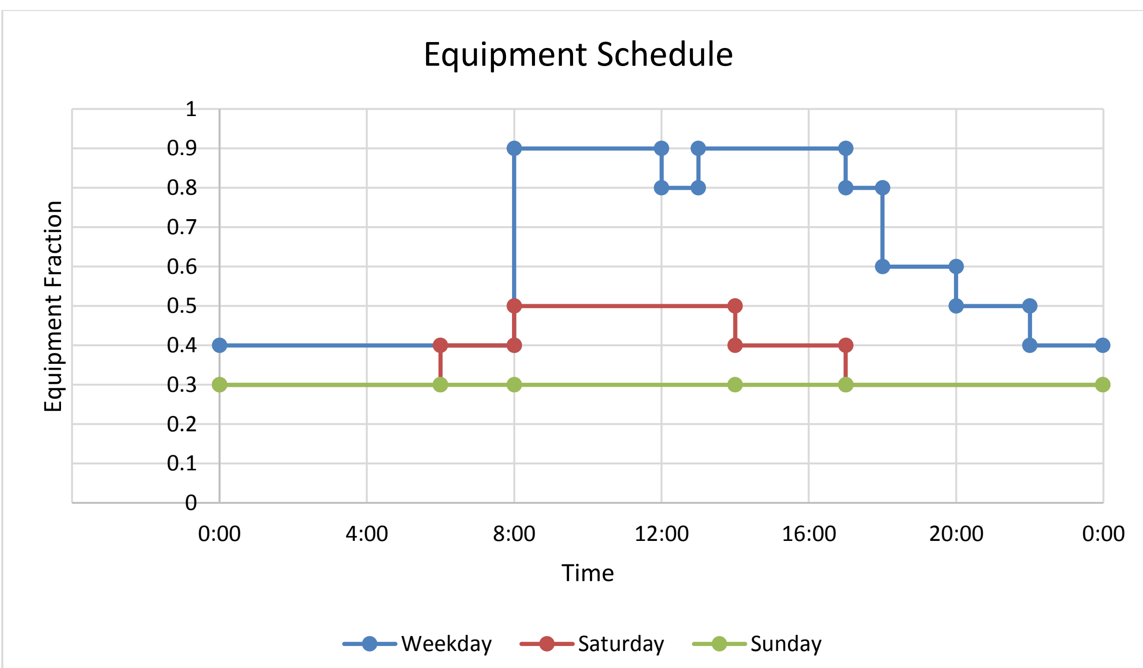

Figure 5. Equipment schedule profiles of both building models

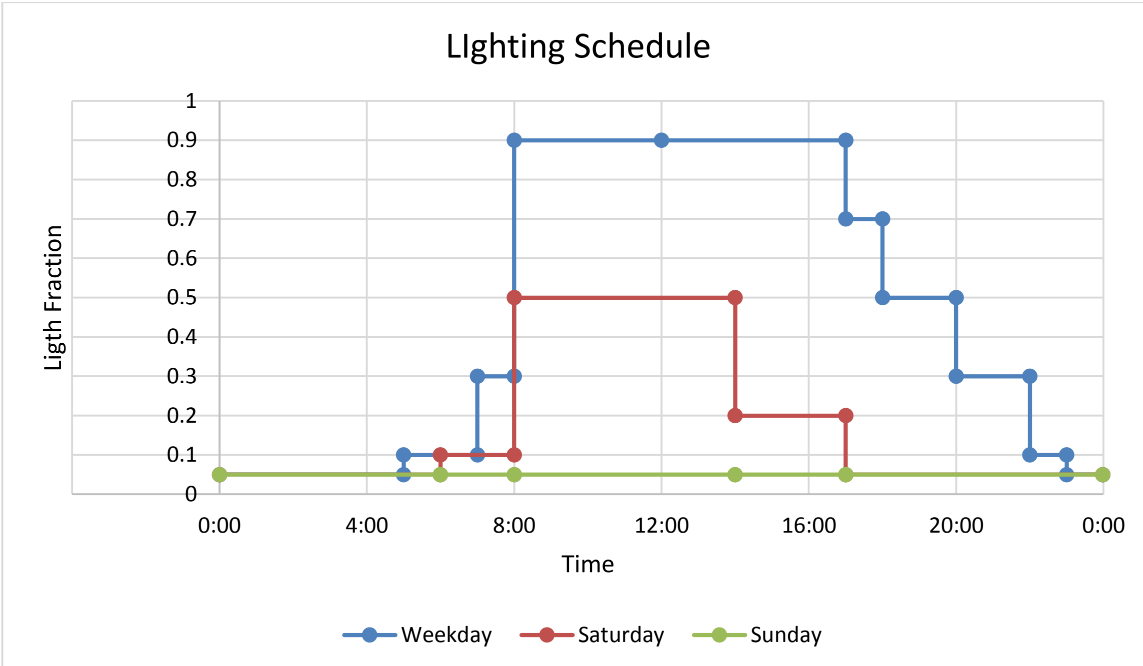

Figure 6. Lighting schedule profiles of both building models

Table 4. Zone Summary of UFAD model in metric units

	Area m^2	Volume m^3	Gross Wall Area m^2	Window Area m^2	Lighting W/m^2	People m^2/person	Plug and Process W/m^2
East Thermal Zone	98	329	102	41	10.7	17.7	7.6
North Thermal Zone	98	329	102	41	10.7	17.7	7.6
South Thermal Zone	98	329	102	41	10.7	17.7	7.6
West Thermal Zone	98	329	102	41	10.7	17.7	7.6
Interior Thermal Zone	536.61	1799.14	0	0	10.7	17.7	7.6

Table 5. Zone Summary of UFAD model in imperial units

	Area ft^2	Volume ft^3	Gross Wall Area ft^2	Window Area ft^2	Lighting W/ft^2	People ft^2/person	Plug and Process W/ft^2
East Thermal Zone	1056	11616	1100	440	1	191	0.71
North Thermal Zone	1056	11616	1100	440	1	191	0.71
South Thermal Zone	1056	11616	1100	440	1	191	0.71
West Thermal Zone	1056	11616	1100	440	1	191	0.71
Interior Thermal Zone	5776	63536	0	0	1	191	0.71

The baseline UFAD system has an outside air damper which mixes return and outside air at a constant flow rate of 3212 cfm which is 0.11 cfm/ft^2. The UFAD AHU is shown in **Figure 7**. The cooling coil and the heating coil modulate to meet the SAT set point measured after the fan. The fan has minimum flow rate corresponding to 0.3 cfm/ft^2, and the maximum flow rate is oversized to meet the cooling load at the peak cooling conditions during the design day with a safety factor of 1.2. The fan motor is simulated to be in the air stream. The motor efficiency is 0.93 and the fan efficiency is 0.6. The pressure loss of the system is taken from Table 5, and is 2.83 in w.c. The supply air is connected to 3 supply plenums. Only a single supply plenum is shown in the diagram.

Each supply plenum splits the airflow into each of the 5 zones within the floor. The heat transfer calculations are done assuming that the concrete slab has a single surface temperature and heat transfer coefficient. Each of the raised floors has its own surface temperature and heat transfer coefficient for the supply plenum heat transfer. There is reheat available for both interior and exterior zones. The air leaves each zone at a temperature calculated by the UFAD modules mentioned previously. The air streams from each room are mixed in a single return plenum per floor. The return air from each of the floors is then mixed and the appropriate fraction is exhausted, and replenished by the outside air.

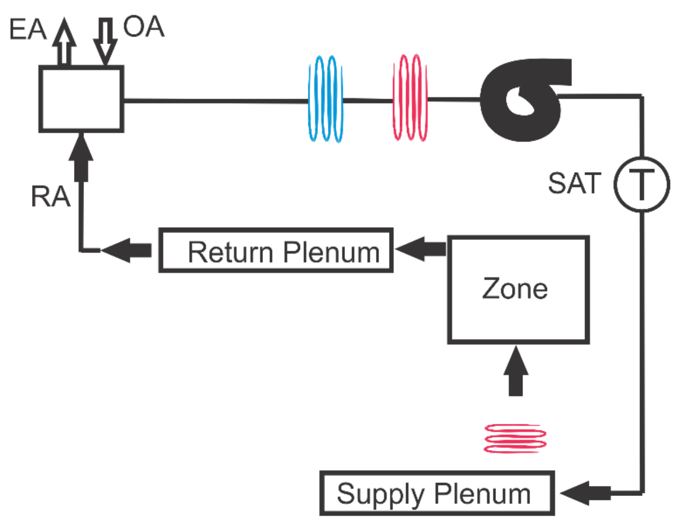

Figure 7. Baseline UFAD AHU system

The overhead AHU shown in **Figure 8** is almost identical to the UFAD AHU. The difference between the two air handling systems is that the overhead system has ducted supply air; thus no supply plenums are simulated. The OH system also has return plenums. The return plenums are simulated as separate zones, calculating the heat transfer from all surfaces similar to the UFAD model. The fan pressure loss is also taken from Table 6; however due to higher pressure losses in ductwork, VAV boxes, and diffusers the pressure loss is assumed to be 4.28 in wc.

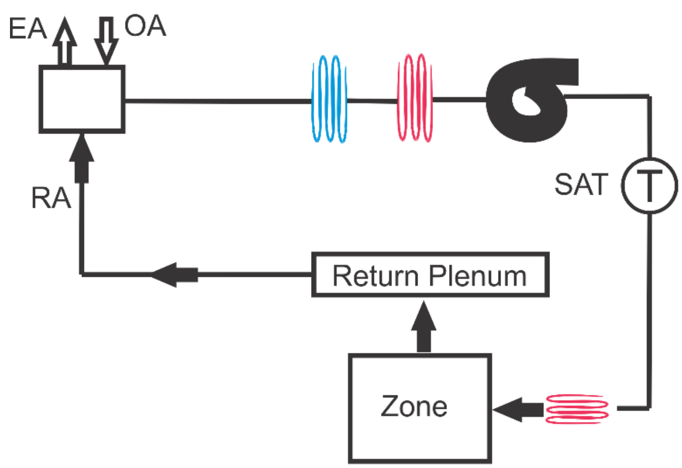

Figure 8. Baseline OH AHU system

The set point for the base line models is 55°F with no reset. 55°F is a common set point for buildings in hot and humid climates.

Table 6. Typical Supply/Return Pressure Requirements Comparison (Bauman and Dally 2013)

Pressure Loss Item	Overhead		UFAD	
	Office Supply, in. wc	Office Return/Relief, in. wc	Office Supply, in. wc	Office Return/Relief, in. wc
AHU (clean filters, coils louvers, etc.)	1.1	0.3	1.1	0.3
Dampers	0.1	0.1	0.1	0.1
Dirty filter allowance	0.75		0.75	
Ductwork, shafts	0.08	0.03	0.08	0.03
Ductwork, branches	1.25	0.02	0.75	0.02
VAV boxes	0.5		0	
VAV box reheat coil	0.2		0	
Diffusers and low pressure ductwork	0.3	0.1	0.05	0.1
Total	**4.28**	**0.55**	**2.83**	**0.55**

In order to study the energy performance of the UFAD and OH systems, each zone's cooling and heating energy rates are examined. There are multiple ways of looking at the energy entering the zone within the EnergyPlus simulation software. The mass flow rates as well as enthalpy and temperature are available for all the nodes. One could choose the nodes that represent the input and the output of each zone and apply a simple formula to calculate sensible heating or cooling. With assumption of constant pressure the cooling or heating sensible energy is proportional to the product of mass flow and the difference of temperatures of the input and the output states. EnergyPlus has another output that calculates the system's sensible heating and cooling energy. This variable outputs heating or cooling energy that is supplied to the zone by the HVAC system. The reported values are calculated based on the difference between average zone temperature and supply temperature and the supply air mass flow rate for the specified time stamp.

The models created for this treat both supply plenum and the return plenum as separate zones. This is helpful because it simplifies the output procedures and allows greater accuracy of simulation. An alternative way of simulating the return plenum is adding an air gap in the construction set for the ceiling. The construction set method would only do heat transfer calculations for top and bottom surfaces and ignore the convective heat transfer directly to the slab.

Figure 9 shows the cooling energy for each of the zones on the first floor. The energy is calculated at hourly time steps. The total energy is then scaled by the zone's area. This graph is for the design cooling day which is Aug 21 with a high temperature of 98.6 °F (37 °C) and an average temperature of 87.8 °F (31.1 °C). The ground floor supply plenum gains heat at 2.3 Btu/ft^2 during unoccupied hours and peaks out at 3.4 Btu/ft^2 at 5 pm. Since the plenum zone is shared by all the zones the peak rate occurs due to the high load of the west zone. During unoccupied hours between 11pm and 6am all the loads in the non-plenum zones are around 4.1 Btu/ft^2. The peak load of the interior zone is 5.1 Btu/ft^2, the north zone's peak load is 9.6 Btu/ft^2, the south' zone's peak load is 12.3 Btu/ft^2, the east zone's peak load is 15.2 Btu/ft^2, and the west zone's peak load is 17.7 Btu/ft^2. The return plenum has no cooling load, which means that the temperature in the return plenum is either equal to or lower than the air temperature returned to the plenum.

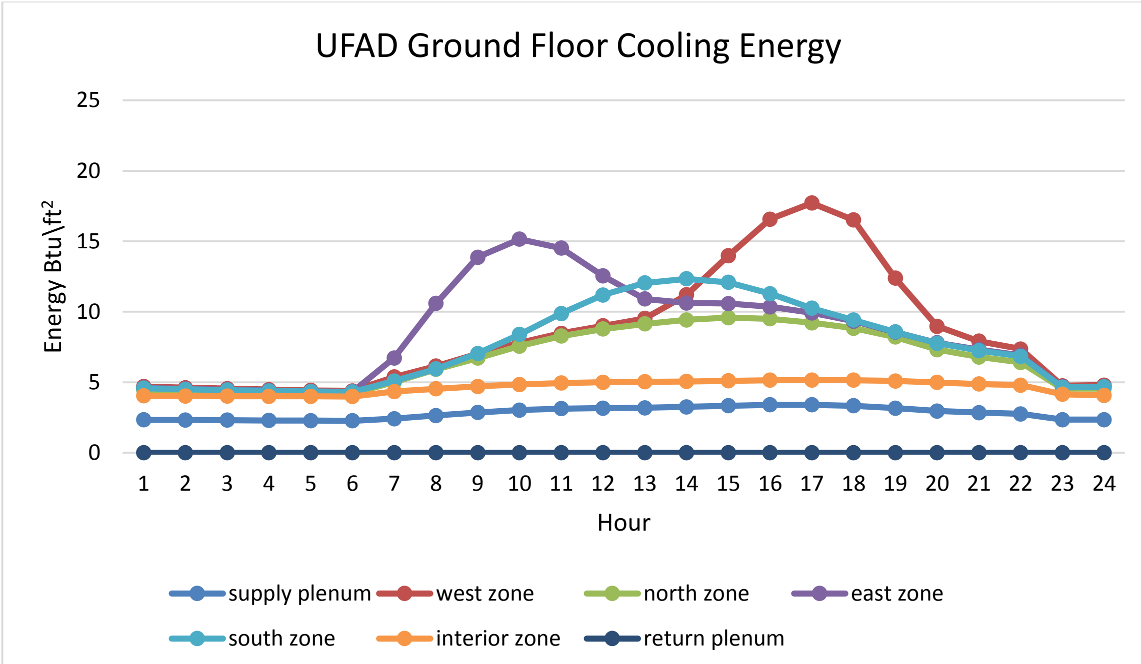

Figure 9. UFAD ground floor cooling energy during cooling design day

Figure 10 shows the cooling energy consumption of all zones of the middle floor of the UFAD model building. The supply plenum, and all the occupied zones have heat gain of 4.0 Btu/ft^2 during unoccupied hours. There is a linear increase in cooling consumption from 6am to 7am where supply plenum heat gain goes close to its peak of 5.0 Btu/ft^2. The interior zone also peaks out at 7am at 6.2 Btu/ft^2, the north zone peaks out at 10.5 Btu/ft^2, the south zone peaks out at 13.7 Btu/ft^2, the east zone peaks out at 16.8 Btu/ft^2, and the west zone peaks out at 19.2 Btu/ft^2. It is important to note that the supply plenum peak heat gain went from 3.4 Btu/ft^2 on the ground floor to 5.0 Btu/ft^2 on the middle floor, which is a 47% increase in heat gain. The increased heat gain also implies that the supply temperatures into the zones were higher, requiring a higher flow rate. The return plenum has no cooling load just like the first floor.

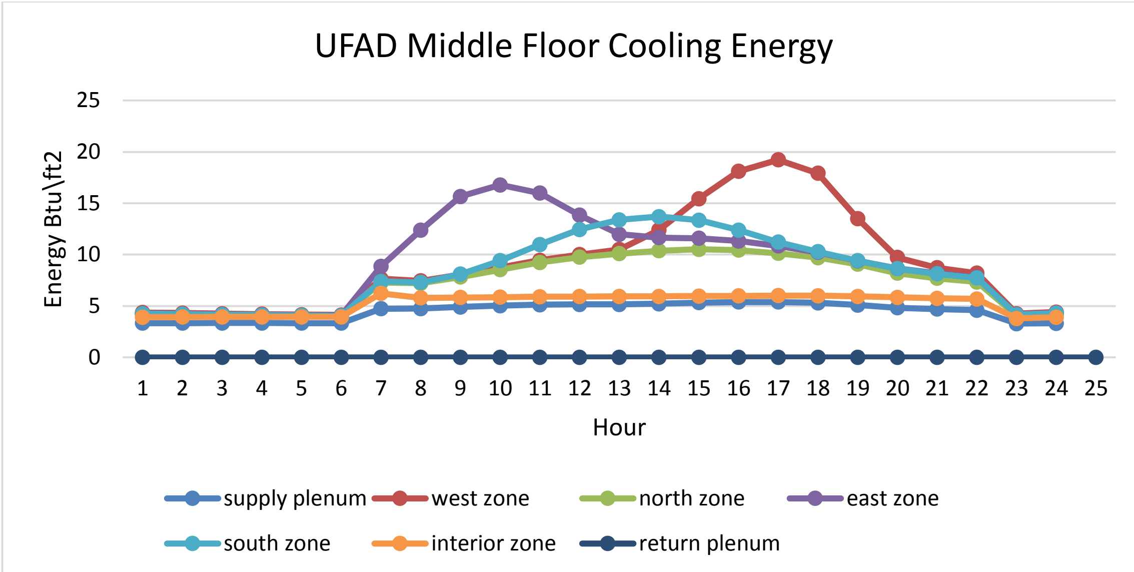

Figure 10. UFAD middle floor cooling energy during cooling design day

Figure 11 shows the top floor cooling energy during the design cooling day. During unoccupied hours the heat gain in all the zones is 4.4 Btu/ft$^{2.}$ There is again a linear increase in cooling consumption from 6am to 7am where supply plenum heat gain goes close to its peak of 5.8 Btu/ft^2 and the interior zone also peaks out at 7.5 Btu/ft^2. The north zone peaks out at 12.6 Btu/ft^2, the south zone peaks out at 14.8 Btu/ft^2, the east zone peaks out at 18.0 Btu/ft^2, and the west zone peaks out at 20.5 Btu/ft^2. The return plenum also has a peak cooling load of 0.6 Btu/ft^2. The heat gain in the return plenum and extra load in the space is due to the roof load.

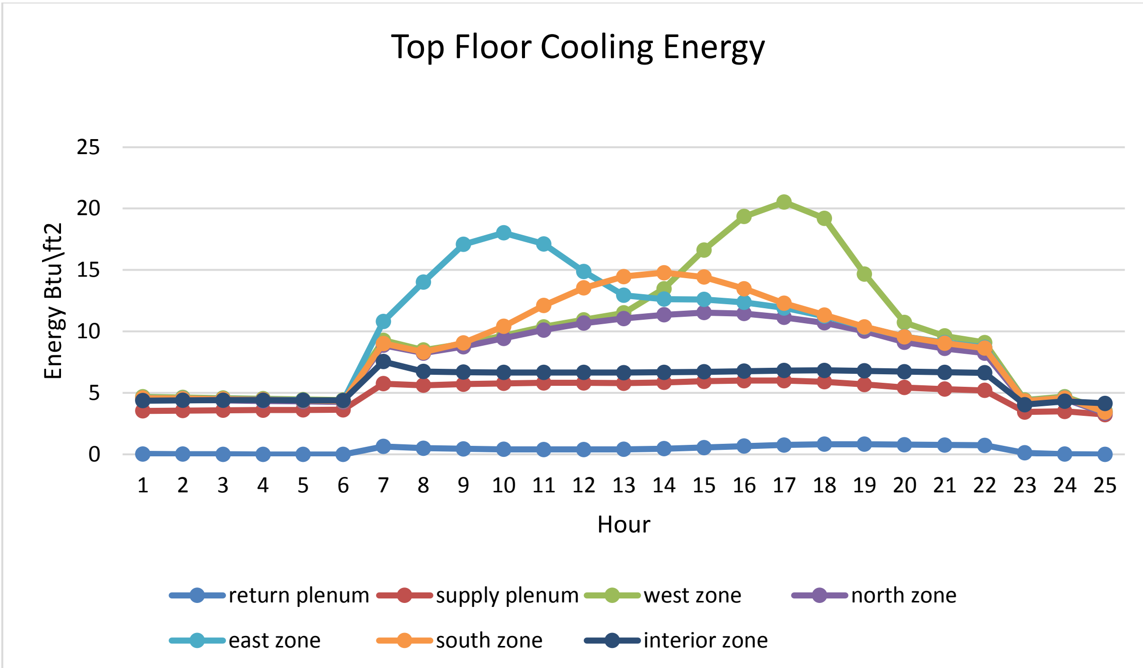

Figure 11. UFAD top floor zone cooling energy during cooling design day

Figure 12 shows the ground floor zone loads of the OH model during design cooling day. The interior zone cooling load ranges from 5 Btu/ft^2 to 5.5 Btu/ft^2 at its peak. The exterior zones have a load of 6 Btu/ft^2 during unoccupied hours. The north zone peaks out at 8.8 Btu/ft^2, the south zone peaks out at 11.1 Btu/ft^2, the east zone peaks out at 12.7 Btu/ft^2, and the west zone peaks out at 15.5 Btu/ft^2. The return plenum also has a cooling load which peaks during unoccupied hours at 0.4 Btu/ft^2 and is about 0.2 Btu/ft^2 during occupied hours.

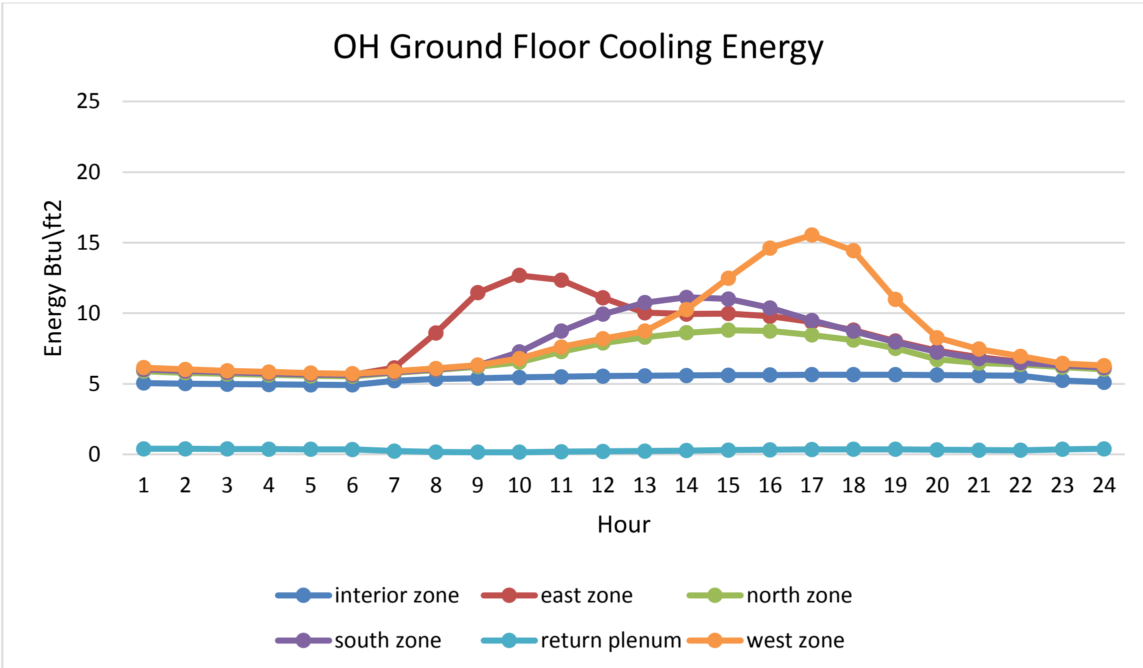

Figure 12. OH ground floor cooling energy during cooling design day

Figure 13 shows the middle floor zone loads of the OH model during the design cooling day. The interior zone cooling load ranges from 6.2 Btu/ft^2 during unoccupied hours to 7.6 Btu/ft^2 during occupied hours. The interior load is larger than that on the ground floor. The exterior zones have cooling loads ranging from 7.4 Btu/ft^2 to 11.9 Btu/ft^2 during unoccupied hours. The peak load for the north zone is 13.3 Btu/ft^2, the south zone's peak load is 16.5 Btu/ft^2, the east zone's peak load is 18.6 Btu/ft^2, and the west zone's peak load is 21.9 Btu/ft^2. The return plenum also has a cooling load which peaks during unoccupied hours at 0.3 Btu/ft^2 and is about 0.7 Btu/ft^2 during occupied hours. The peak loads for all the zones are larger than for comparable zones on the ground floor.

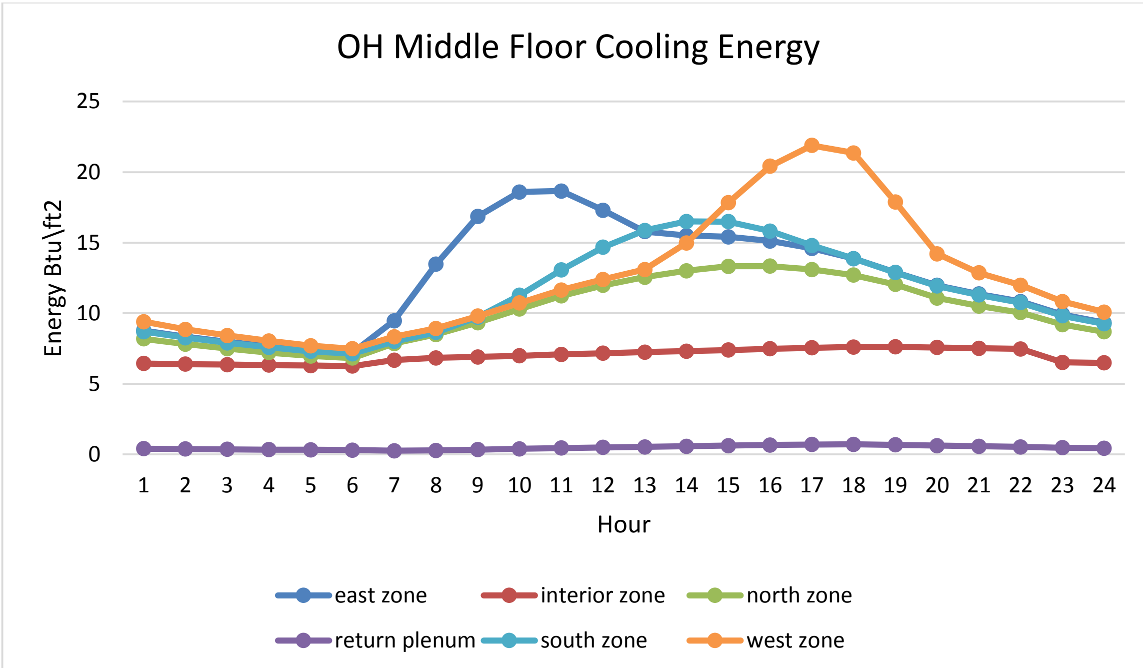

Figure 13. OH Middle floor cooling energy during cooling design day

Figure 14 shows the top floor zone loads of the OH model during the design cooling day. The interior zone cooling load ranges from 6.6 Btu/ft^2 during unoccupied hours to 8.2 Btu/ft^2 during occupied hours. The interior load is larger than that on either the ground floor or the middle floor. The exterior zones have cooling loads ranging from 7.9 Btu/ft^2 to 12.8 Btu/ft^2 during unoccupied hours. The peak load for the north zone is 14.2 Btu/ft^2, the south zone's peak load is 17.4 Btu/ft^2, the east zone's peak load is 19.6 Btu/ft^2, and the west zone's peak load is 22.9 Btu/ft^2. The return plenum also has a cooling load which peaks during unoccupied hours at 0.5 Btu/ft^2 and is about 1.1 Btu/ft^2 during occupied hours. The peak loads for all the zones are larger than for the ground floor and the middle floors.

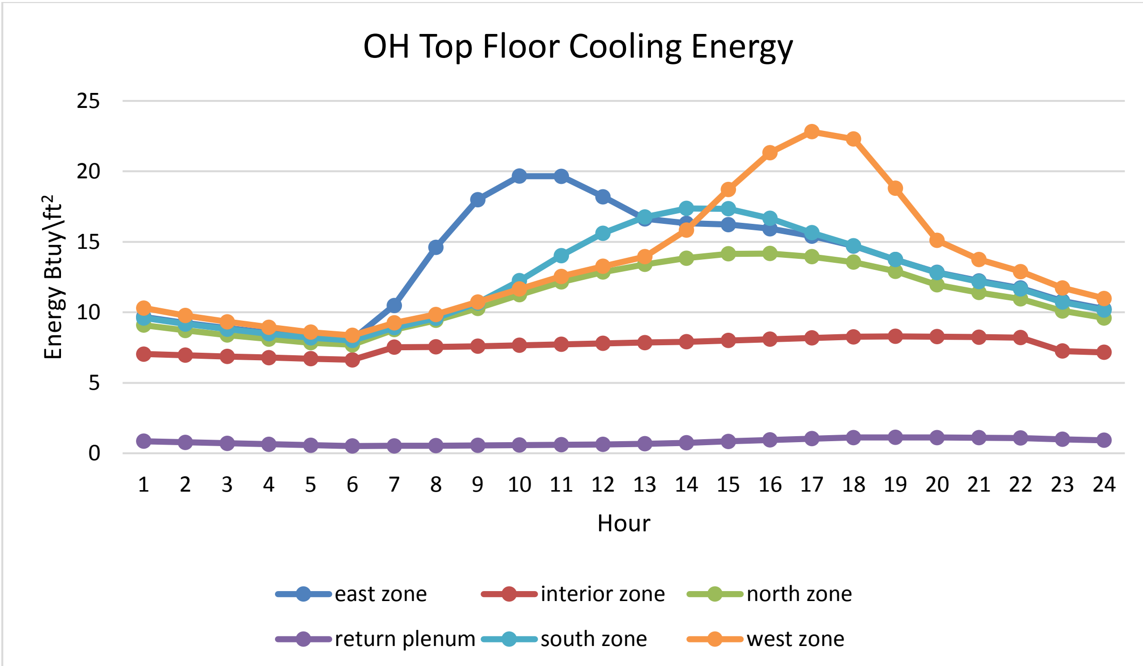

Figure 14. OH top floor cooling energy during cooling design day

Figure 15 shows the plenum loads of the UFAD simulation. The supply plenums deliver cold air to the zone, with the conditioned air gaining heat due to the cooling load. There is heat transfer from the return plenum into the supply plenum above. The return plenum is cooled by the top slab surface; this is called "heating load" since it cools the plenum just as heat loss through a wall can create heating load in an exterior space. The first floor supply plenum is in contact with the floor slab, which is in contact with ground. The ground temperature for the slab on grade contact was assumed to be 64.4 °F (18 °C) which is the average annual temperature of the first floor plenum The first floor supply plenum has heat gain of 2.3 Btu/ft^2 during unoccupied hours and a peak of 3.4 Btu/ft^2. The second floor supply plenum is thermally connected to the first floor return plenum. The second floor supply plenum heat gain is 3.4 Btu/ft^2 during unoccupied hours and 5.3 Btu/ft^2 at its peak. The first floor return plenum is cooled (heating load) by 0.6 Btu/ft^2 during unoccupied hours and 0.9 Btu/ft^2 during the occupied hours. The cooling of the return plenum explains a portion of the extra load in the second floor supply plenum. The higher supply temperature on the second floor also increases the flow rate, which in turn increases the heat transfer coefficient. The second floor supply plenum cooling load is larger than the first floor by more than the energy transferred into the return plenum due to the higher air flow rate.

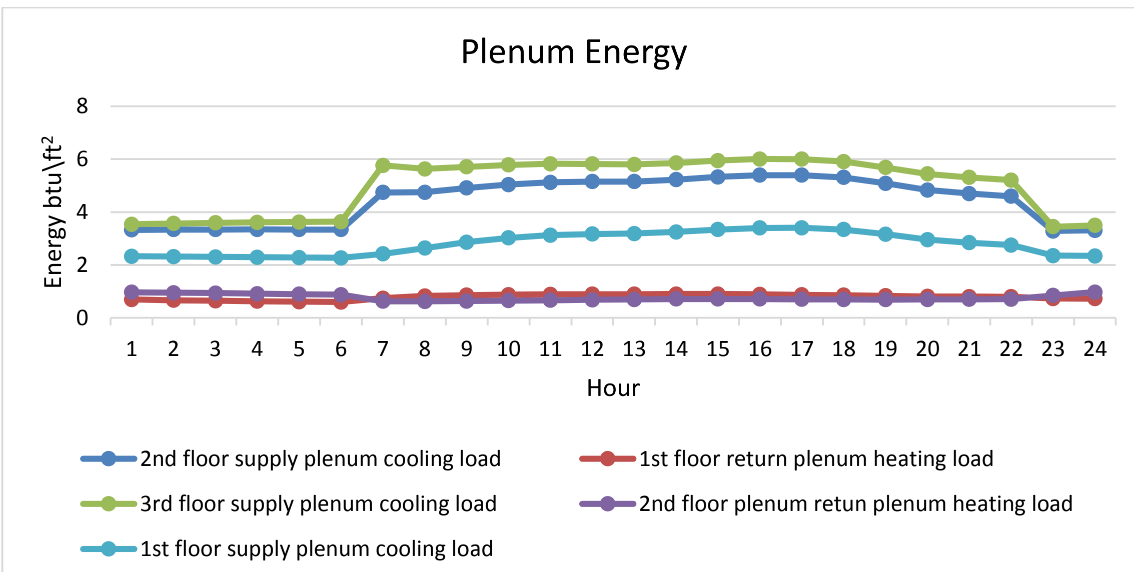

Figure 15. Plenum energy for UFAD model

The third floor supply plenum cooling load is around 3.6 Btu/ft^2 during unoccupied hours and 5.7 Btu/ft^2 at its peak. The second floor return plenum heating load is similar to the first floor ranging from 1 Btu/ft^2 during unoccupied hours to 0.7 Btu/ft^2 during the working hours. The third floor supply plenum load is higher due to an even higher air flow rate due to the extra roof load in the zone.

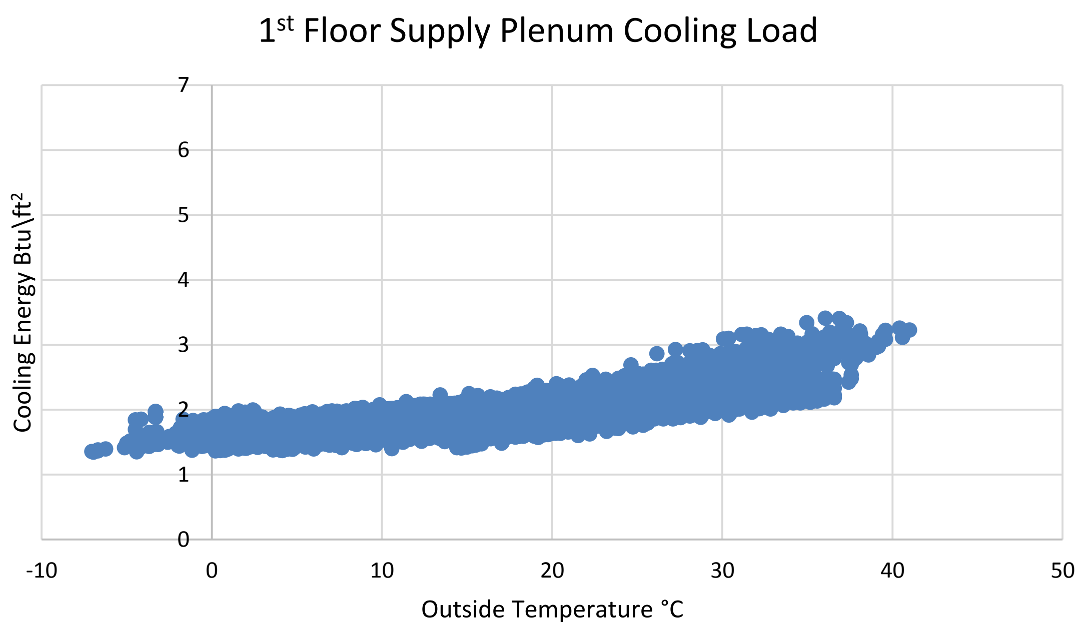

Figure 16. 1st floor supply plenum cooling load

Figure 16 shows first floor supply plenum heat gain (cooling load). The heat gain increases with outside temperature with a minimum of 1.4 Btu/ft^2 during between 0°C (32 °F) and 10 °C (50 °F), an average of 2 Btu/ft^2 between 20°C (68 °F), and 30°C (86 °F),, and a peak of 3.4 Btu/ft^2 at 37°C (98.6 °F),. The variance of heat gain at each temperature is smaller at cold temperatures and larger at the higher temperatures and it is equal to1 Btu/ft^2.

Figure 17 shows the second floor supply plenum heat gain (cooling load). The heat gain increases with outside temperature with a minimum of 0.8 Btu/ft^2 during between 0°C (32 °F) and 10 °C (50 °F), an average of 2.6 Btu/ft^2 between 20°C (68 °F), and 30°C (86 °F), and a peak of 5.4 Btu/ft^2 at 37°C (98.6 °F). The variance of heat gain at each temperature is smaller at lower temperatures and larger at the higher temperatures and is about 1.8 Btu/ft^2.

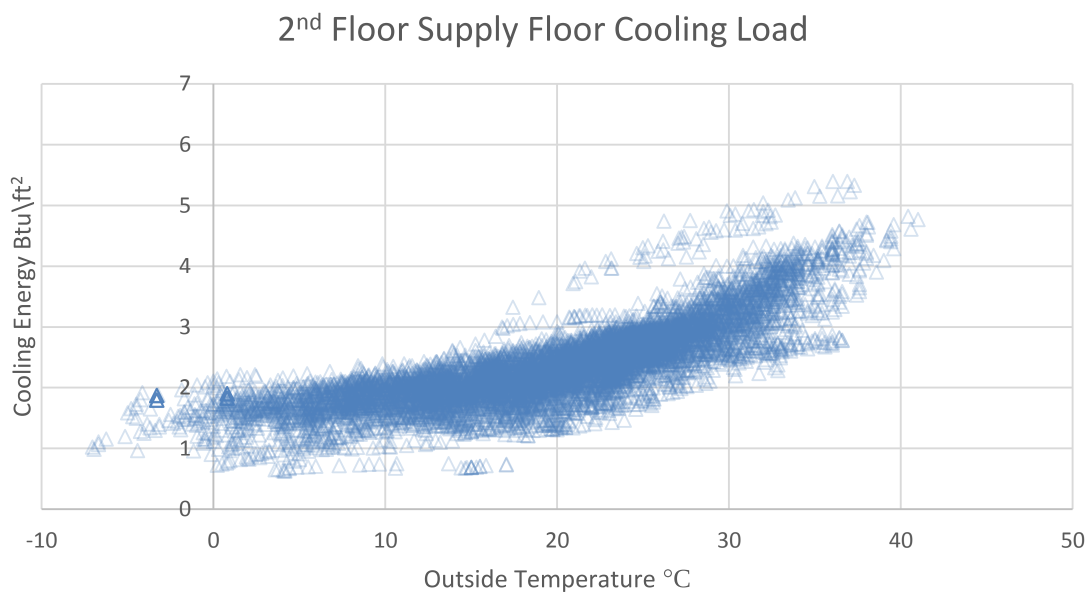

Figure 17. 2nd floor supply plenum cooling load

Figure 18 shows the supply plenum entering temperature from the air handler, supply plenum leaving temperature (into the zone) and the difference between two temperatures. All data is binned into 5 degree Fahrenheit outside temperature intervals. The supply plenum entering and leaving temperatures are averaged within each of the bins. The temperature difference peaks out at 8.18 °F in the 80 °F - 85 °F (26.7 °C – 29.4 °C) outside temperature interval. The cooling load displayed in **Figure 17** continues to increase while the temperature difference starts to taper off. This is due to increased flow rate of the supply air. The air spends less time in the plenum thus, lower temperature differences, however total energy transfer is increased.

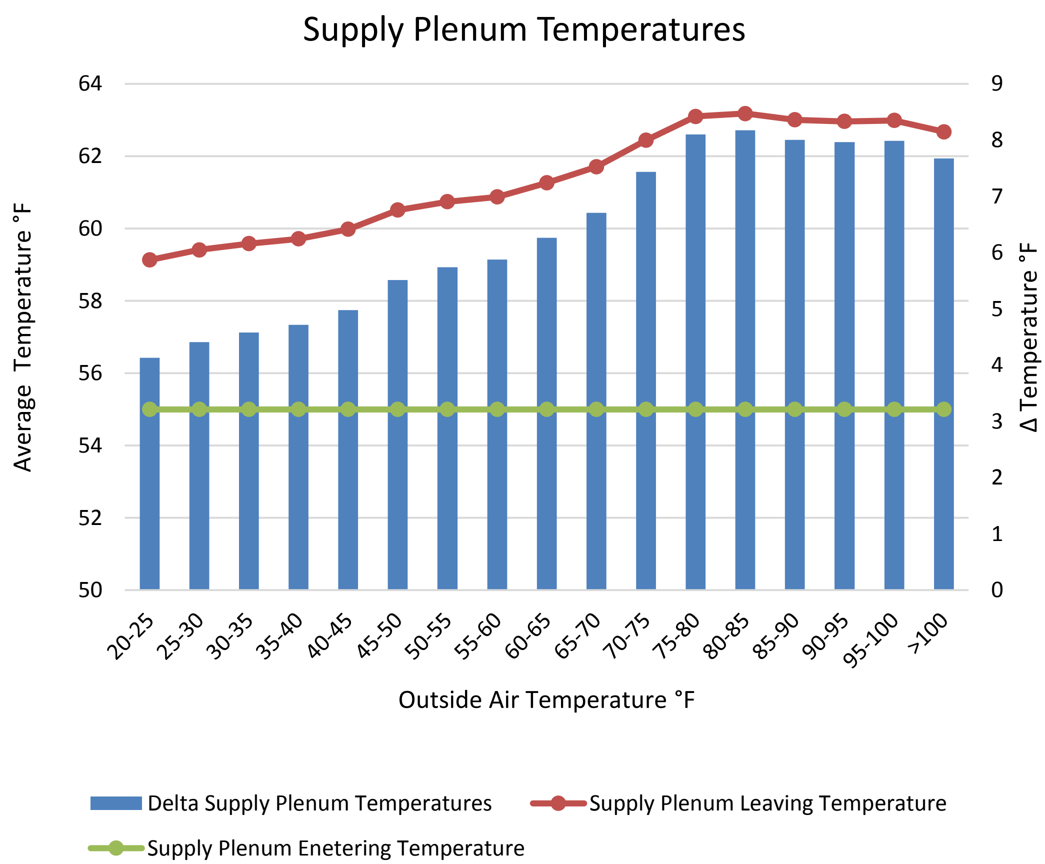

Figure 18. 2nd floor supply plenum temperatures

Figure 19 shows the third floor supply plenum heat gain (cooling load). The heat gain increases with increasing outside temperature with a minimum of 0.6 Btu/ft^2 during between 0°C and 10 °C, an average of 2.9 Btu/ft^2 between 20°C and 30°C, and a peak of 5.9 Btu/ft^2 at 37°C. The variance of heat gain at each temperature is smaller at lower temperatures and larger at the higher temperatures and is about 2.1 Btu/ft^2.

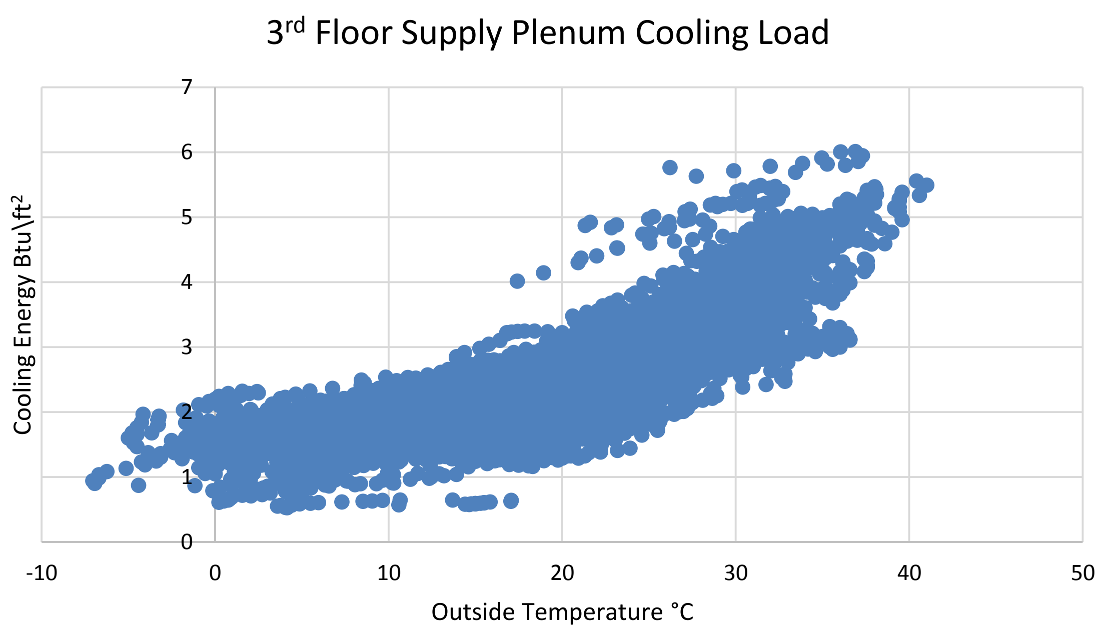

Figure 19. 3rd floor supply plenum cooling load

Figure 20 shows the return plenum heat loss for the 2nd floor. The return plenum heat loss is independent of outside air temperature; however there is great variance within the temperature ranges. The average heat loss is 1 Btu/ft^2 with maximum heat loss of 2 Btu/ft^2.

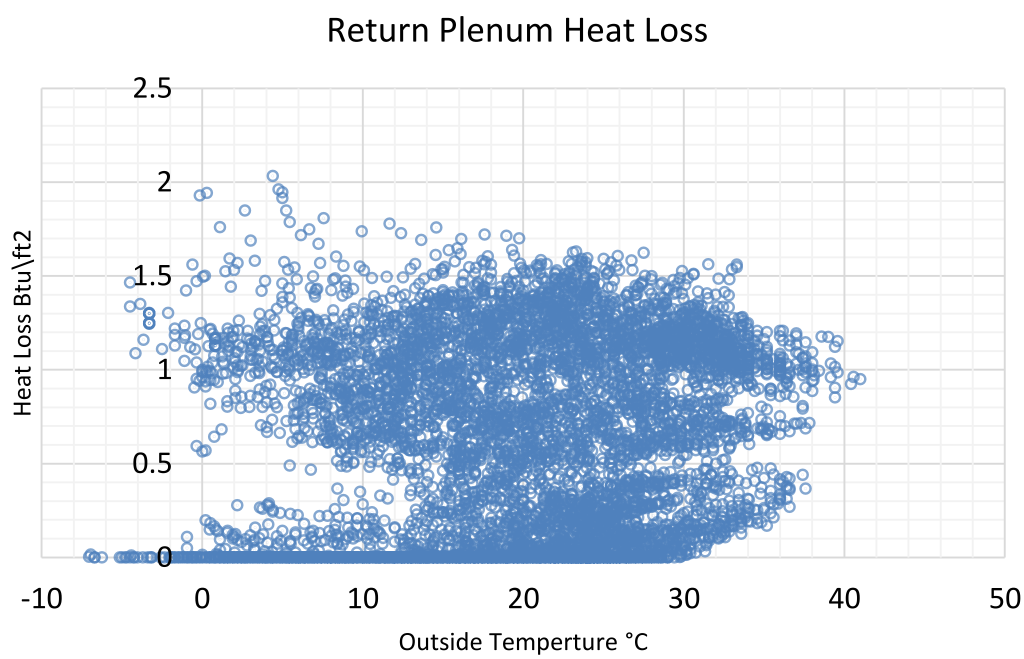

Figure 20. 2nd floor return plenum heat loss (heating load)

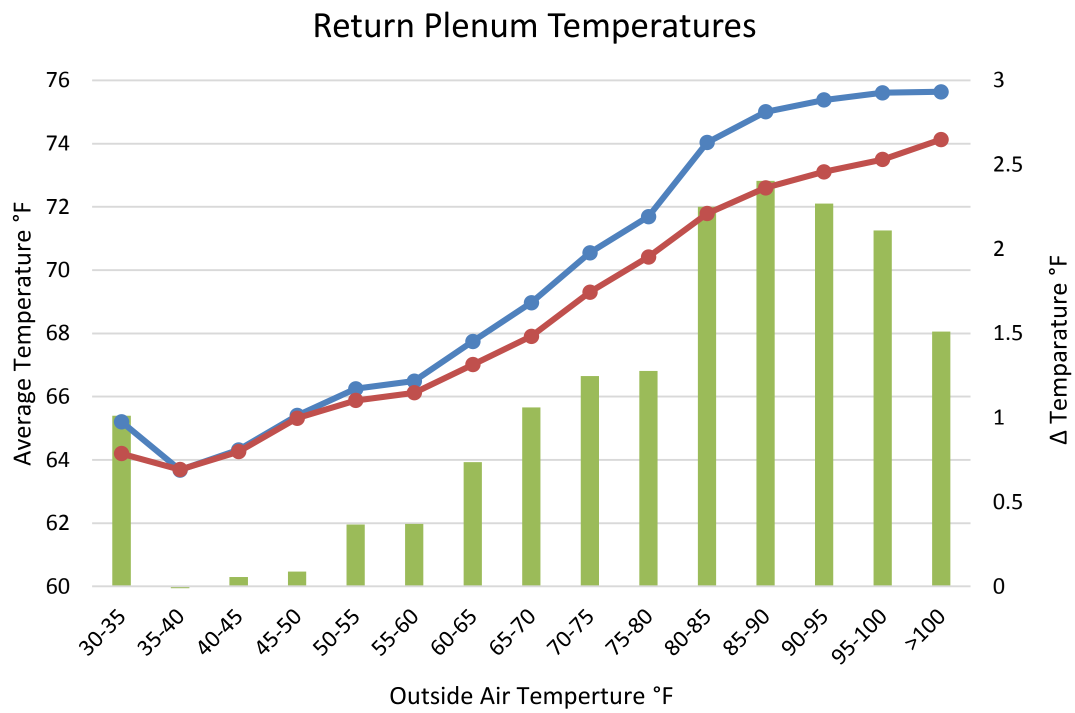

Figure 21. Return plenum temperatures with blue line representing return plenum entering temperature and red line representing return plenum leaving temperature.

Figure 21 shows the return plenum entering and leaving temperatures. The mixed subzone temperature is the upper layer temperature inside the zone. The return plenum leaving temperature is the temperature output at the exit node of the return plenum.

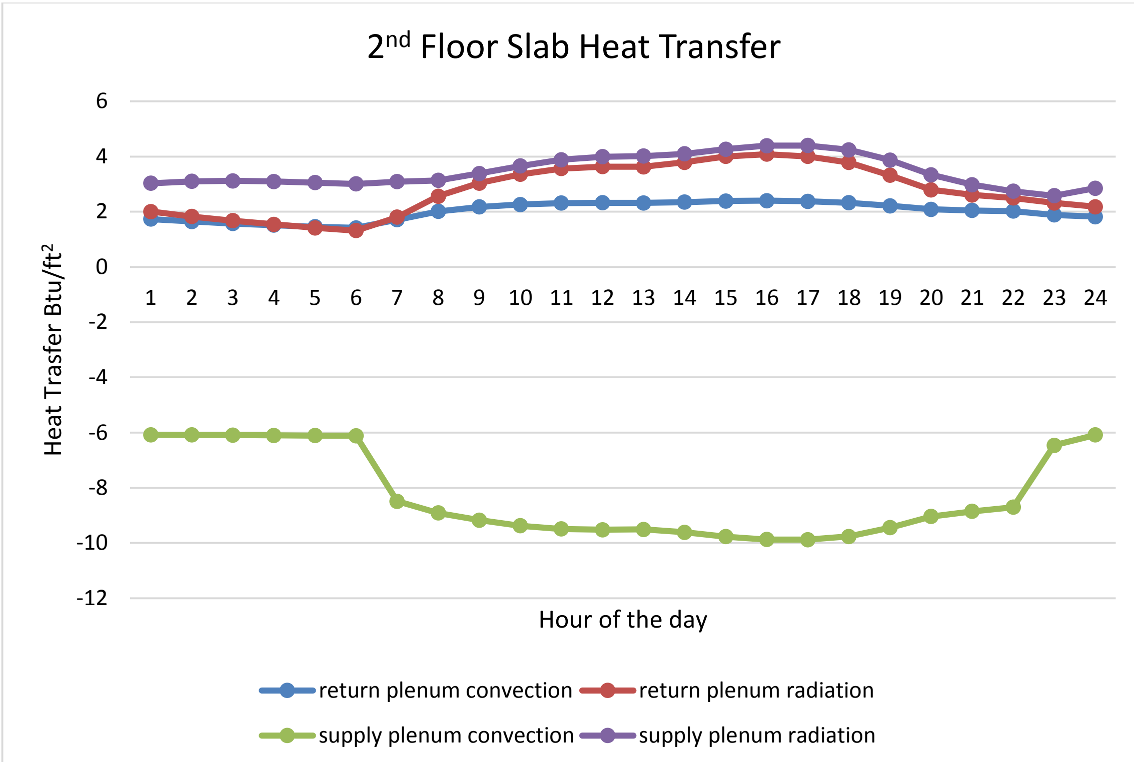

Figure 22. 2nd floor slab convection and radiation heat transfer on a design cooling day

Figure 22 shows the heat transfer of the slab during the design cooling day. The largest component of slab thermal balance is the convection heat transfer from conditioned air to the slab from -8 Btu/ft^2 to -10 Btu/ft^2. The negative heat transfer represents the cooling of the slab. The heating of the slab mostly occurs by net radiation exchange. The supply plenum radiation represents the net exchange between the bottom of the raised floor and the face of the slab facing the conditioned air (from 3 Btu/ft^2 to 4.5 Btu/ft^2). Similar in magnitude is the return plenum radiation which represents the radiation from the bottom of the slab to the top of the acoustic tile (from 2 Btu/ft^2 to 4 Btu/ft^2). The hot air inside the return plenum also contributes to the heat balance of the slab by convection. The magnitude of return plenum convection to the slab is from 1.3 Btu/ft^2 to 2.4 Btu/ft^2.

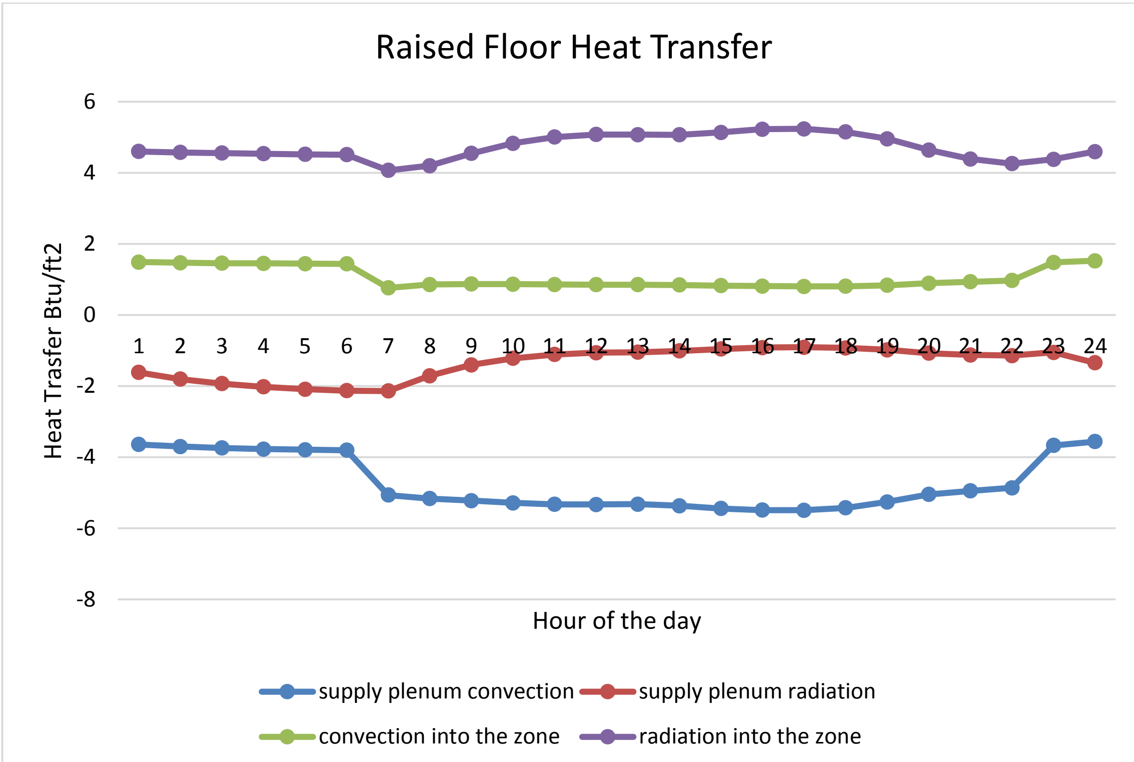

Figure 23. Raised floor convection and radiation heat transfer on a design cooling day.

Figure 23 shows the heat balance of the raised floor. The two largest components of the heat balance are convection from conditioned air in the plenum and radiation into the room. The raised floor is mostly cooled by the conditioned air from below with magnitude of -5 Btu/ft^2 to -5.5 Btu/ft^2. Another source of cooling is the radiation from the slab which is around -2 Btu/ft^2 during unoccupied hours and -1.2 Btu/ft^2 during occupied hours. This cooling is countered by the net radiation into the room which is from 4 Btu/ft^2 to 5.2 Btu/ft^2.

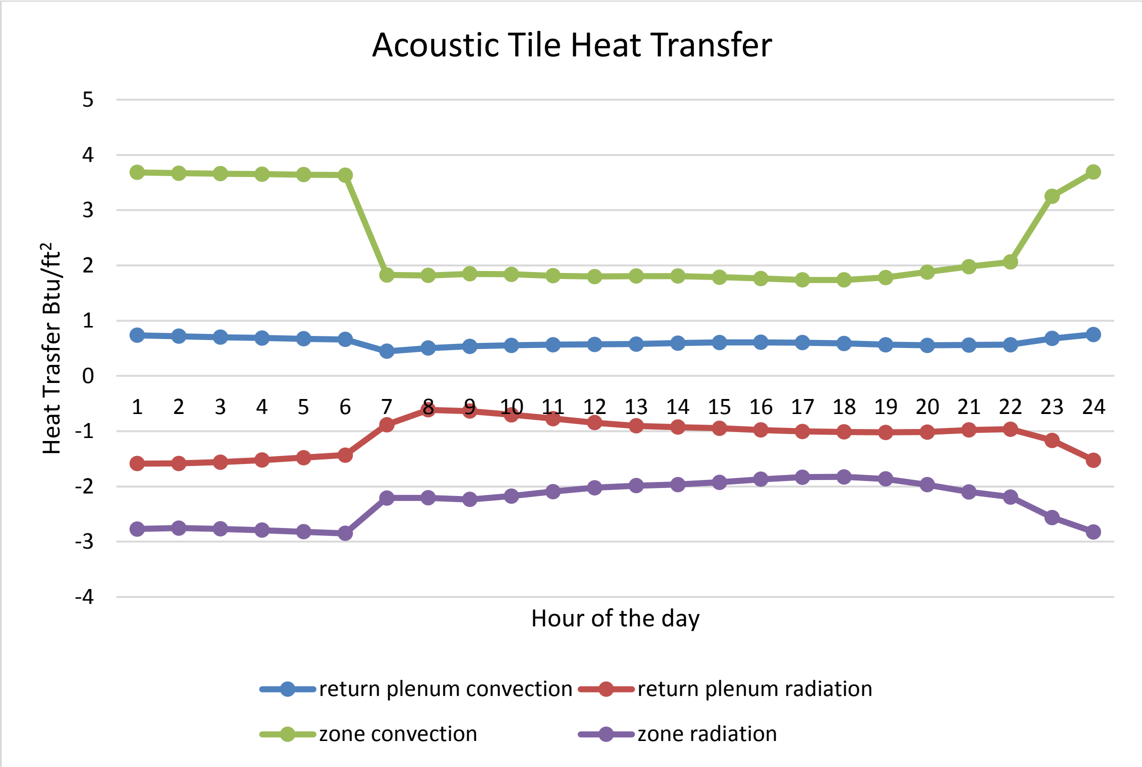

Figure 24. Acoustic tile convective and radiation heat transfer on a design cooling day.

Figure 24 shows the heat transfer of the acoustic tile layer. The acoustic tile is heated by the convection resulting from the room air stratification. The inside of the return plenum is also at a higher temperature than the acoustic tile which also adds to the convective heating of the tile. The acoustic tile is exposed to two colder surfaces which are the raised floor and the slab which both cool the acoustic tile. The convective cooling of the top layer of the interior zone is 3.5 Btu/ft^2 during unoccupied times and 1.7 Btu/ft^2

during occupied periods. The convective heat transfer inside the return plenum is 0.7 Btu/ft^2 during unoccupied times and 0.6 Btu/ft^2 during occupied periods.

During the design day, zone loads in the UFAD system are lower than the OH system. The UFAD system has an extra supply plenum zone which has a significant load. The supply plenum load increases with temperature. Some of the cooling load in the supply plenum ends up cooling the return plenum of the floor below. The return plenum cooling is independent of outside temperature. This implies that the rest of the plenum heat gain is ether transferred to the slab or is transferred to the occupied zone.

Figure 25 shows the cooling energy and the fan power for both OH and UFAD systems on a design cooling day. The UFAD system uses slightly less cooling energy during unoccupied hours, but uses more cooling throughout the day. The UFAD system used 10% more cooling energy throughout the whole day. Since there is lower pressure drop in the UFAD system, the fan energy is significantly lower during the night time. During the design day, supply plenum heat gain increases the supply air temperature to the zone. The higher supply temperature requires a higher flow rate, deteriorating the fan savings due to the pressure drop. The UFAD system uses less fan power throughout the day by a total of 9.8%.

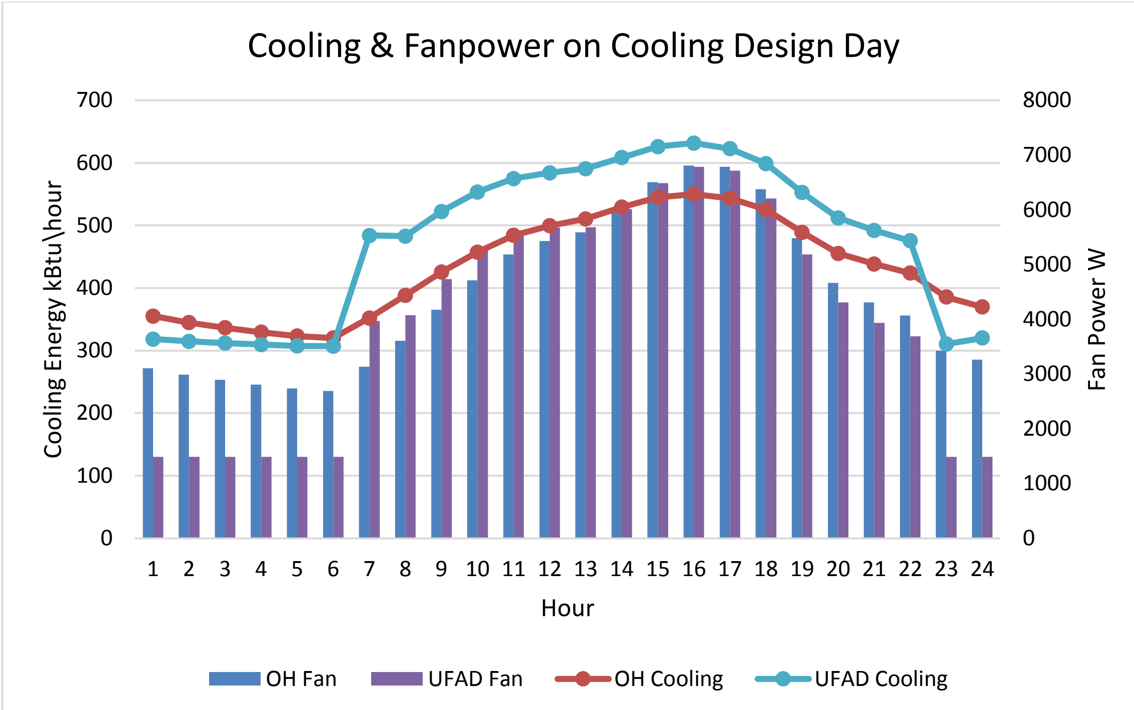

Figure 25. Cooing and fan power on a cooling design day for both UFAD and OH systems

Figure 26 shows cooling and fan consumption on a mild day. The data is taken from April 20th with a minimum temperature of 59.7 °F (15.4 °C), average temperature of 69.8 °F (21 °C) and maximum of 78.8 °F (26.6 °C). The cooling energy profile for UFAD and OH are almost identical between 8pm to 11am. The fan energy of the UFAD system is consistently lower at all times. The UFAD system used 2% more cooling energy than the OH system on a mild day. The UFAD system used 36% less fan energy than the OH system on a mild day.

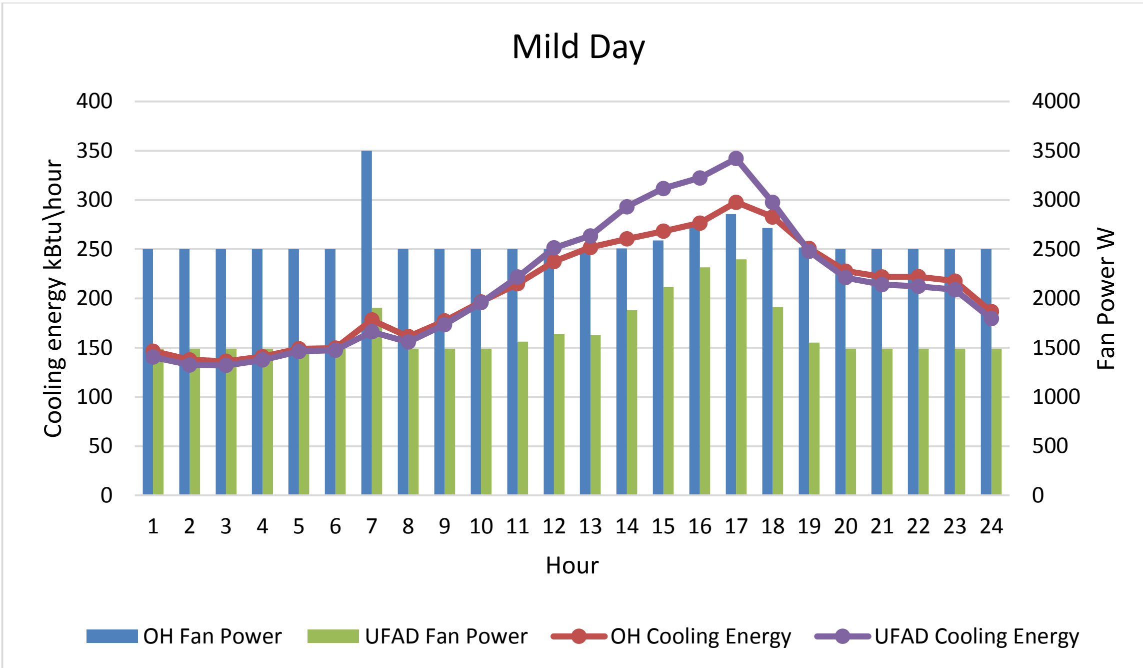

Figure 26. Cooling and fan power on a mild day for both UFAD and OH systems

Figure 27 shows the heating energy of UFAD and OH on April 20th. The UFAD system used 49% less heating energy. This is due to the heat gain in the supply plenum, which reduces the need to reheat the air at the minimum flow rates.

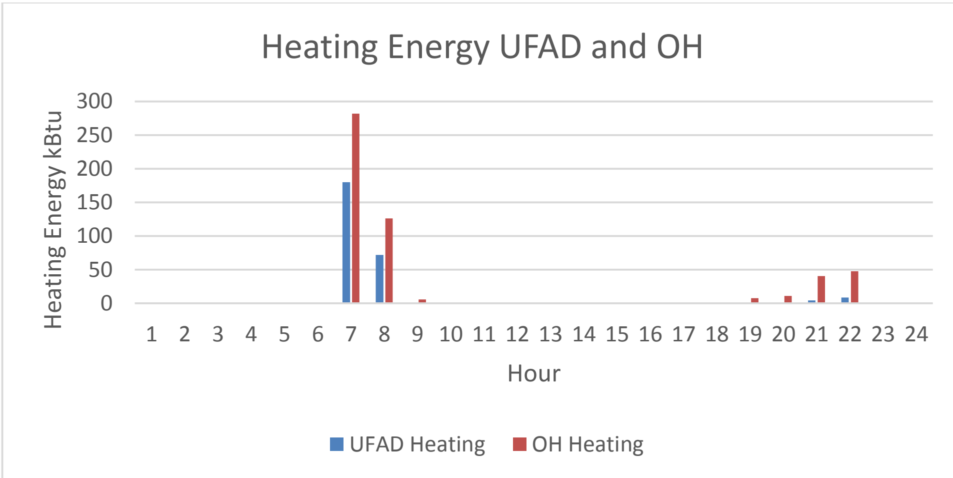

Figure 27. UFAD and OH heating energy on a mild day

Figure 28 shows the heating and fan energy on the coldest day in the simulated data set. The day occurred on January 7 which has coldest temperature of 23.9°F (-4.5 °C) and the average temperature of 30.4°F (-0.8°C). The overhead system uses 18% more heating energy during the period. The UFAD system uses 43% less fan energy during the period. This lower heating energy UFAD system can be explained by the heat transfer from supply plenum into return plenum. The return air is heating up the supply air requiring less heat to be added by the reheat coils.

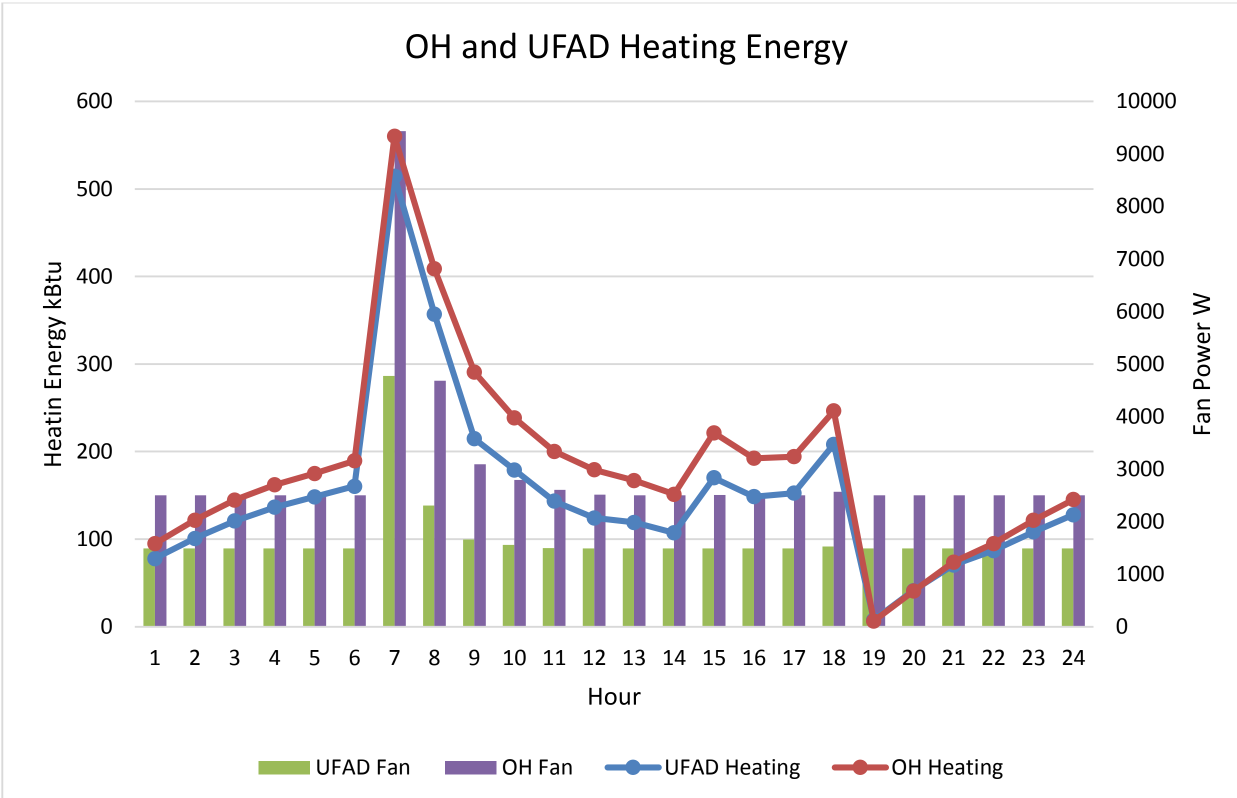

Figure 28. UFAD and OH heating energy on design heating day

2.2 Minimum Flow Rates

Conventional VAV systems have design or maximum flow rate and the minimum flow rate. The minimum flow rate usually determined by the ventilation standards and the outside air strategy. The cheapest and the least efficient outside air control is a damper that is manually controlled. This type of damper usually left in a constant position such that 10%-20% of supply air is outside air. An office requires 0.06 cmf/ft^2 + 5cmf/person of outside air. As an example constant air fraction of 20% outside air would require a minimum of 0.3cfm/ft^2 to meet the standard. If building has building has CO_2 sensor in the return duct, a demand control outside air strategy can be implemented. CO_2 based demand control ventilation does not rely on the minimum flow rate to meet the standard, thus the minimum flow rate can be 0.

In this section, the EnergyPlus models are simulated at different minimum flow rates to assess the energy performance of both overhead and UFAD systems. The ventilation strategy is constant outside air flow, which means that minimum flow rate of optimized system would equal to this outside air flow rate. The models are ran at different flow rates to understand the energy penalties of higher minimum flow rate of both systems. The outside air system stays the same for different minimum flow rates in order to study the impact of the minimum flow rate energy consumption by itself.

As described earlier in this thesis the peak load for the UFAD system is larger than for the OH system. The larger peak load requires a slightly larger HVAC system at design to meet those loads. This means that the minimum flow rates cannot be designed as a fraction of maximum flow rate. The zones were designed with fixed minimum flow rates to match the 0.1 cfm/ft^2, 0.2 cfm/ft^2, 0.3 cfm/ft^2, 0.4 cfm/ft^2.

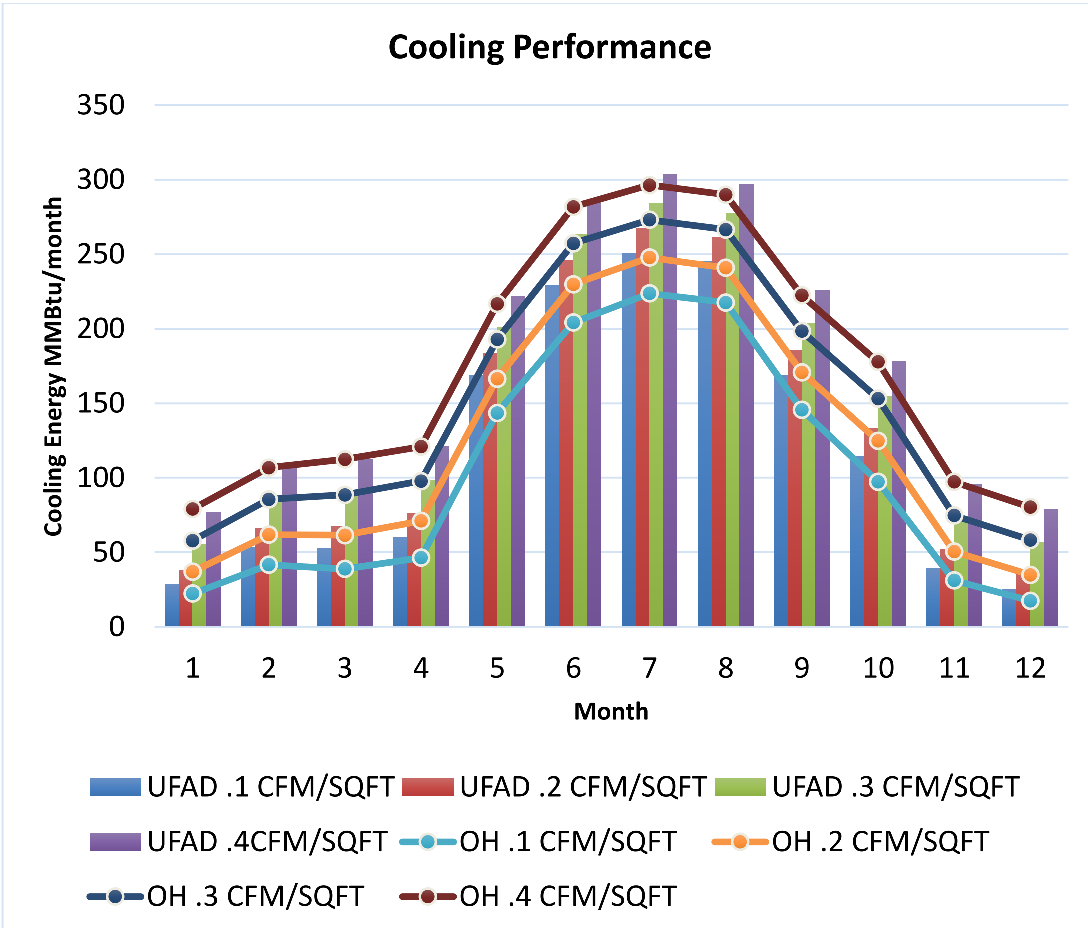

Figure 29. Cooling Performance of UFAD and OH systems at different minimum flow rates

Figure 29 shows the cooling energy of the UFAD and OH systems throughout the year. The OH system significantly outperforms the UFAD system at lower minimum flow rates. The UFAD system has very similar performance at the high 0.4 cfm/ft^2 minimum flow rate.

Table 7. Cooling energy consumption difference UFAD vs. OH

Minimum Flow Rate	0.1 cfm/ft^2	0.2 cfm/ft^2	0.3 cfm/ft^2	0.4 cfm/ft^2
OH (MMBtu)	1230	1497	1804	2081
UFAD (MMBtu)	1436	1613	1842	2104
(OH-UFAD)/OH (%)	-16.8%	-7.8%	-2.1%	-1.1%

Table 7 shows the exact cooling energy comparison between the overhead and UFAD systems. At 0.1 cfm/ft^2, which is the ventilation requirement, the UFAD system uses 16.8% more chilled water than the overhead system. If the system requires less cooling than the minimum flow rate requirement the air is reheated at the terminal level. Earlier we established that the supply plenum adds heat to the supply air. Since the supply air is now at higher temperature in UFADs due to the added heat, the flow rate that is required to meet the load will also be higher. This phenomenon reduces the amount of time that the system spends in the mode where the minimum flow rate cooling rate is higher than the load in the space. In other words the amount of time that the system spends in reheat mode is reduced, because of natural reheat in the supply plenum. Since the reheat energy is never added to the system, it does not need to be removed by the system, thus lowering cooling consumption. This phenomenon made possible by the heat from the return air plenum being transferred to supply air plenum discussed earlier in the thesis.

This result also has implications on optimization measure savings estimation. If an overhead system is operating at a high flow rate, and the measure is to reduce the minimum flow rate from 0.4 cfm/ft^2 to 0.1 cfm/ft^2 the expected savings in cooling were 40.9%. In the UFAD system the same measure will produce only 31.7% in cooling energy savings.

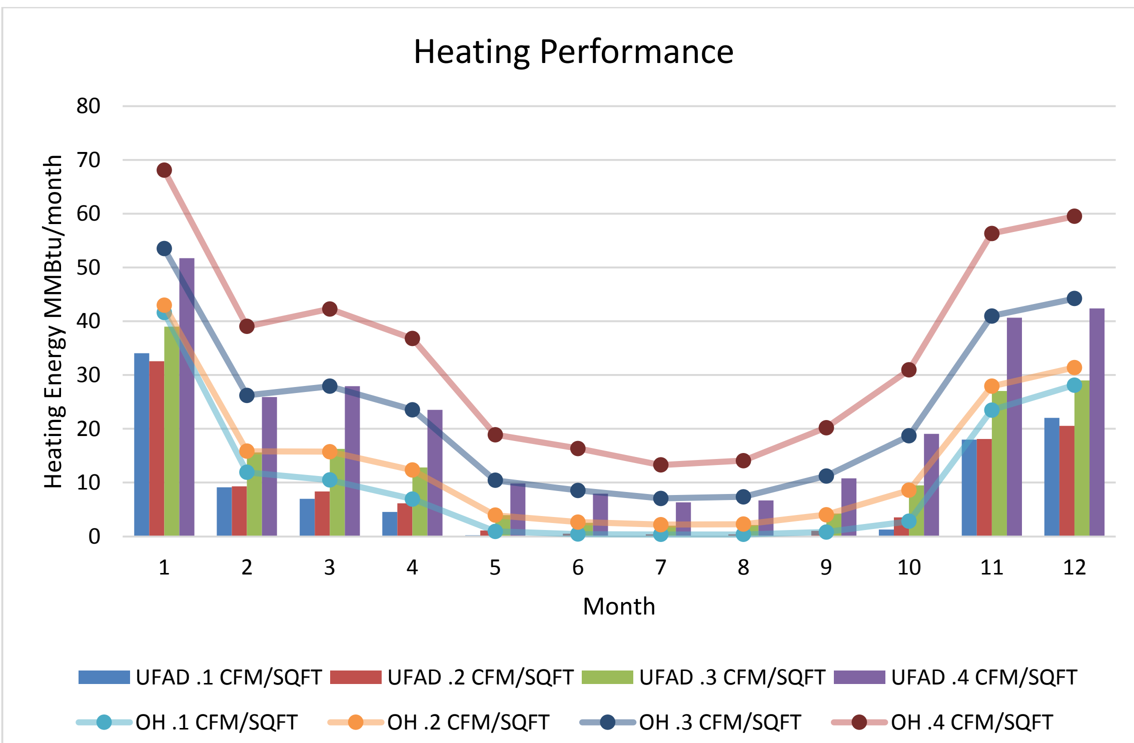

Figure 30. Heating Performance of UFAD and OH systems at different minimum flow rates

Figure 30 shows the heating energy of the UFAD and OH systems throughout the year. The UFAD system uses consistently less heating energy than the OH system. This can be explained by the higher supply temperature into the zone due to heat gain in the supply plenum. The UFAD system fundamentally requires less reheat.

Table 8 shows the heating energy consumption and the percent difference between the UFAD and OH systems. The negative sign means that UFAD uses less energy. At the low minimum flow rate (0.1 cfm/ft^2) the savings are the lowest (24.9%), due to low reheat in the OH system. For the medium minimum flow rates (0.2 cfm/ft^2 and 0.3 cfm/ft^2) the savings are the largest (40% and 41.4%). The high savings in heating energy can be explained by very little or no reheat in the UFAD system. The heating savings start to deteriorate at the highest minimum flow rate of 0.4 cfm/ft^2, because even with the supply plenum heat gain, the system now requires reheat, just like OH system. At high minimum flow rate, there is heating consumption even during the summer months.

Table 8. Heating energy difference between UFAD and OH

Flow	0.1 cfm/ft^2	0.2 cfm/ft^2	0.3 cfm/ft^2	0.4 cfm/ft^2
OH (MMBtu)	**128.**	**170**	**280**	**416**
UFAD (MMBtu)	**96**	**102**	**164**	**273**
(OH-UFAD)/OH (%)	**24.9%**	**40.0%**	**41.4%**	**34.4%**

The heating energy savings from reducing minimum flow rate in both systems are similar. The reduction of minimum flow rate from 0.4 cfm/ft^2 to 0.1 cfm/ft^2 will produce 69.1% savings in the UFAD system and 64.7% in the OH system. In this case the UFAD system will produce a higher heating energy savings percentage than the OH system, even though OH uses more heating energy.

Figure 31 shows the fan performance of UFAD and OH systems at different flow rates. The UFAD system has 2.83 in w.c. system pressure drop while the OH system has 4.28 in w.c. Both systems have the same fan efficiency of 60% and motor efficiency of 93%. Both systems also use the same coefficients for the 4th order PLR polynomial curve. The UFAD system uses less fan energy than the OH system. There is unusual observation that the UFAD system at 0.1 cfm/ft^2 minimum flow uses more fan energy than at 0.2 cfm/ft^2 from May through

August. This is due to the extra fan energy required to cool down the concrete slab and the plenums in the morning. This will be discussed later in the fan shutdown and optimization strategies.

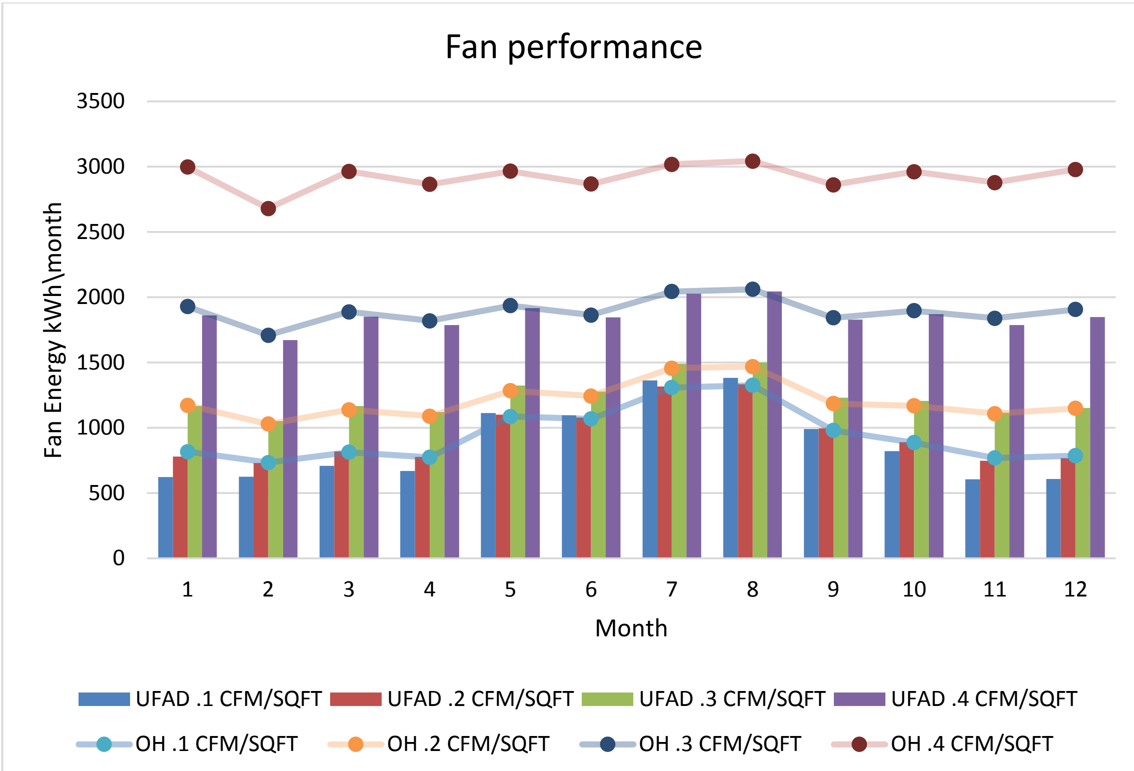

Figure 31. Fan Performance of UFAD and OH systems at different minimum flow rates

Table 9 shows fan energy in kWh/month and the percent differences between the UFAD and OH systems at different minimum flow rates. The UFAD uses less energy due to the lower pressure drop; however the higher flows that are required during the peak loads offset some of those savings.

Table 9. Fan energy difference between UFAD and OH systems

Minimum Flow Rate	0.1 cfm/ft^2	0.2 cfm/ft^2	0.3 cfm/ft^2	0.4 cfm/ft^2
OH (kWh)	11349	14495	22732	35079
UFAD (kWh)	10602	11334	14799	22335
(OH-UFAD)/OH (%)	6.6%	21.8%	34.9%	36.3%

2.3 Supply Air Temperatures

Supply air temperature models were run with no outside air in the air handling loop. This was done to avoid any energy discrepancies due to outside air humidity levels between different supply air temperatures. Both UFAD and OH models use 0.3 cfm/ft^2 minimum flow rate.

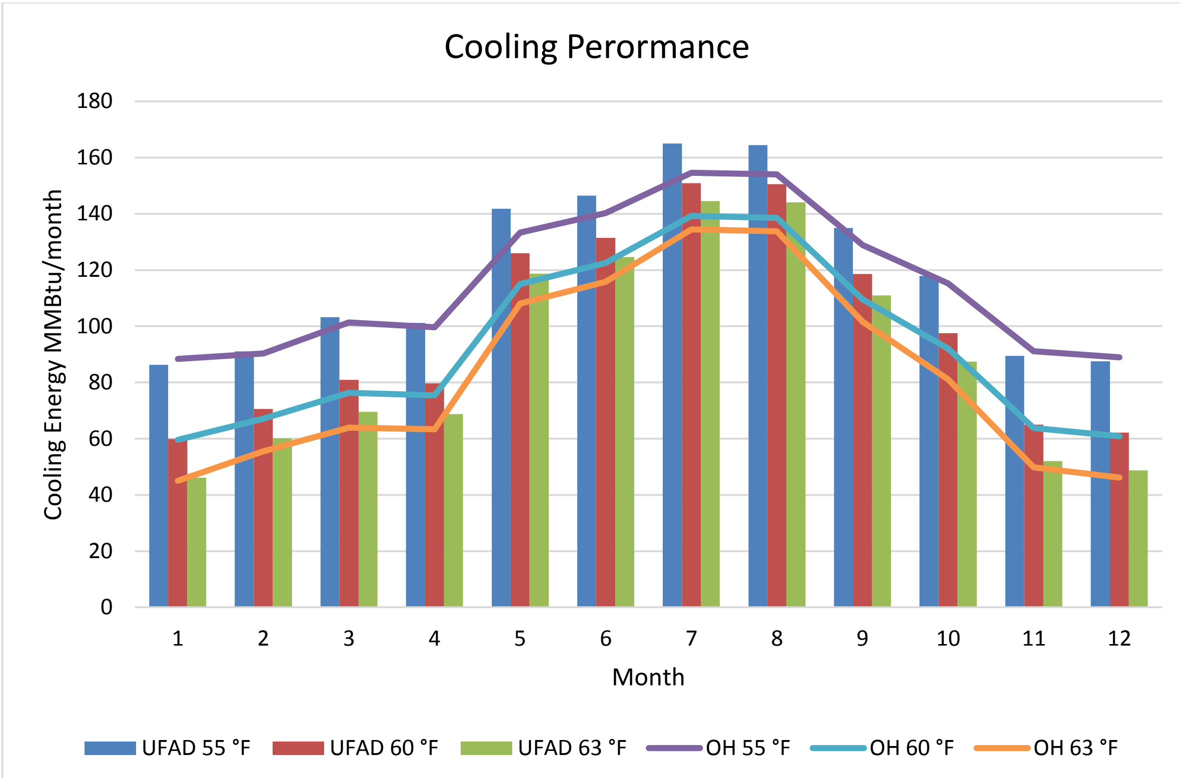

Figure 32. Cooling performance of UFAD and OH systems at different supply air temperatures.

Figure 32 shows cooling energy used by both UFAD and OH systems over the period of the year. The UFAD system consistently uses more cooling energy than the OH system. All systems use less cooling energy as the supply air temperature (SAT) increases. If there is no reheat the amount of cooling energy would be the same regardless of SAT. Increasing the SAT reduces reheat, but increases the fan energy required to move the larger volume of air to meet the same load

.

Table 10. Chilled Water Consumption at different supply air temperatures

	Chilled Water Consumption MMBtu					
	UFAD 55 °F	UFAD 60 °F	UFAD 63 °F	OH 55 °F	OH 60 °F	OH 63 °F
January	86	60	46	88	60	45
February	91	71	60	90	67	56
March	103	81	70	101	76	64
April	101	80	69	100	75	63
May	142	126	119	133	115	108
June	146	131	125	140	122	116
July	165	151	145	155	139	134
August	164	151	144	154	139	134
September	135	119	111	129	110	102
October	118	98	87	115	92	81
November	89	65	52	91	64	50
December	88	62	49	89	61	46
Total	1,429	1,193	1,076	1,386	1,120	999

Table 11. Cooling, Heating and Fan energy use of UFAD vs OH system

	Cooling	**Heating**	**Fan**
55 F SAT	3.1%	-42.2%	-34.9%
60 F SAT	6.5%	-38.7%	-29.2%
63 F SAT	7.7%	-34.2%	-25.7%

Table 10 shows the UFAD vs OH system chilled water energy use and **Table 11** shows the percent difference. The present values are calculated by subtracting the OH energy use from UFAD energy use and divided by the OH energy use. The higher the supply temperature the better the OH cooling performance is compared to UFAD. This is similar to the finding that UFAD cooling performance gets closer to the OH system at higher minimum flow rates. At higher SAT temperatures the model’s flow rate of 0.3

cfm/ft^2 gets closer to the optimal flow rate. Cooling energy savings from increasing SAT from 55 °F to 63 °F will result in 24.7% in UFAD system and 28.0% in OH system.

Figure 33 shows the heating energy use of each month throughout the year, for both UFAD and OH systems. The UFAD system requires less heating energy throughout the year than the OH system at all SATs. The advantage of the UFAD system's performance decreases as the SAT increases. Table 10 shows that the UFAD system uses 42.2% less heating energy at 55 °F and only 34.2% less heating energy at °63F.

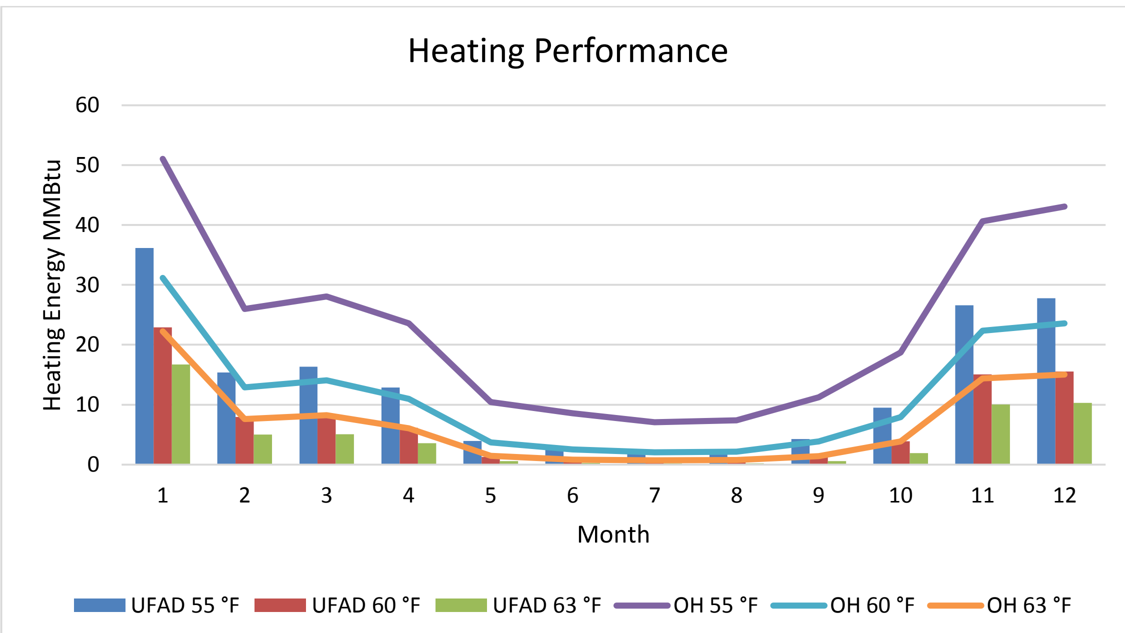

Figure 33. Heating performance of UFAD and OH systems at different supply air temperatures.

Table 12.Heating Consumption at different air supply temperatures

	Heating Consumption MMBtu					
	ufad 55 °F	ufad 60 °F	ufad 63 °F	oh 55 °F	oh 60 °F	oh 63 °F
January	36.2	22.9	16.7	51.1	31.2	22.2
February	15.4	7.9	5.0	26.0	12.9	7.6
March	16.3	8.3	5.1	28.1	14.1	8.3
April	12.9	6.1	3.5	23.6	11.0	6.1
May	4.0	1.3	0.6	10.4	3.7	1.4
June	2.6	0.7	0.2	8.6	2.5	0.8
July	2.0	0.5	0.2	7.1	2.0	0.7
August	2.1	0.6	0.2	7.4	2.1	0.7
September	4.2	1.3	0.6	11.3	3.8	1.4
October	9.5	3.9	1.9	18.7	7.9	3.9
November	26.6	15.1	10.0	40.6	22.4	14.4
December	27.7	15.5	10.3	43.1	23.6	15.0
Total	159.4	84.1	54.3	275.8	137.2	82.6

Figure 33 shows fan performance of both UFAD and OH systems. The UFAD uses less fan energy at all SATs. The profiles of fan energy use are similar between the UFAD and OH systems. From **Table 10**, the UFAD system provides the greatest fan energy savings compared to the OH system at 55 F° (-34.9%) with savings decreasing slightly with increasing SAT to 63 F (-25.7%).

Implementing the SAT reset from 55 to 60 (units) will result in 24.7% cooling energy savings, 65.9% heating energy savings, and will increase fan energy by 47.3% in the UFAD system. The same SAT reset for OH system will result in 28.0% cooling energy savings, 70% heating energy savings and will increase the fan energy use by 22.5%. The OH system benefits more from SAT optimization than the UFAD system.

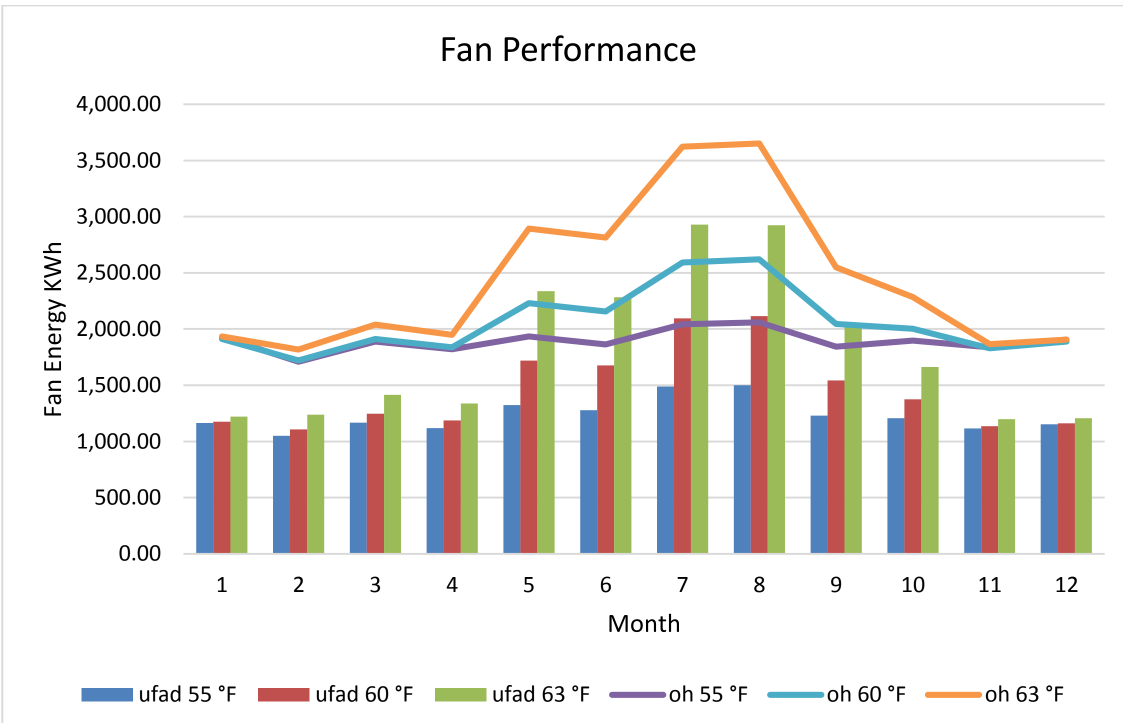

Figure 34. Fan performance of UFAD and OH systems at different supply air temperatures.

Table 13. Fan energy consumption for different supply air temperatures

	Fan energy consumption (kWh)					
	ufad 55 °F	ufad 60 °F	ufad 63 °F	oh 55 °F	oh 60 °F	oh 63 °F
January	1,165	1,175	1,222	1,928	1,912	1,934
February	1,050	1,108	1,238	1,709	1,722	1,817
March	1,167	1,246	1,415	1,888	1,912	2,040
April	1,119	1,187	1,337	1,819	1,838	1,949
May	1,325	1,719	2,338	1,936	2,232	2,893
June	1,278	1,676	2,282	1,864	2,157	2,815
July	1,490	2,095	2,929	2,043	2,592	3,624
August	1,501	2,115	2,924	2,061	2,622	3,651
September	1,230	1,542	2,042	1,843	2,045	2,550
October	1,206	1,374	1,662	1,896	2,003	2,284
November	1,114	1,135	1,197	1,839	1,829	1,866
December	1,152	1,162	1,207	1,906	1,890	1,906
Total	14,797	17,534	21,792	22,731	24,752	29,328

2.4 Outside Air

Ventilation in hot and humid climates uses a significant portion of HVAC energy. Multiple strategies can be used to mitigate the energy cost of ventilation. The most common methods for reducing ventilation includes energy recovery ventilation (ERV), economizers, and demand control ventilation. In this section the baseline OH and UFAD system models are run with different outside air ventilation strategies. The models have a 0.3 cfm/ft^2 minimum flow rate and a constant 55 °F supply air temperature set point.

Table 14. Cooling Energy performance of different outside air ventilation strategies

	UFAD		OH	
	kBtu/ft²/year	% savings	kBtu/ft²/year	% savings
NO OA	13.77	22.4%	13.93	23.2%
ERV	10.47	17.1%	10.57	17.6%
ECONOMIZER	3.94	6.4%	3.99	6.6%
ERV + ECONOMIZER	16.81	27.4%	16.92	28.1%

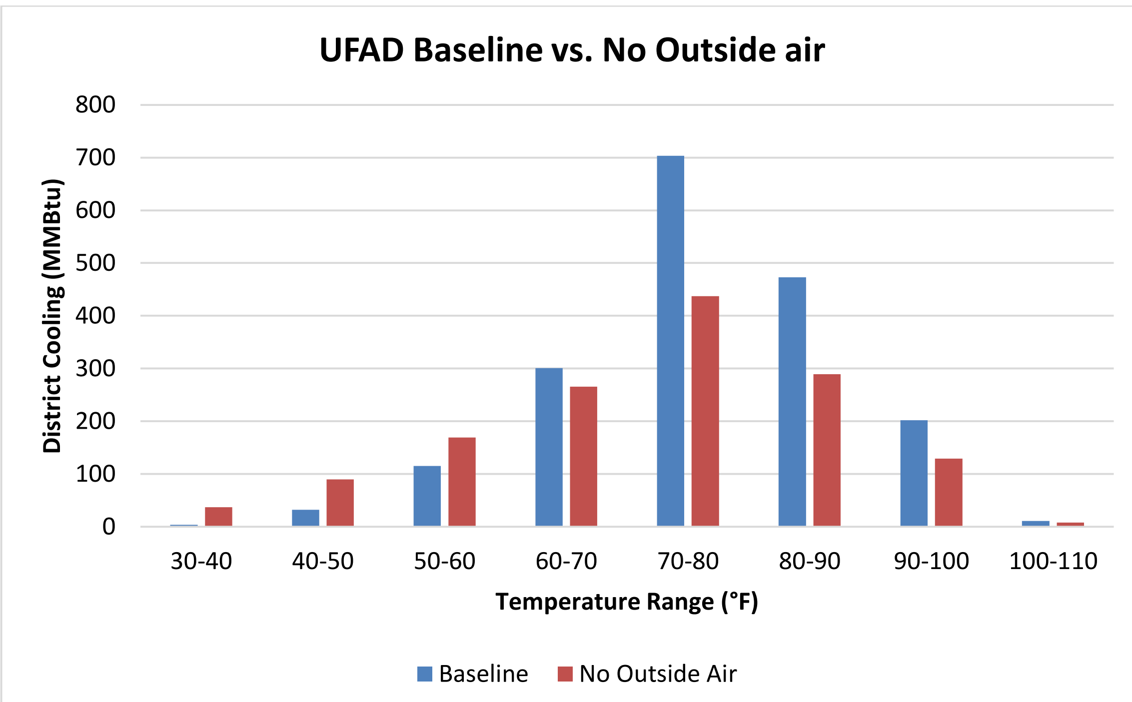

Figure 35. Chilled water consumption of UFAD Baseline and UFAD with no outside air models

Figure 35 shows the UFAD cooling consumption baseline case and a model with no outside air with binned consumption at different temperature ranges. The "no outside air" model uses 100% return air as supply air; thus no ventilation energy load is added to the energy consumption. The energy savings over the baseline model are 13.7 kBtu/ft^2/year or 22.4%. The largest savings come from the 70°F – 80°F bin range, due to the large number of hours within this temperature range. The baseline outperforms the no outside air model in all ranges below 70°F. The lower energy consumption is cause by lower mixed air temperature, which is closer to the supply air temperature set point than the return air.

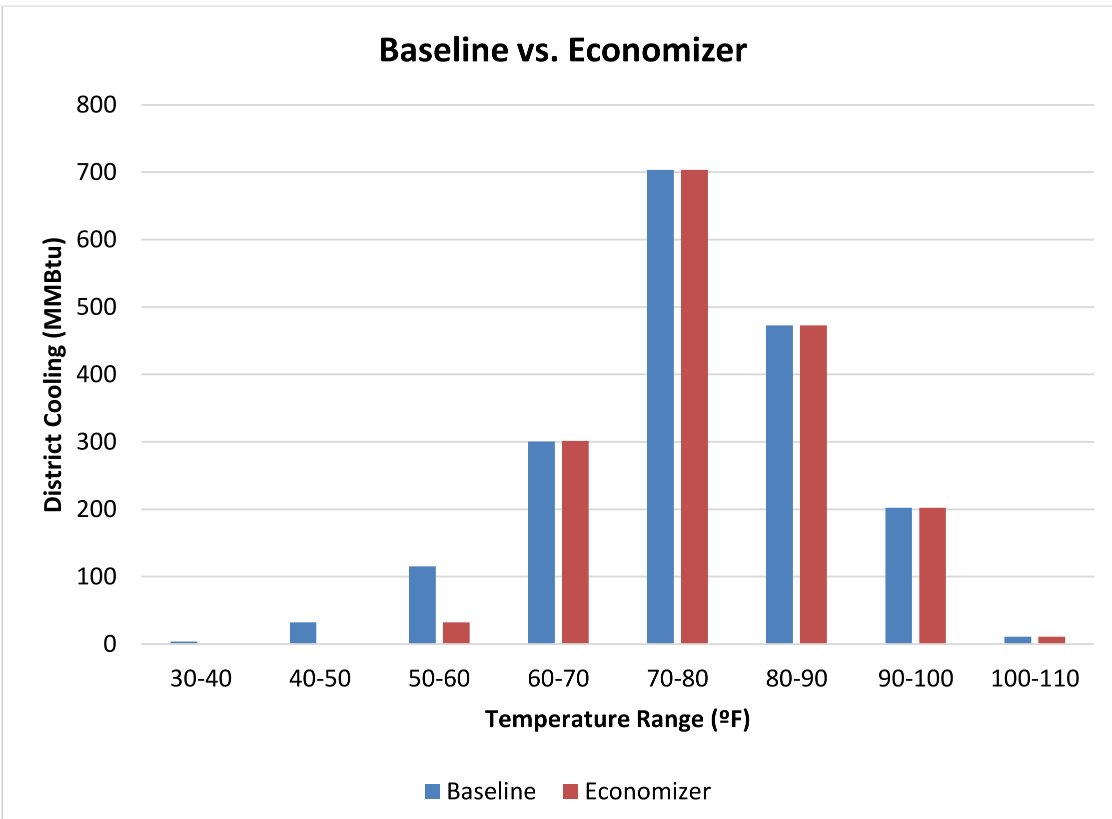

Figure 36. Baseline and Economizer chilled water consumption

Figure 36 shows chilled water consumption of the baseline and economizer models. The economizer is set to 100% outside air below 65°F and modulates to meet the supply air temperature setpoint at the lowest outside air temperatures. The economizer produces 3.94 kBtu/ft^2/year or 6.4% of savings. The economizer is producing savings only below 60°F. Any energy sensible energy that would be saved from the 60°F - 65°F range of 100% economizer operation is canceled out by extra latent load.

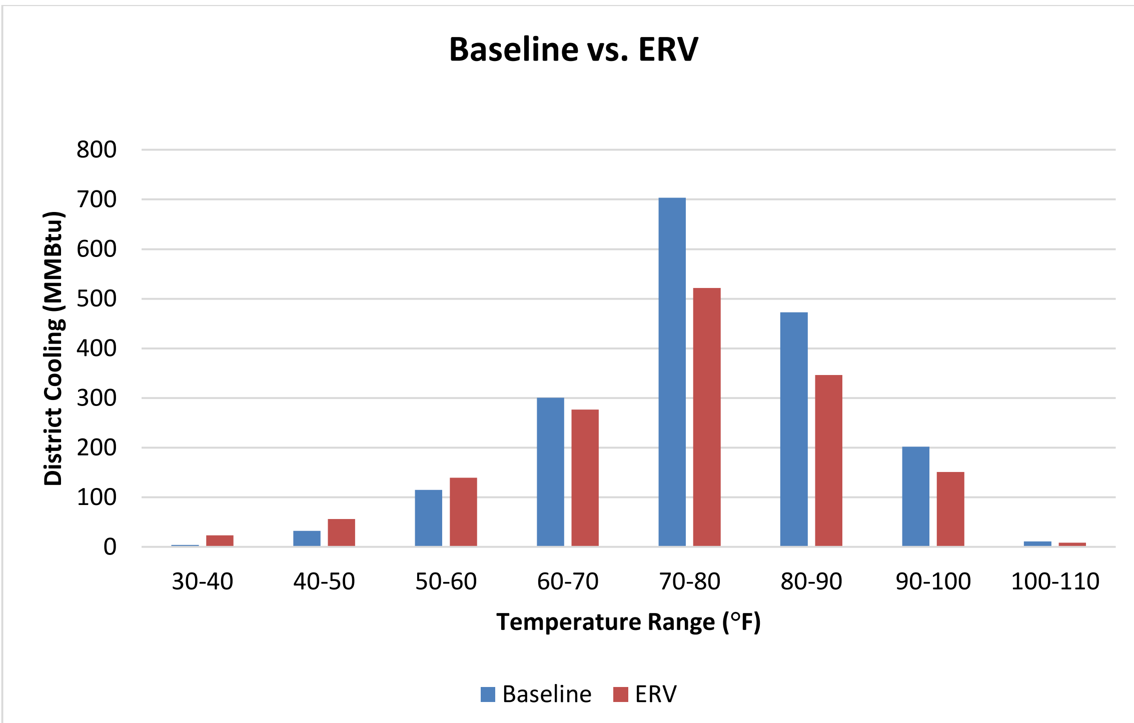

Figure 37. Baseline model and model with energy recovery ventilation district cooling consumption.

Figure 37 shows the baseline model and the model with the ERV continually running. The ERV produces savings of 10.47 kBu/ft^2/year or 17.1% over the baseline model. The ERV has savings in all temperature bins above 60 °F. The cooling energy consumption is higher for the ERV model below 60 °F. The higher energy consumption is due to not taking advantage of free cooling provided by cold outside air. This is not ideal way to operate an ERV, the ERV with economizer configuration is described further down in the thesis. If the ERV is shut down during the lower temperatures the cooling consumption will be identical to the baseline model.

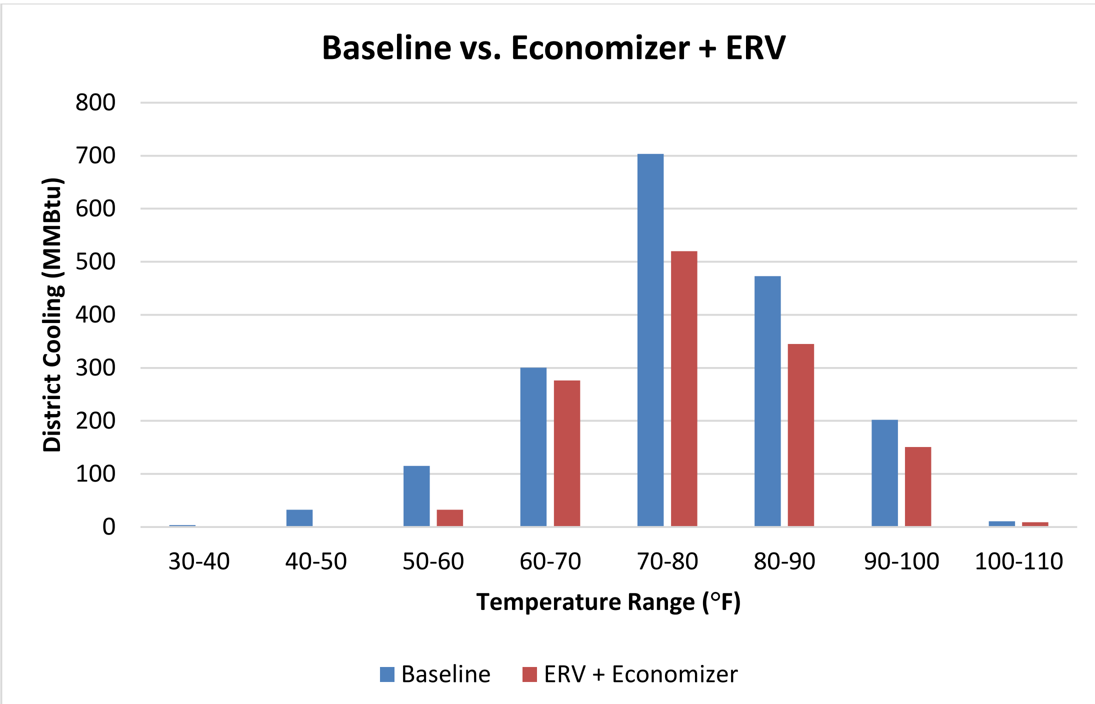

Figure 38. Baseline model and model with economizer as well as ERV district cooling consumption.

Figure 38 shows the district cooling consumption of combining the ERV with economizer compared to the baseline model. The combined model outperforms the baseline model in all temperature bins. When the energy recovery ventilation and economizer are operated such that ERV operates above 65 °F and the economizer operates below 65 °F the total energy consumption is 16.81 kBtu/ft^2/year or 27.4% lower than the baseline.

Table 15. Annual Energy consumption of different outside air ventilation strategies.

	UFAD	OH
Baseline (MMBtu)	1,842.24	1,804.01
Econ (MMBtu)	1,723.87	1,667.47
ERV (MMBtu)	1,528.06	1,486.77
ERV+Econ (MMBtu)	1,337.52	1,273.50

Having 100% return air instead of 0.11 cfm/ft^2 outside air will save 13.9 kBtu/ft^2 in OH and 13.8 kBtu/ft^2 in UFAD systems. The ventilation cost for both UFAD and OH systems is within 1% of each other. The savings are not identical because return air temperatures can be different between the two systems. The stratification inside occupied spaces increases the return temperature. Increased air return temperature, makes ventilation more efficient during cooling operation. The return heat transfer from return plenum into the supply plenum, cools the return air, counteracting the increase of temperature due to stratification. The ventilation costs being close between OH and UFAD systems implies that the combination of stratification and return plenum cooling in totality has very little to no effect on ventilation energy performance.

The economizer that was used in this simulation uses simple temperature control. The fixed dry bulb temperature was set to 65 °F; above this temperature the economizer damper supplies the minimum outside air flow rate designed by the system (0.11 cfm/ft^2). Below 65 °F the economizer is set to modulate to best meet the supply air temperature set point up to 100% outside air. This type of economizer control uses 100% outside air when the outside air temperature is between the SAT and 65, and modulates the damper for free cooling when the outside temperature is below the SAT.

Other types of economizer control include fixed enthalpy, differential dry bulb temperature and differential enthalpy. Constant enthalpy works the same way as fixed temperature, but instead of controlling to a particular dry bulb temperature, it uses the enthalpy sensor. Differential temperature compares the return dry bulb temperature to outside dry bulb temperature and will use outside air when the return temperature is higher than the outside air temperature. This type of control is not suitable for a hot and humid climate, because of outside air humidity. Differential enthalpy control is theoretically the best way to control economizer. This type of control activates the economizer when enthalpy of the return air is higher than the enthalpy of outside air. For the weather file in this simulation, enthalpy control and fixed temperature economizer control produced similar savings as with a differential enthalpy economizer. The fixed temperature economizer has an advantage of relying on one sensor as opposed to two enthalpy sensors in the differential enthalpy case and temperature sensors are generally more reliable than enthalpy sensors.

The energy recovery ventilation was simulated with 0.76 sensible effectiveness and 0.68 latent effectiveness. The use of an ERV will save 10.5 kBtu/ft^2 annually in the UFAD system and 10.6 kBtu/ft^2 in the OH system. The slight discrepancy can again be explained by the different return air temperatures of the two systems. The use of an ERV will save 76% of the ventilation energy (76.1% for UFAD and 75.9% for OH). The total effectiveness of the ERV is below 76% because the latent effectiveness of the wheel is set to be 68%. The savings are slightly higher than total effectiveness due to periods of time when the outside temperature conditions are more favorable than the return air.

Combining the economizer and the ERV is the optimal ventilation strategy, slightly outperforming the “no outside air” model simulation. To achieve such performance, the return air fraction has to be equal to the supply air fraction, otherwise the ERV performance will degrade.

2.5 Optimization Strategies

Table 16. Baseline energy cost UFAD vs OH

	UFAD-baseline	**OH-baseline**
Fans (kWh)	**14,799.28**	**22,732.44**
Pumps (kWh)	**4,355.26**	**4,563.85**
Cooling (MMBtu)	**1,842.24**	**1,804.01**
Heating (MMBtu)	**164.02**	**279.788**
Total HVAC cost ($)	**$ 32,233.08**	**$ 34,084.78**
(OH-UFAD)/OH (%)	**5.43%**	

Table 16 shows the energy and the cost at current utility rates. The campus utility rates are $0.087/kWh for electricity, $15.264 /MMBtu for chilled water, and

\$14.971 /MMBtu for heating hot water. In the baseline case the fan energy savings and the heating hot water savings outweigh the extra cooling consumption cost of UFAD system. The total cost savings of using the UFAD system over the overhead system operated with 55°F supply air temperature and 0.3 cfm/ft^2 minimum flow rate is 5.43%. The optimized model reduced the minimum flow rate to 0.1 cfm/ft^2, with the supply air temperature increased to 60°F. The optimized model also has an ERV and economizer installed as well as air handler shutdown from 12am – 6am.

Table 17. Optimized model energy cost of UFAD vs OH

	UFAD	**OH**
Fans (kWh)	**14278.782**	**9742.726**
Pumps (kWh)	**1739.904**	**1921.759**
Cooling (MMBtu)	**963.515**	**844.905**
Heating (MMBtu)	**32.539**	**62.393**
Total HVAC cost (\$)	**\$ 16,586.10**	**\$ 14,842.16**
(OH-UFAD)/OH (%)	**-11.75%**	

Flow rate decrease and supply air temperature reset, eliminated most of the reheat inside the overhead model. UFAD system still has the plenum heat entering the supply plenum requiring higher flow rates reducing the times that the system can operate at minimum flow rate. The extra energy cost of operating the UFAD system is 11.75%.

CHAPTER III FIELD MEASURMENTS

3.1 Error Analysis

Field measurements are needed to establish stratification, plenum temperature, and air handler operation within the offices inside the building. In order to measure stratification the temperature loggers were placed at 0.5 ft, 1 ft, 2 ft, 3 ft, 4 ft, 5 ft, 6 ft, 7 ft, 8 ft, 9 ft, 10 ft, and 11 ft above the floor and at the return from the room. The loggers were set to record temperature at 5 minute intervals. The measurements were made from September 27th to October 9th. The loggers were set to start recording at a synchronized time. In order to establish the error of temperature readings, the loggers were first placed inside a closed table drawer and were set to measure temperature over 4 days.

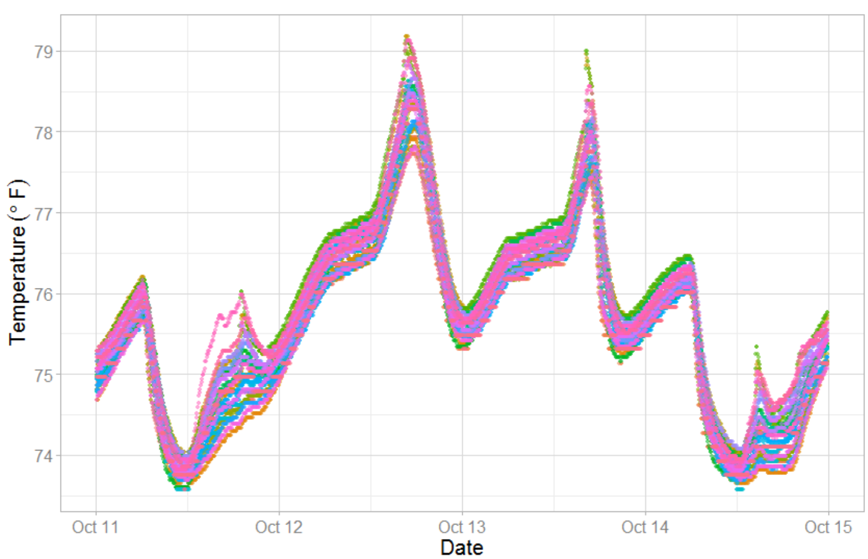

Figure 39.Calibration temperature data

Figure 39 shows the data from the temperature logger was synchronized with respect to time and temperature readings were interpolated when needed. This plot shows that the measured temperatures are close, within 0.5 °F at some times and around 1.5 °F during temperature changes.

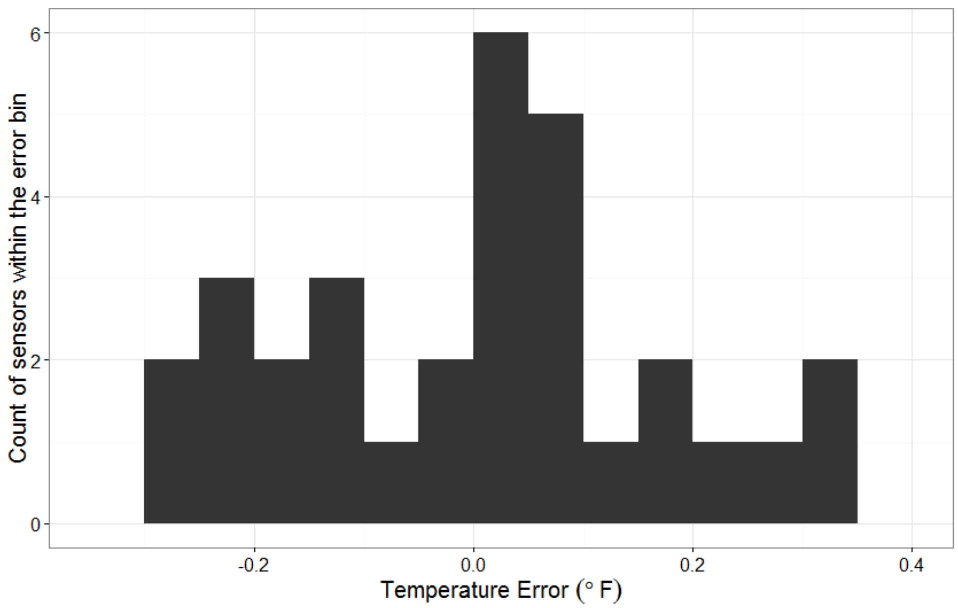

Figure 40. Calibration Error

To adjust for any calibration error of temperature loggers, first each logger's mean temperature was calculated throughout the whole measurement period. The average of all temperature readings then was considered as the accurate temperature. The calibration error was calculated by subtracting the mean of all temperature readings from the mean of each temperature logger readings. Figure 40 shows the histogram of the calibration errors for all the loggers.

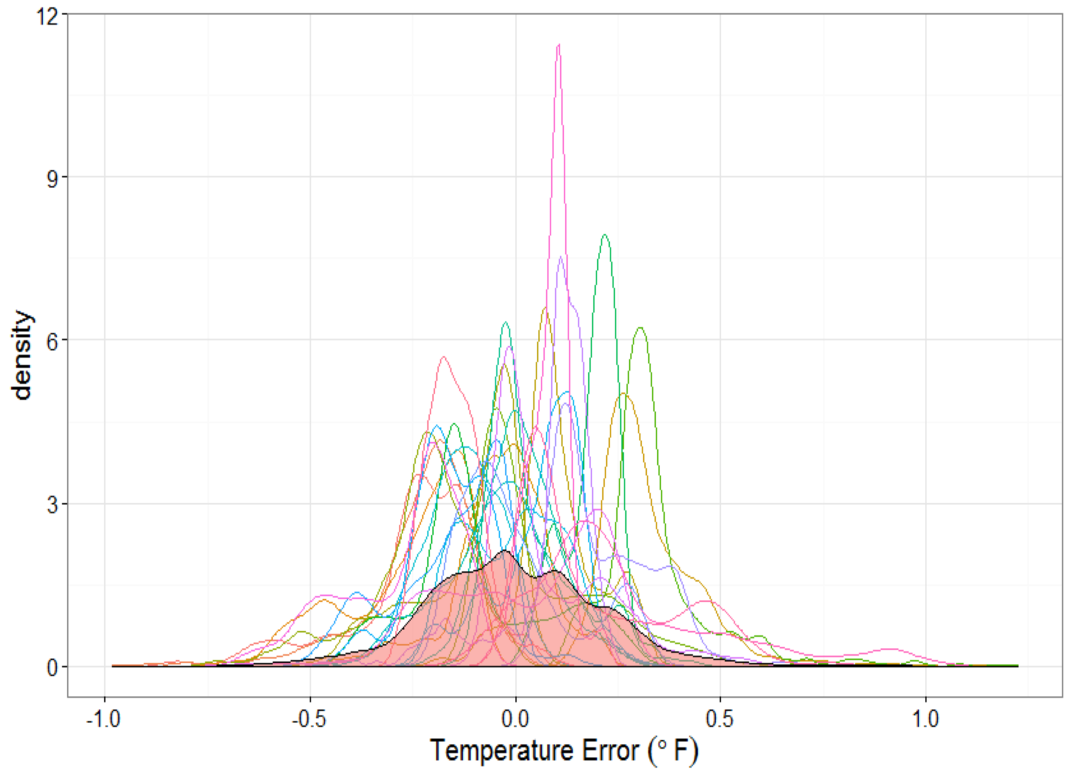

Figure 41. Sensor error individual sensor and combined probability density distributions.

Figure 41 shows the sensor error probability densities. The lines represent the individual sensor errors while the semi-transparent area represents the combined error density. A density curve integrated over x will have a value of 1. To get this plot the 31 sensors were averaged at each point in time. The error was then calculated by subtracting the measured value from the mean temperature. Each density line takes into account 1151 observations that were recorded during the calibration period. The total density curve represented by the semi-transparent area takes into account all 35681 observations from 31 sensors. The un-calibrated error distribution has a median of -.01 °F, 5% quantile of -0.34, and 95% quantile of 0.34 °F.

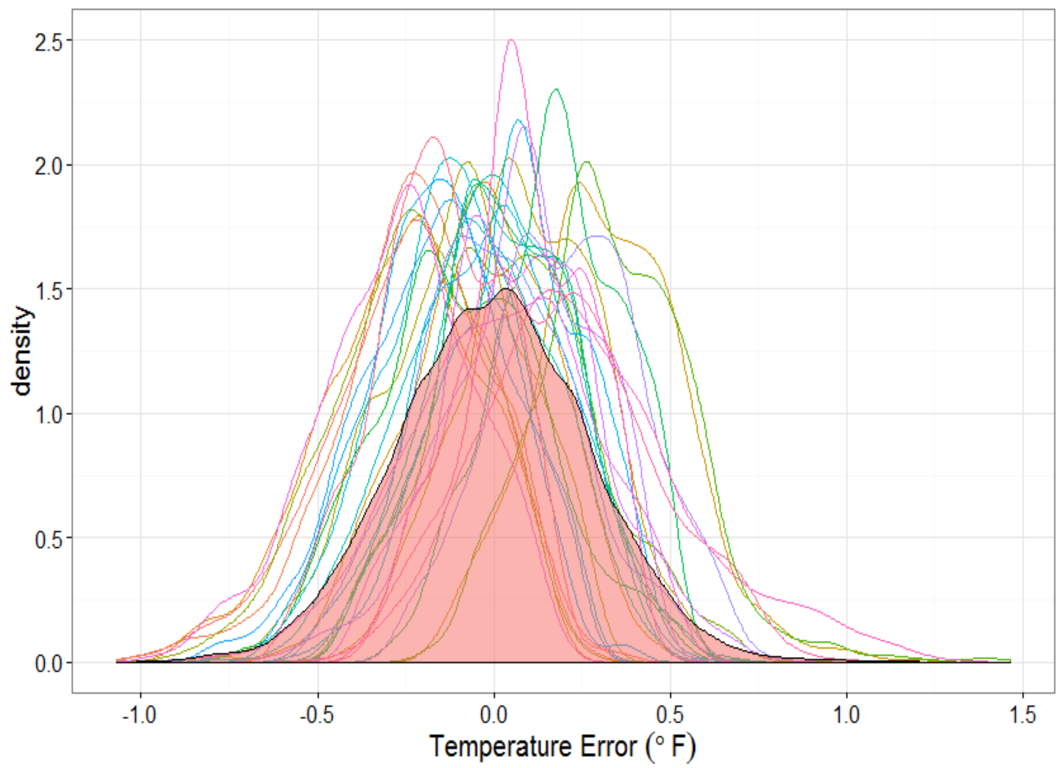

Figure 42. Calibrated error individual sensor and combined probability density distributions.

Figure 42 shows the error after calibrating the sensor data by subtracting the average deviation (error) for each sensor from the mean. To clarify, the averaging was done for each sensor through 1151 to come up with a single value that was then subtracted from the combined average of 35681 observations from 31 sensors. This new calibrated data represents the measured data minus the sensor error. This means that the average for each sensor is now identical to the average of all sensors.

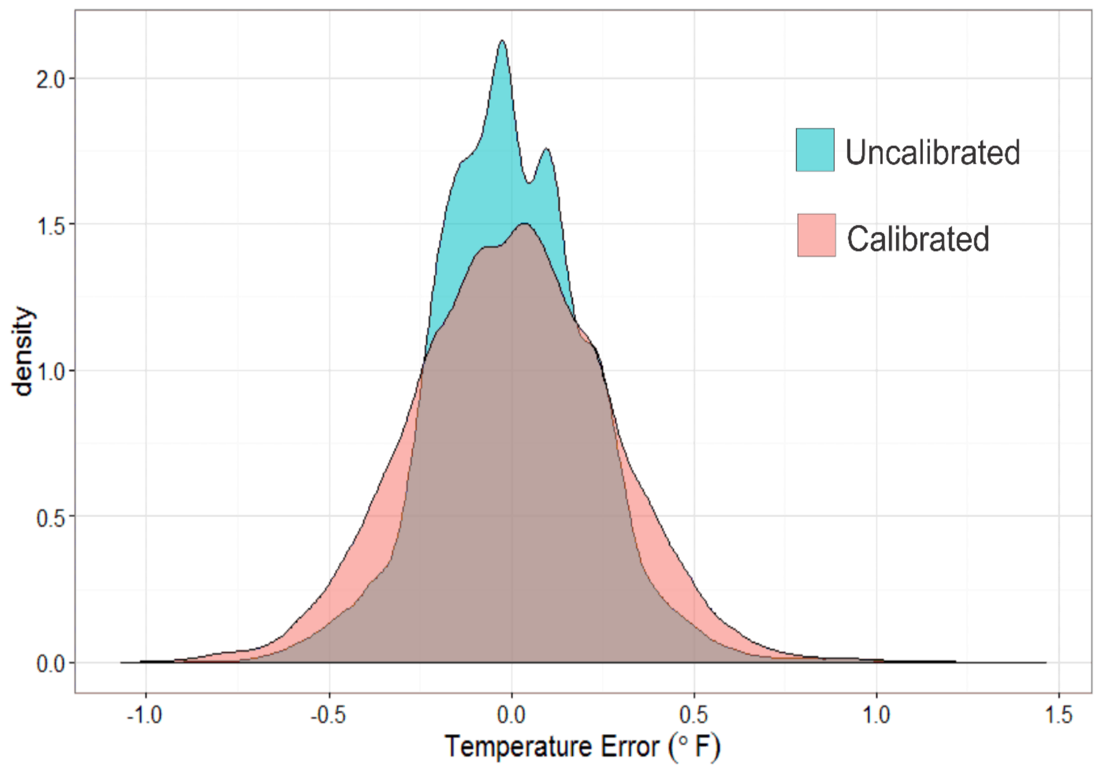

Figure 43. Error probability densities for calibrated and uncalibrated data sets

Figure 43 shows the probability densities before and after the calibration described above. The probability distribution after the calibration became wider increasing the error. Calibrated distribution's 5% and 95% quantiles are -0.45 °F and 0.45 °F and the median is 0.001 °F. Calibrating the sensors moved the median from 0.01 °F to 0.001 °F while widening the rest of the distribution.

Looking at **Figure 39** which shows that temperature data from the loggers it can be seen that temperature sensors seems to deviate ¾ into the day or around 18:00. The reason for the higher deviation at this time has to do with the calibration procedure rather than sensor error itself. The most likely scenario is that the air conditioning was off during that time, and the table drawer was unevenly heated due to occupants of the office creating a slightly uneven temperature distribution within the drawer. The calibration procedure was not implemented. The total error from table calibration procedure is slightly inflated, however still valid. The 5% and 95% quantiles for the 12 loggers that are used to measure stratification in room 411 are (-0.29 °F, 0.32 °F) and (0.35 °F, 0.39 °F) in room 423.

3.2 Stratification Measurements

The stratification measurements were made starting on Friday September 27th 2013 and the loggers were removed from the building at 8 am on October 9th 2013. Throughout the measurement period the data was captured through 7 week days and 4 weekend days. **Table 18** shows the average and maximum outside air temperatures recorded during the stratification measurement period. The temperature logger that was used to record temperatures was placed in the outside air duct of the air handler serving the building. The office relative location is shown on **Figure 51**.

Table 18. Week day and outside air temperature summaries for stratification measurement period.

Date(year:2013)	Day of the week	Outside Air Average Temperature	Outside Air Maximum Temperature
27-Sep	Friday	86.6	88.5
28-Sep	Saturday	81.1	90.8
29-Sep	Sunday	74.2	76.8
30-Sep	Monday	76.8	85.2
1-Oct	Tuesday	80.5	87.8
2-Oct	Wednesday	78.3	83.2
3-Oct	Thursday	79.3	86.9
4-Oct	Friday	81.0	87.8
5-Oct	Saturday	80.4	87.8
6-Oct	Sunday	68.1	77.3
7-Oct	Monday	70.9	79.3
8-Oct	Tuesday	72.6	79.8
9-Oct	Wednesday	70.2	78.1

The stratification is created by the plumes generated by occupants and equipment. The stratification is reduced with high cold air flow rates. This means that the stratification is higher when the occupant and equipment load is high relative to the envelope load. The stratification is lower when the envelope load dominates in times of low occupancy or extremely hot weather.

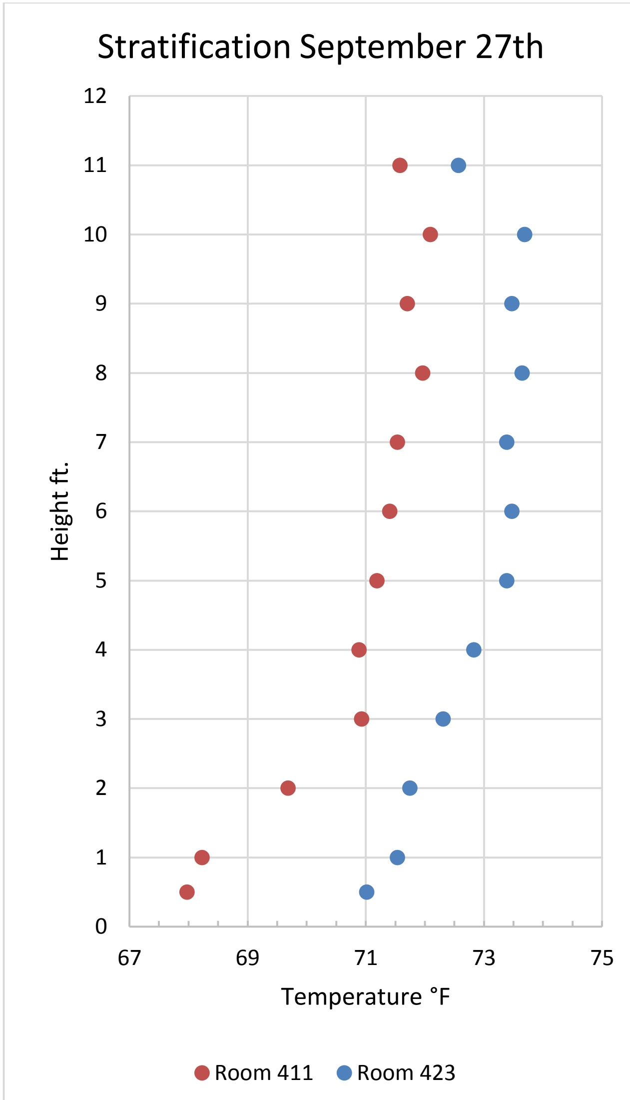

Figure 44. Stratification on Friday September 27th

Figure 44 shows the temperature recorded by the loggers as the x-axis and the height of logger location as the y-axis. The outside temperature recorded during this period is 86 °F. This profile was taken at 12:05pm on Friday. The stratification within the occupied region (in this case defined as the first 6 feet) is 3.4 °F in room 411 and

2.5°F in room 423. The total stratification defined as the difference between the temperature at 10 feet and 0.5 feet is 4.1 °F in room 411 and 2.7°F in room 423.

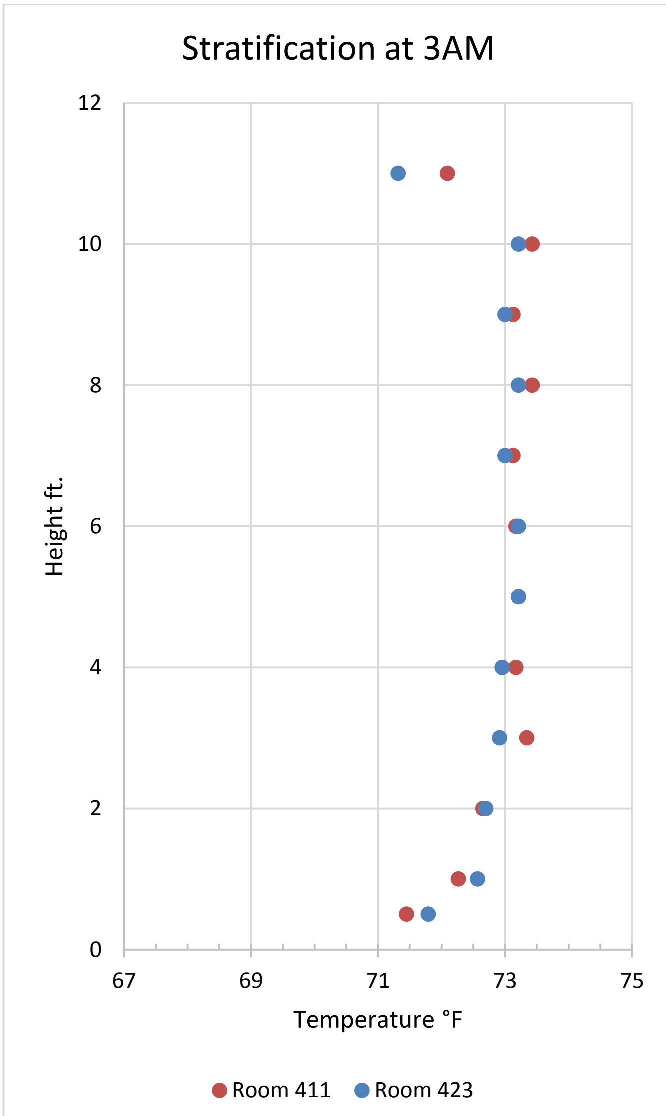

Figure 45. Room stratification during shutdown

Figure 45 shows the stratification at 3 am in the morning. The HVAC system has shut down at 12 am, and the stratification only exists due to cooling from the raised floor and the slab on top. From 2 feet to 10 feet the temperature is 73 °F. The total and occupied stratification is the same in this case and equal to 2°F in room 411 and 1.4°F in room 423.

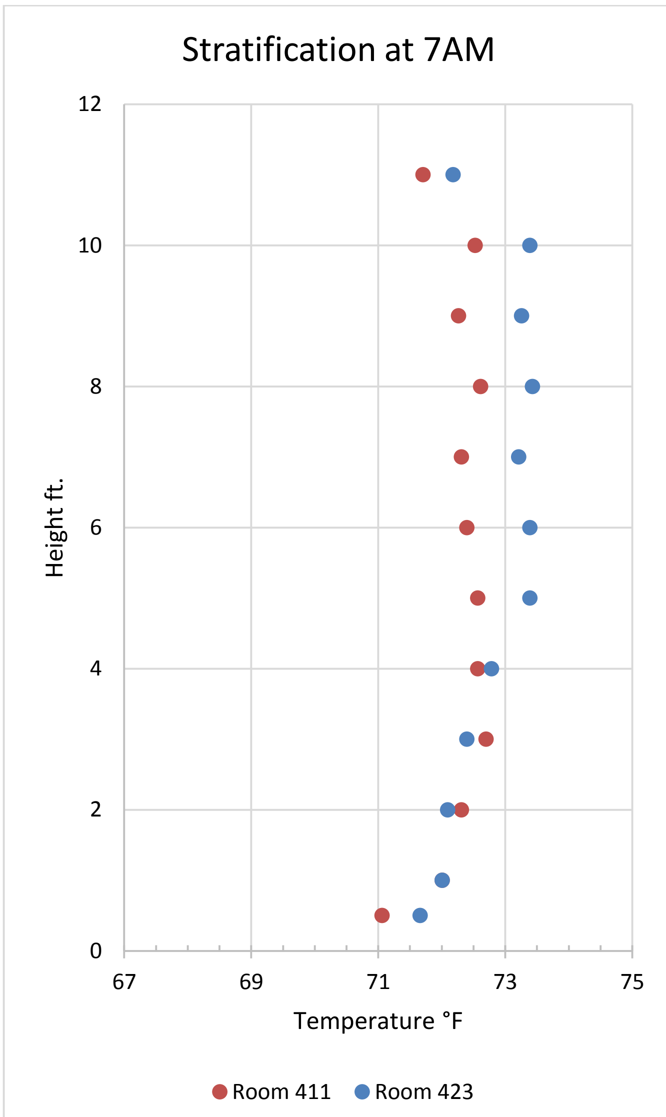

Figure 46. Low occupancy stratification at 7am.

Figure 46 shows the stratification early in the morning at 7 am on September 28th. The stratification is 1.5°F in room 411 and 1.7°F in room 423. The stratification in the morning is lower than that at 12 pm shown in Figure 44. In this case, since the office is not occupied, the temperature should be allowed to drift closer to the 75 °F set point. The temperature at 4 ft. which is the thermostat height is 72.7 °F implying that the air supplied to the room is at the minimum. This minimum flow rate is too high because the temperature near the thermostat is not allowed to go to its upper set point, and it is also evident due to low stratification within the room.

In order to represent the stratification using this large dataset, a box whisker plot was used for each data logger. The box plot sides represent the first and third quartiles and the band in the middle represents the median, while the whiskers represent the extremes, ignoring the outliers. The outliers in this case defined by being outside of the "whiskers" of the boxplot or 1.5 times the interquartile range above the upper quartile or below the lower quartile. The mean is also plotted as the white circle inside the box plot for each height.

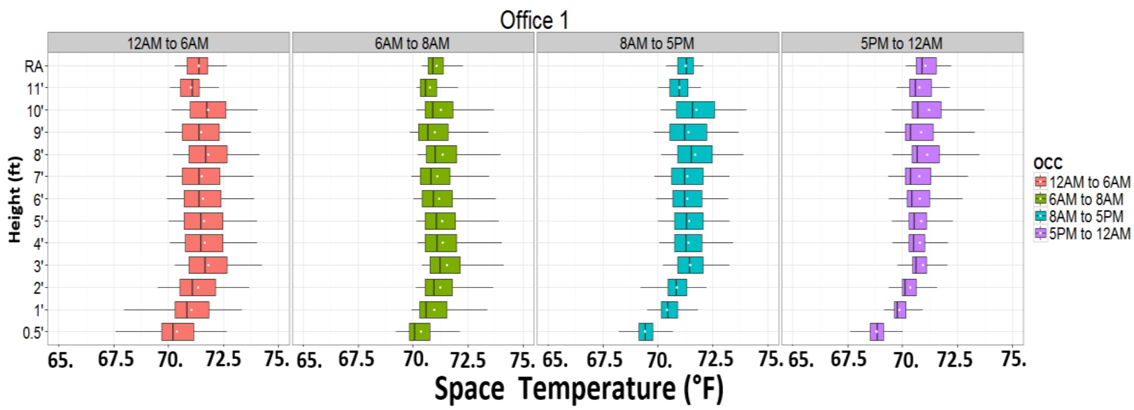

Figure 47. Office 1 (Rm # 423) vertical stratification temperature at different times of day (Zhao 2014)

In **Figure 47**, the stratification in office 1 is displayed at different times of the day. There is an air handler shut down during the first period (12am - 6am). The system should come to set point during the 6am - 8am period. The periods 8am - 5pm and 5pm - 12am are both occupied with more occupancy during the 8am - 5pm period. The solar and envelope gains are higher during the 8am - 5pm period.

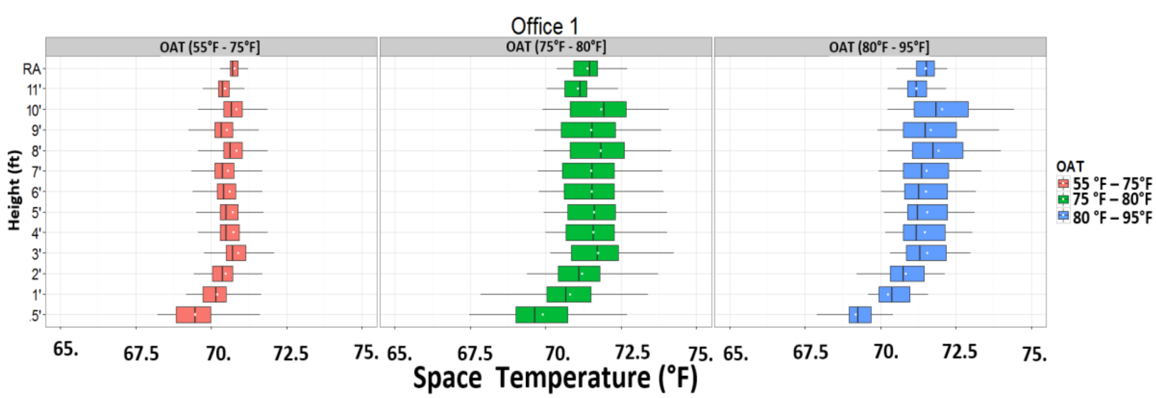

Figure 48. Office 1 (Rm # 423) temperature stratification for different outside air temperatures (Zhao 2014)

In **Figure 48** the office 1 stratification is displayed for different outside air temperature ranges. Higher temperatures correlate to higher envelope load, as well as solar load. The temperature data from office 1 suggest that the temperatures within the occupied zone range from a minimum of 67.5 °F, to a maximum of 74°F throughout the measured period. The minimum temperature occurs at the lowest level near the supply plenum. The temperature is maximum at the 10 foot level, or 1 foot below the acoustic tile. The temperature on top of the acoustic tile is consistently cooler than the temperature at the 10 foot level, in all graphs. The average stratification during the occupied periods is 1.5°F. The average stratification in this case is defined by subtracting the average temperature at 0.5 ft. from the average temperature at 10'.

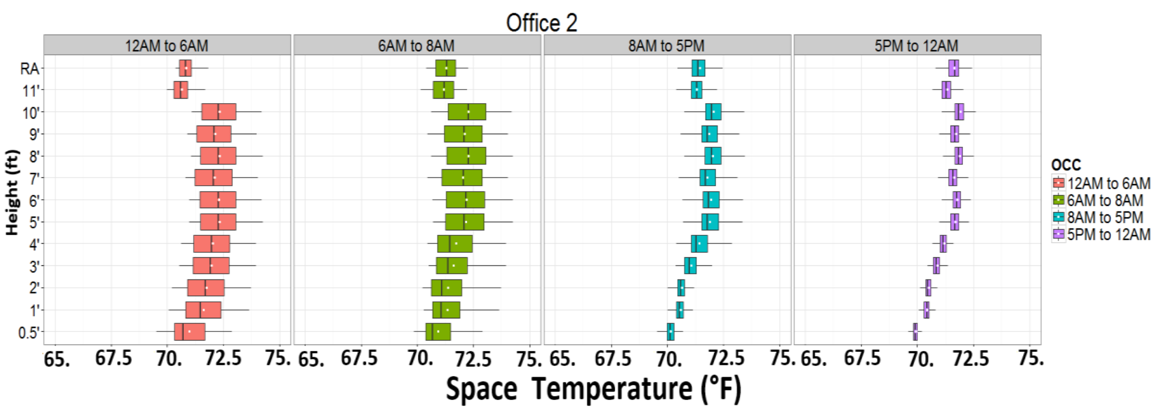

Figure 49. Office 2 (Rm # 411) vertical stratification temperature at different times of day (Zhao 2014)

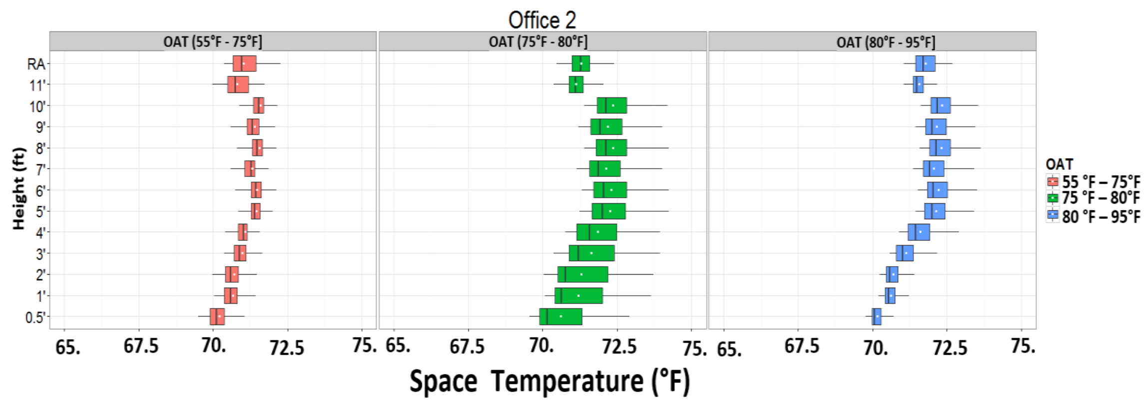

Figure 50. Office 2 (Rm # 411) vertical temperature stratification for different outside air temperatures (Zhao 2014)

The office 2 measurements are very similar to the measurements in the first office **Figure 49** and **Figure 50**. The maximum temperature is at 10ft. The average stratification during the occupied periods is 1.8 °F. The temperature of the return air is again cooler than the temperature at 10ft. The data during the occupied period in office 2 is much less spread out than in the first office. The much skinnier box and whisker plots represent very constant temperatures throughout the occupied periods.

Figure 47 and Figure 48 indicate there is very little stratification within the occupied spaces, since the average temperature in the occupied zone (the first 6 feet) and the upper mixed air zone (from 6 feet to 11 feet) differ by only 0°F to 1.0 °F on average.

The temperature loggers were also placed inside the underfloor diffusers. The temperature readings can show plenum thermal decay, as well as any reheat that occurs inside the system. Figure 8 shows the locations of the loggers that were placed during the study. Figures 9 and 10 show the recorded temperature time series, as well as outside air temperature. The supply air temperature during this period was 55°F.

In office 1 the average temperature leaving the supply plenum is 65°F or 10°F temperature gain compared to the discharge air temperature. The average temperature leaving the supply plenum in the second office is closer to 67.5°F or 12.5°F temperature gain compared to the discharge air temperature.

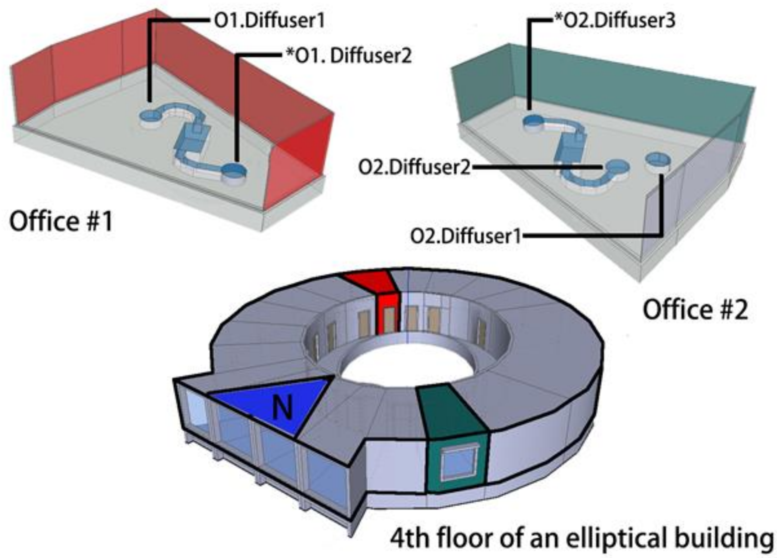

Figure 51. Location of diffuser temperature data loggers in the Mitchell Physics Building.

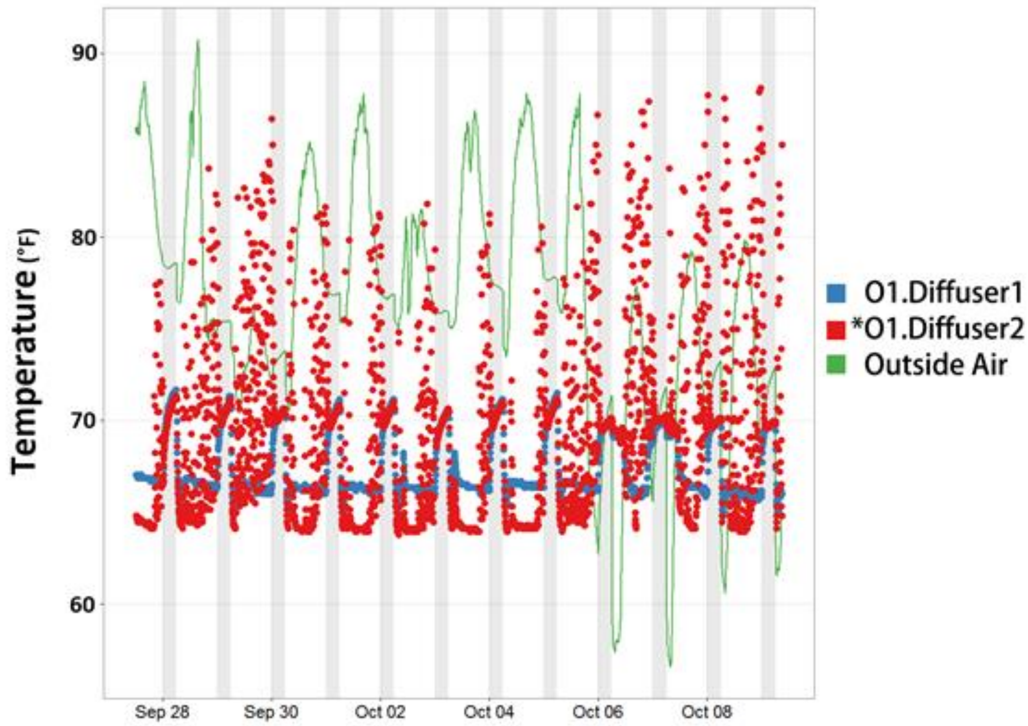

Figure 52. Office 1(Rm #423) diffuser temperatures

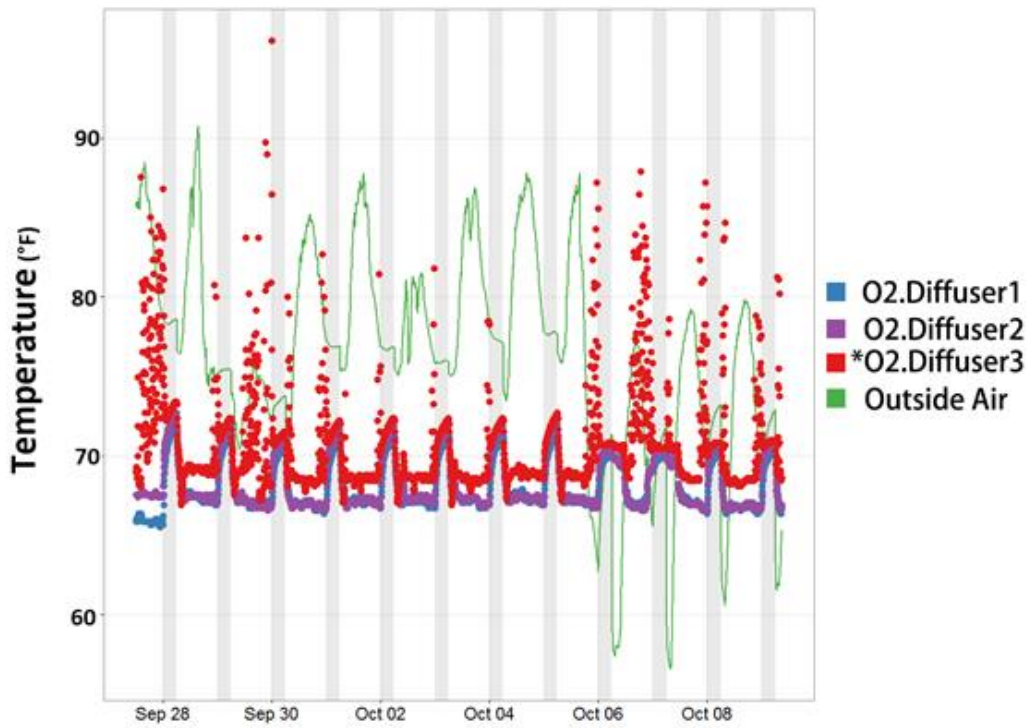

Figure 53. Office 2 (Rm #411) diffuser temperatures

CHAPTER IV AHU SYSTEM ANALYSIS

5.1 UFAD System

The UFAD systems monitored have electrical reheat, which is not sub metered. The UFAD systems are the only systems with electrical reheat, since the rest of the boxes use heating hot water. By looking at the electrical consumption correlation with outside air temperature it is possible to demonstrate that reheat is used. **Figure 54** below shows the charts that represent all available electric metered data from the beginning of the building operation. All the data found to be erroneous by the data quality group was deleted. The data year 2013 only includes data through July 31. Each year of operation is graphed separately. The weekends and the weekdays are separated by different colors. The data is then divided into different temperature groups: below 60°F, 60°F to 75°F, 75F to 80°F and above 80°F. A linear regression model was fit through each of the temperature groups for both weekdays and weekends.

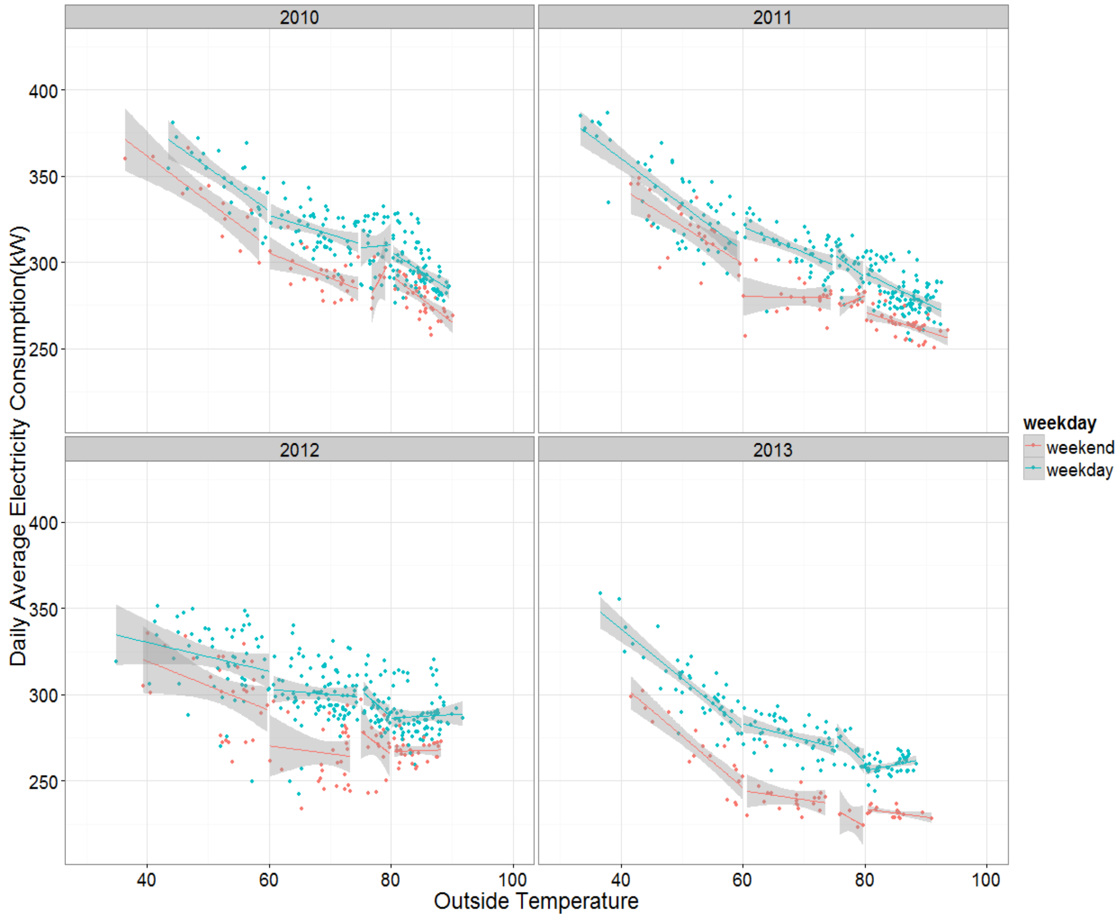

Figure 54. Electrical consumption vs. OAT correlation for Mitchell Physics Building

Looking at **Figure 54**, it is clear that the electric use has a negative slope as a function of temperature for most of the times when the temperatures are above 60°F when there should be no need for heating, suggesting that reheat is being used. This is particularly clear in the weekday data for 75°F to 80°F for all except the 2010 data.

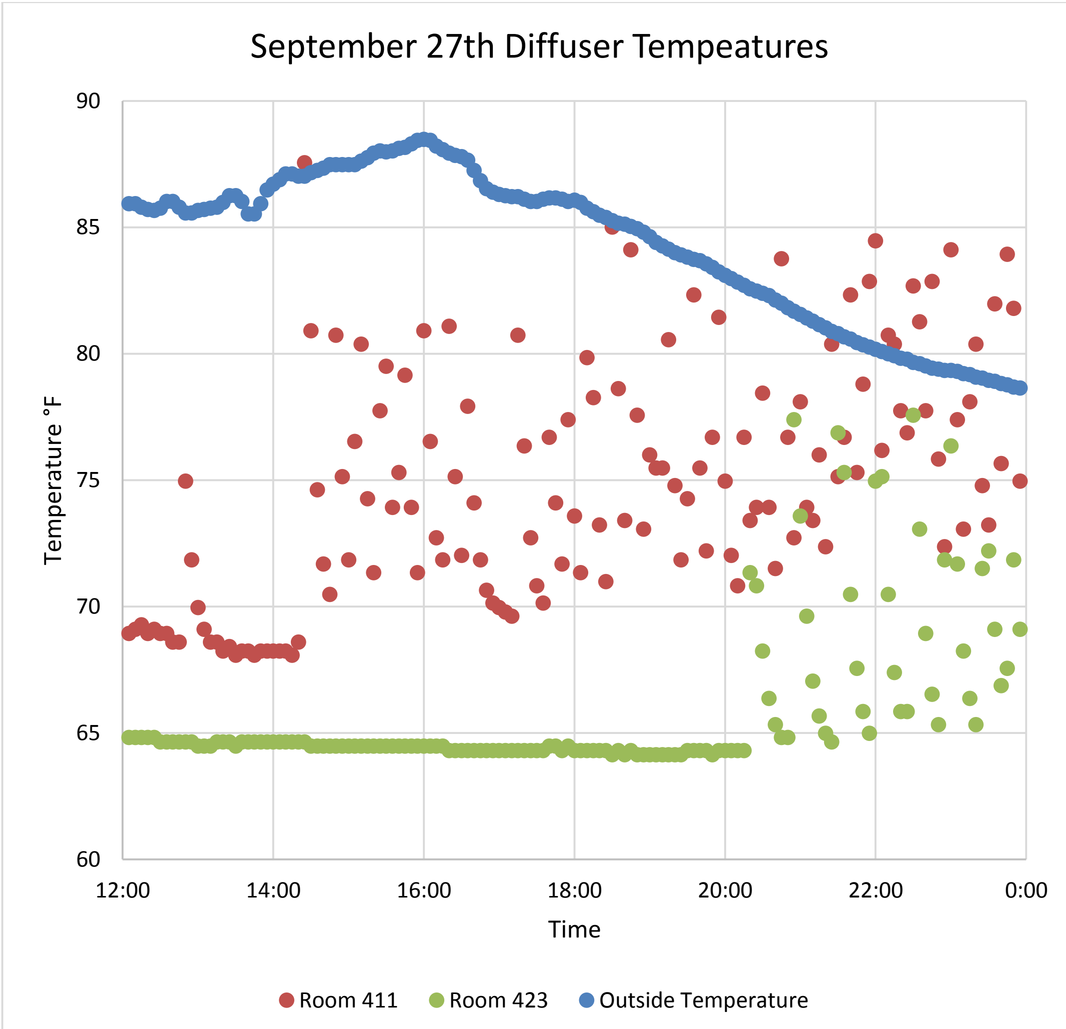

Figure 55. Diffuser temperature for September 27th.

Figure 52 and Figure 53 show the temperatures measured below each of the underfloor diffusers. Both figures show that the building is in reheat operation at least some of the time because supply temperatures are well above room temperatures. Figure 55 shows only the reheat diffusers for both offices on September 27th. The UFAD unit in room 411 switched to heating operation starting at around 2:30 pm while the UFAD unit in room 423 switched to heating operation at 10 pm.

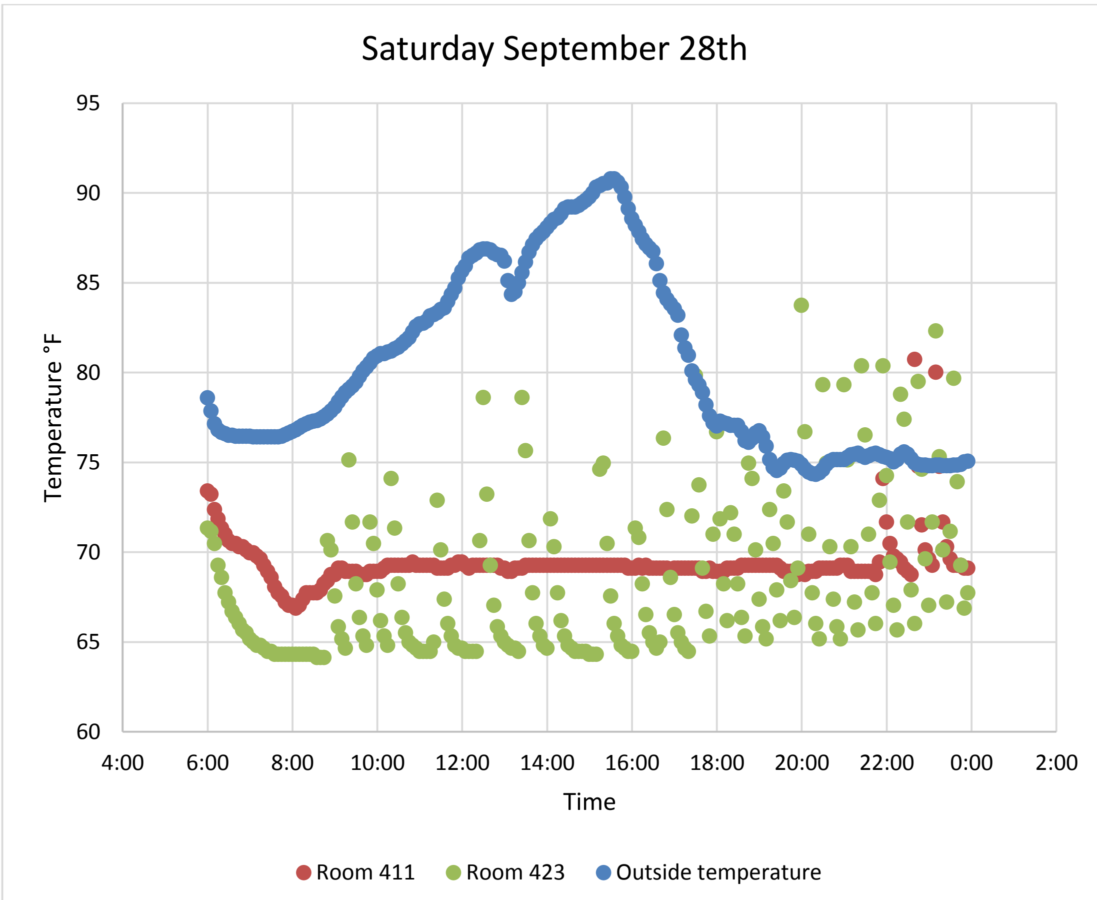

Figure 56. Diffuser temperature on Saturday September 28th

Figure 56 shows diffuser temperatures on Saturday. Office 423 has reheat, and the outside temperature is between 76°F and 90°F. Office 423 most likely was unoccupied during this day. Instead of lowering the flow rate, the system went into heating operation. This can only happen if the system operating at minimum flow rate delivers more cooling than the load inside the zone. As the outside temperature went down after 4 pm to near 75 °F at 6 pm, the supply temperature in room 423 increased. The reheat in room 411 didn't startuntil 10pm, and the amount of time spent in reheat mode is less. One of the reasons for this is the supply temperature in cooling mode is around °4 F higher. The higher supply temperature could be caused by plenum geometry, as well as the direction of air as it enters the plenum from the air handler.

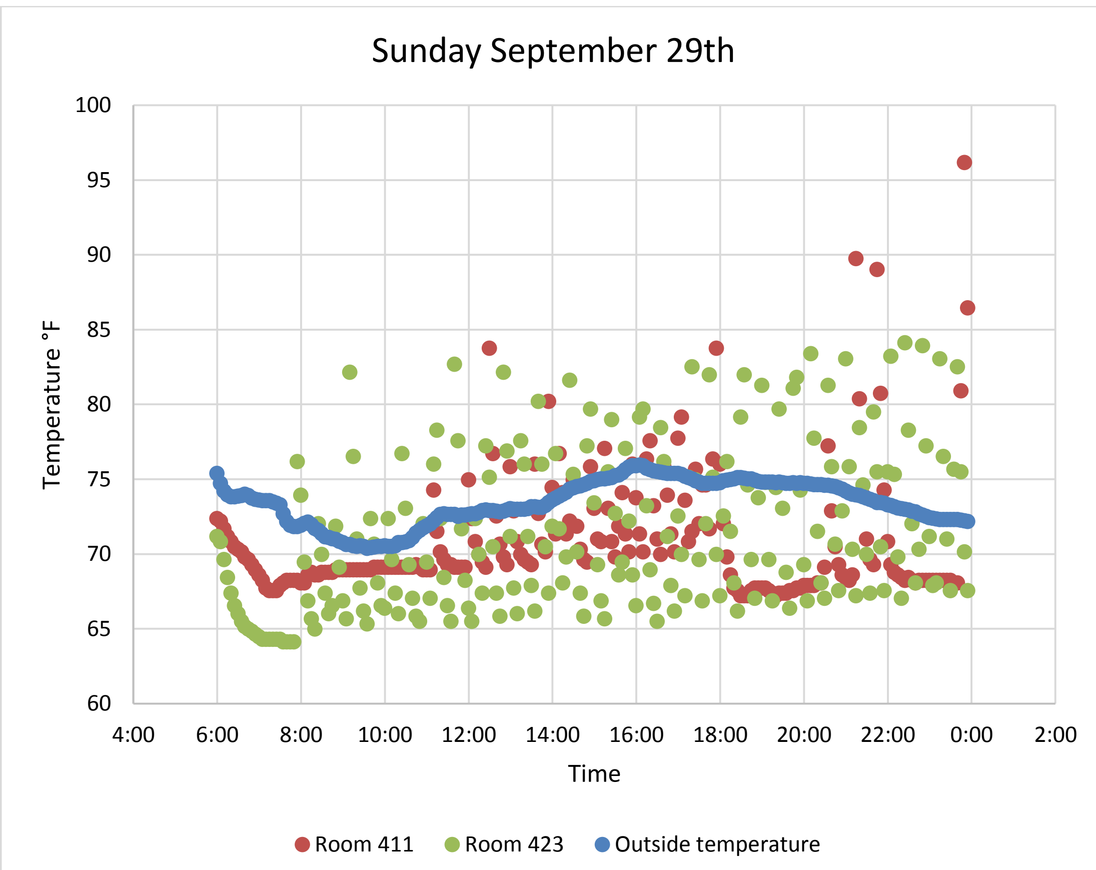

Figure 57. Diffuser temperatures on Sunday September 29th.

Figure 57 shows the diffuser temperature on Sunday September 29th. The weather was colder during this day ranging between 70 and 75. Room 423, is in reheat mode throughout most of the day. The pattern of the heating mode seems to follow the inverse of the occupancy with it turning on when the room is likely unoccupied. To further demonstrate the point Figure 58 shows the diffuser temperature on the week day. The heating mode in room 411 activates from 6am to 8 am and from 9pm until the end of the day.

The plenum decay in room 411 is slightly higher represented by the higher supply temperature measured at diffuser level (68 °F in room 411 and 64 °F in room 423). The outside temperature is also lower during the reheat period; however the reheat is likely caused by the low occupancy because it occurs on the weekends even when the outside temperature is in the 75 °F to 85 °F range.

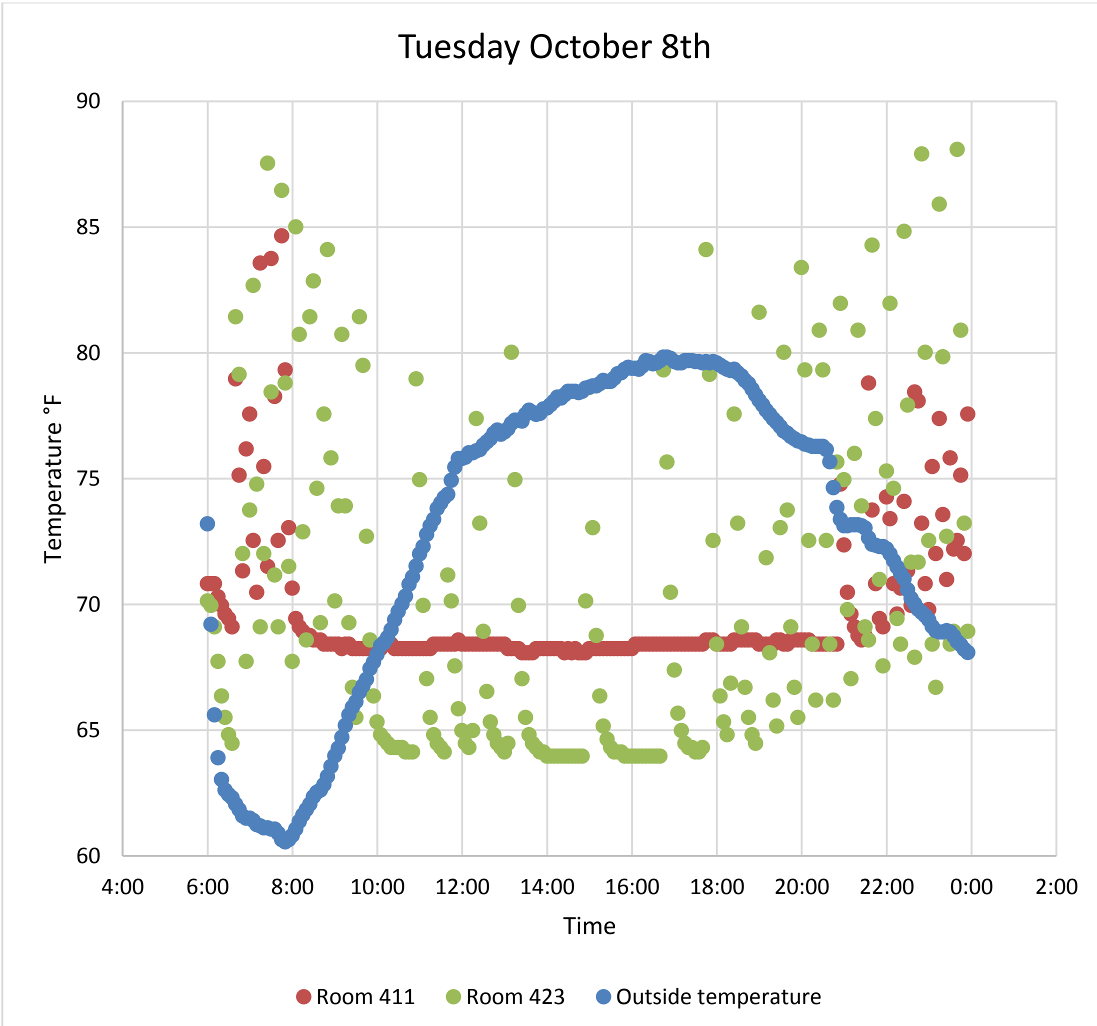

Figure 58. Diffuser temperatures on Tuesday October 8th.

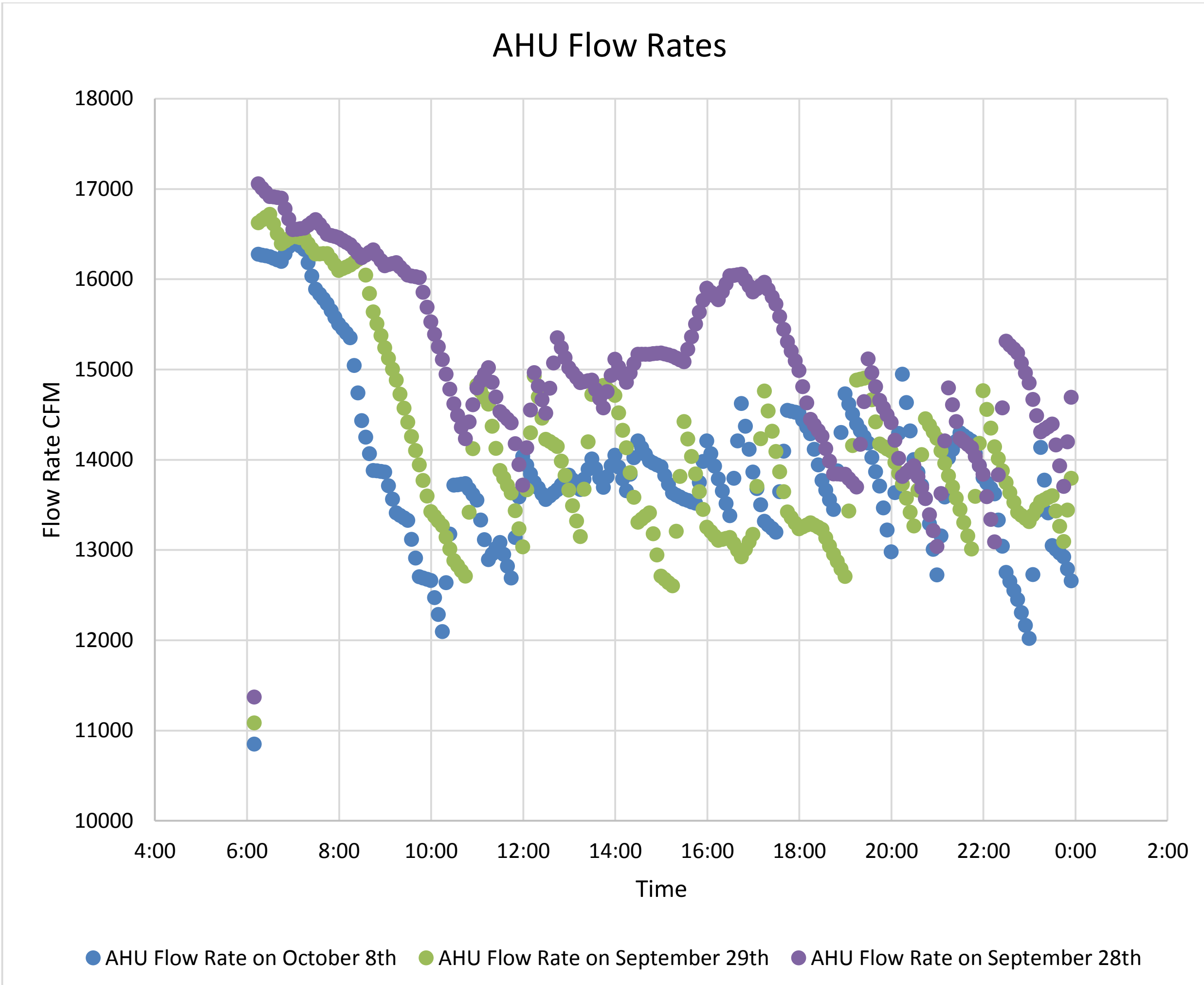

Figure 59. Supply air flow rates for September 28th, September 29th, and October 8th

The air handler's fan has an integrated air flow measurement station. The supply air flow data from the building automation system is plotted in Figure 59 for the three days of September 28th, September 29th, and October 8th. At 6am the system comes online to pressurize the plenums. For the first two hours the air handler fan is operating close to the design air flow rate of 17,000 cfm. The building gross area is 43,770 square feet with this air handler serving 5 out of 6 floors. The building also has a hollow core which takes up 30% of the floor area. The net area served by the UFAD system is 25,533 ft^2. The design flow for this system is 0.67 cfm/ft^2. The minimum flow rate recorded during this period is 12,000 cfm/ft^2, or 0.47 cfm/ft^2.

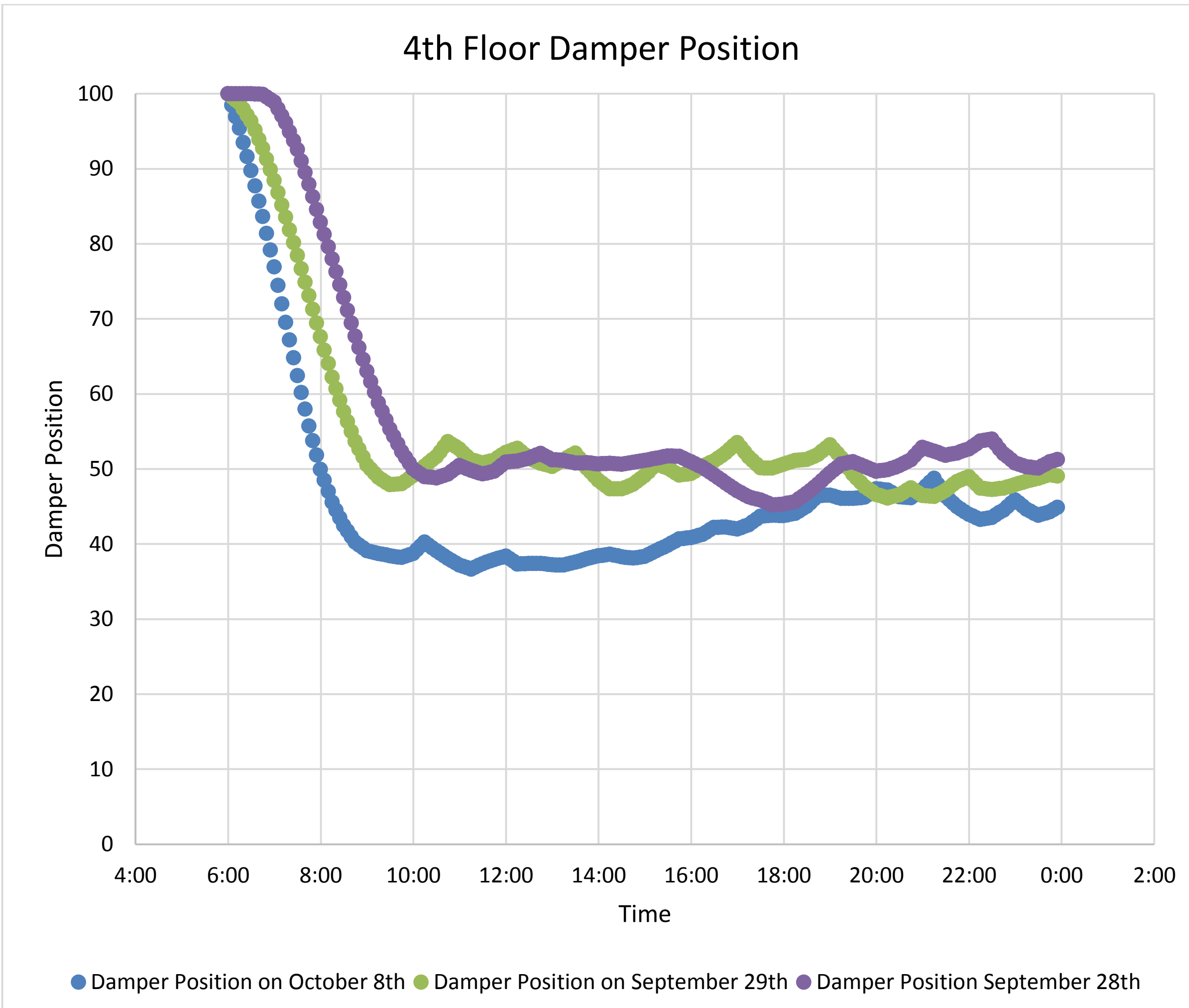

Figure 60. 4th floor damper positions for September 28th, September 29th, and October 8th

Figure 60 shows the damper positions recorded by the building management system on the fourth floor of the building, where the offices are located. The damper is located at the floor level to balance out the air going to this particular floor. If any of the dampers are at 90% or higher, the static pressure will reset such that none of the floor dampers are fully open.

Examining the period between 22:00 and 23:59 when the outside temperature for all 3 days is below 75 °F, both of the rooms are in heating mode and neither the damper nor the air handler significantly lowered the flow rate which is between 12,000 and 15,000 cfm (0.47 cfm/ft^2 to 0.59 cfm/ft^2). If this was a conventional overhead system the amount of reheat would be significantly higher. The UFAD system is able to maintain the set point with only some reheat due to higher supply air temperature at the diffuser level.

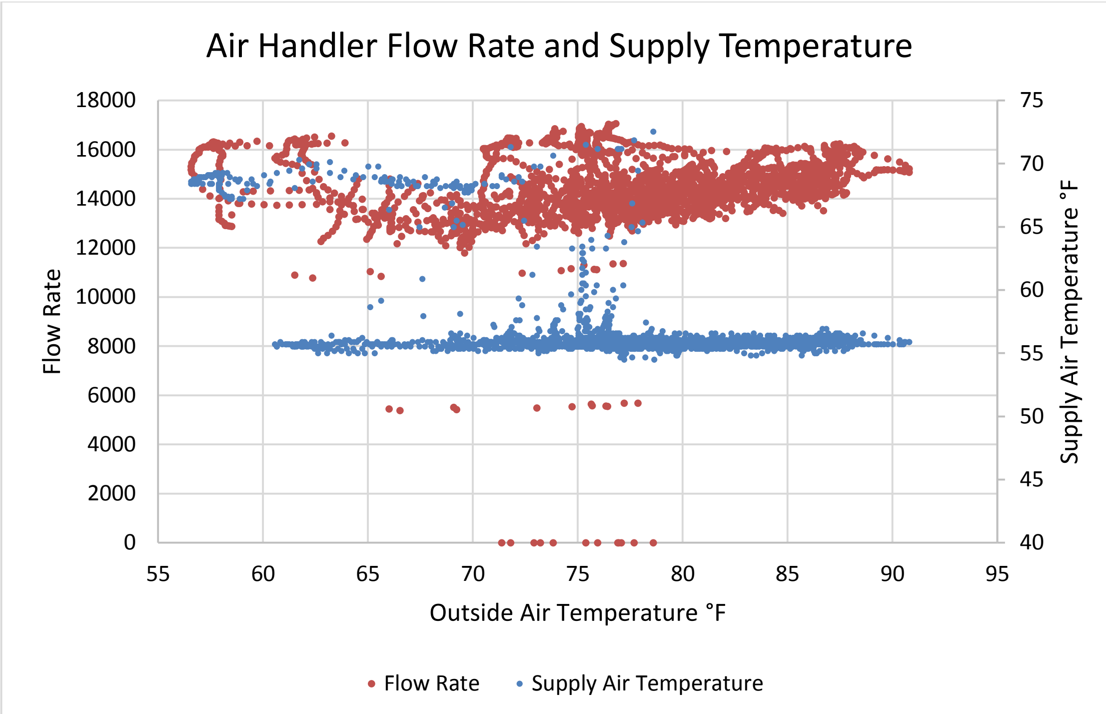

Figure 61. Supply Air flow rate and temperature for stratification measurement period plotted against outside temperature.

The supply air flow rate and supply discharge air temperature are shown on Figure 61. The supply air temperature is recorded by the temperature data logger that was placed after the fan in the supply air stream. The flow rate is from the fan integrated airflow measurement station which was tracked by the building management system. The flow throughout the period shows similar trend as shown in Figure 59 such that it is between 12,000 cfm and 17,000 cfm, with little dependence on outside air temperature. The supply air temperature has a brief period where it was reset from 55°F to 65°F. The lack of any points between the two supply air temperatures suggests that the control strategy for air reset is sub optimal where the system is hunting between two operation modes.

5.2 ERV Effectiveness

There is data available for benchmarking ERVs inside the building. The system optimum operation will depend on extra ERV characteristics. The ERV performance can be simplified by looking at ERV effectiveness. There are two ways to calculate wheel effectiveness, one using return air flow, QRA, and another using supply airflow, QSA,

$$\varepsilon_x = \frac{Q_{SA\,(x_2 - x_1)}}{Q_{min\,(x_3 - x_1)}}$$

$$\varepsilon_x = \frac{Q_{RA\,(x_3 - x_4)}}{Q_{min\,(x_3 - x_1)}}$$

where x can be temperature, specific humidity or enthalpy for sensible, latent, or total effectiveness. The subscripts 1-4 correspond to the points shown in Figure 62.

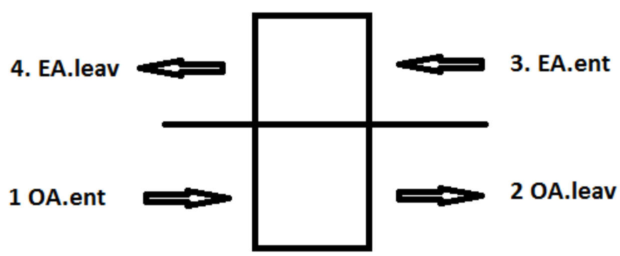

Figure 62. Airstream Numbering Convention

In this building, the supply air stream is measured with an air station; however the return air flow is a virtual point based on pressure drop and fan speed. The return air flow is at all times lower than the supply air flow. The building design documentation suggests that this particular air handling unit should have return air flow equal to the supply air flow. Another air handling unit will be able to pressurize the building. According design information this energy recovering wheel total effectiveness is 0.93.

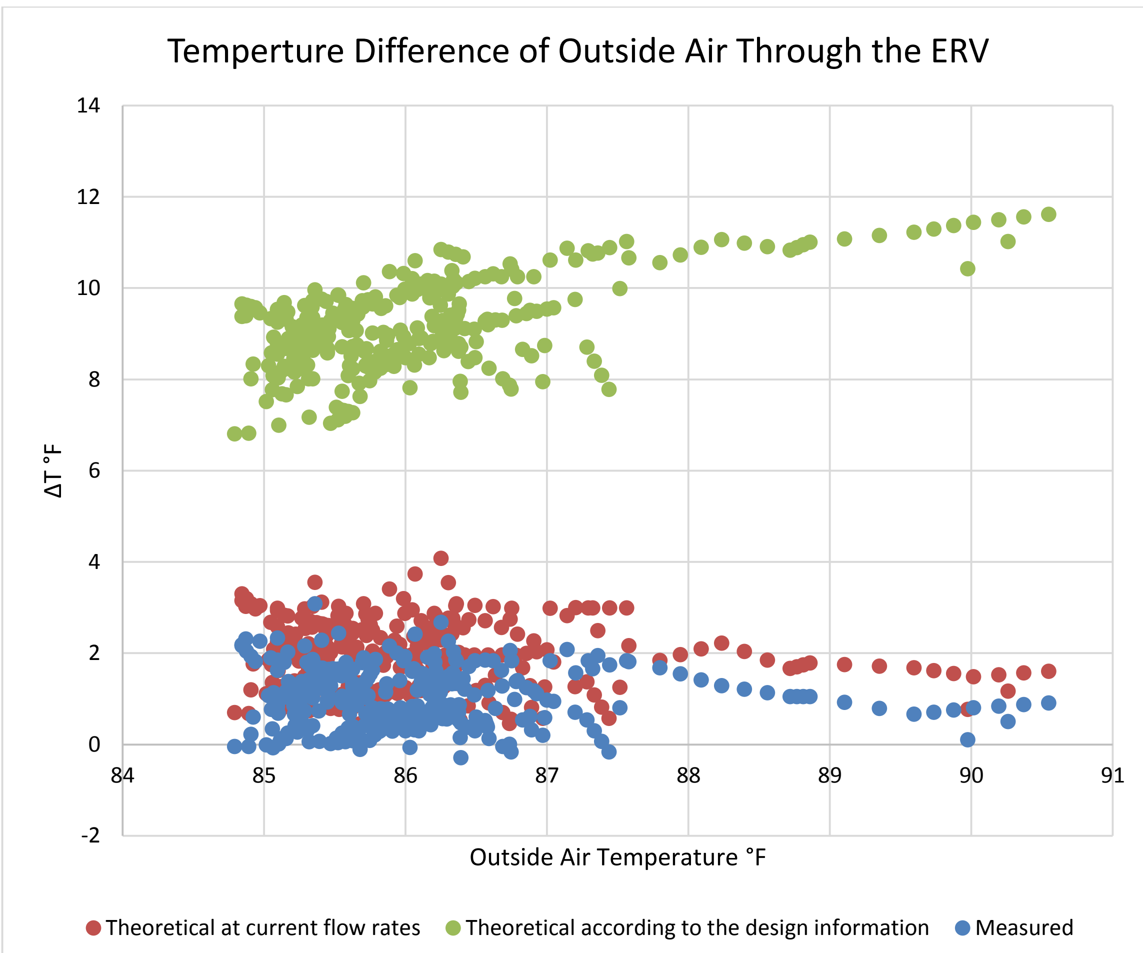

Figure 63. Temperature difference of outside air going through energy recovering ventilation.

The return air flow for this air handler is lower than the supply air flow rate. The average ratio of exhaust flow rate to outside air flow rate during the energy recovering wheel operation is 0.2. Figure 63 shows the temperature difference measured by the temperature sensors located on both sides of the ERV. The theoretical ΔT represents the temperature difference that should be recorded if the ERV’s sensible effectiveness was 0.93. The theoretical design temperature difference is calculated at a sensible effectiveness of 0.93 and return supply air flow rate ratio of 1.

The ERV specified by design has total effectiveness of 0.93 which combines both sensible and latent effectiveness. By having an exhaust flow rate at 0.2 instead of 1 restricts the amount of energy that can be transferred into the outside air flow. Running the enthalpy wheel at this return rate, would be equivalent to running an enthalpy wheel with 0.186 total effectiveness at exhaust to outside air fraction of 1.

CHAPTER V CONCLUSIONS

The thermal decay and stratification changes the energy performance of a UFAD system compared to an overhead system. Minimum flow rate variation showed that UFAD relative performance to overhead system gets better with higher minimum flow rates. However for both systems the lower the minimum flow rate, the better the cooling, heating and fan performance for both systems. The overhead system consumed 16.8% less cooling energy at 0.1 cfm/ft^2 while only 1.1% less cooling energy at 0.4 cfm/ft^2. The UFAD system had only 6.6% heating energy savings at a minimum flow rate of 0.1 cfm/ft^2 vs. the overhead system while at 0.4 cfm/ft^2 the heating energy savings are 36.3%.

A higher supply air temperature reduces the cooling and heating energy consumption at the expense of higher fan energy consumption for both systems. The UFAD system has an advantage when operating at lower pressure so the higher supply temperature has a lower fan energy penalty than the overhead system. Operating both systems at 60 °F supply air temperature will have the UFAD using 6.5% more cooling energy but save 38.7% of heating energy and 29.2% of fan energy compared to the overhead system.

The outside air strategy has similar savings for both systems. In other words the outside air savings can be calculated independent of the type of system in this particular climate. Energy recovery ventilation provides the majority of the savings. The economizer on its own provides only 6.4% of the savings. The best strategy is a combination of Economizer and ERV which provides 27.4% total savings compared to the constant outside air flow strategy.

The supply temperature into the zone from a UFAD system will be higher than that of an overhead system. This higher supply temperature will be achieved without any extra heating added to the supply air stream. This free heating can be an advantage when the minimum flow rate is above that of the flow rate needed to cool the space. When the minimum flow rate is above the flow rate that is required to cool the space at a particular supply air temperature, the overhead system requires the reheating of the air, to maintain the adequate temperature set point. The UFAD system reduces or eliminates this need to reheat due to naturally higher air temperature entering into the zone. The same plenum heat gain also increases the cooling load when the supply air required is above the minimum flow rate. At the peak load, not only does the HVAC system have to cool the same space to the thermostat set point but also cool the supply plenum which is constantly gaining heat through radiation onto the raised floor and conduction into the return plenum below.

The UFAD system outperforms the overhead system when the supply air temperature is low or when minimum flow rate is much higher than needed. The UFAD baseline model which has an air supply temperature of 55°F and a minimum flow rate of 0.3 cfm/ft^2 saves 5.43% of HVAC energy cost over the overhead system. If both systems are optimized such that the overhead system requires no reheat, the UFAD system is no longer the most efficient system. With both system operating at supply air temperatures of 60°F and a minimum flow rate of 0.1cfm/ft^2, the overhead system will save 11.75% of HVAC operation cost.

The stratification measurements showed that on average the stratification was lower than expected for such systems with office 411 having average stratification of 1.8 °F and office 423 average stratification of 1.5 °F. Temperature measurements at the diffuser level showed some reheat especially during unoccupied periods such as early mornings, late evenings and weekends, even when the outside temperature was above the interior thermostat set point. System level total supply air flow rate showed little variation with a minimum of 0.47 cfm/ft^2 and maximum of 0.59 cfm/ft^2. The analysis of energy recovery wheel operation concluded that the exhaust air flow is only 20% of the outside air flow. The temperature difference in the outside air stream through the ERV low, around 20% of expected value, which assumes exhaust mass flow rate equivalent to outside air flow rate. The recommendation was made to increase the exhaust flow rate on this air handler, and let another air handler pressurize the building as design documents suggested.

REFERENCES

Alajmi, A. and El-Amer, W. 2010. Saving energy by using underfloor-air-distribution (UFAD) system in commercial buildings. Energy Conversion and Management 51 (2010) 1637-1642.

Bauman, F. 2003. Underfloor Air Distribution (UFAD) Design Guide. American Society of Heating, Refrigerating and Air-Conditioning Engineers, Inc. Atlanta, GA.

Bauman, F., Jin, H., and Webster, T. 2006. Heat transfer pathway in underfloor air distribution (UFAD) systems. ASHRAE Transactions 112 (part 2).

Bauman, F. S. and Dally, A. (2013). Underfloor air distribution (UFAD) design guide, American Society of Heating, Refrigerating and Air-Conditioning Engineers.

Claridge, D. E., C. H. Culp, M. Liu, S. Deng, W. D. Turner and J. S. Haberl. 2000. Campus-wide Continuous Commissioning^{SM} of university buildings, Proceedings ACEEE Summer Study on Energy Efficiency in Buildings, 3(1): 3.101-3.112.

DOE, US. (2013). Energyplus engineering reference. The Reference to EnergyPlus Calculations.
http://apps1.eere.energy.gov/buildings/energyplus/pdfs/engineeringreference.pdf

Fisk, W., Faulkner, D., and Sullivan, D. 2005. Performance of underfloor air distribution: Results of a field study. Report of Energy Analysis and Environmental Impacts Department, LBNL-56257.

Ho, S.H., Rosario, L., and Rahman, M.M. 2012. Comparison of underfloor and overhead air distribution systems in an office environment. Building and Environment 46(7): 1415-1427.

Lee, K.H., Schiavon, S., Bauman, F., and Webster, T. 2011. Thermal decay in underfloor air distribution (UFAD) systems: Fundamentals and influence on system performance. Applied Energy 91 (2012) 197-207.

Lee, K. H., et al. 2013. Supply air temperature impact in underfloor air distribution systems under Korean climatic conditions: Energy, humidity and comfort. Energy and Buildings 58(0): 363-371.

Mills, E., N. Bourassa, M. A. Piette, H. Friedman, T. Haasl, T. Powell and D. Claridge. 2005. The cost-effectiveness of commissioning, HPAC Heating, Piping, AirConditioning Engineering, 77(10): 20-24.

Montanya, E., Keith, D., and Love, J. 2009. Integrated design and UFAD. ASHRAE Journal (2009): 30-40.

Schiavon, S., Lee, K.H., Bauman, F., and Webster, T. 2010. Simplified calculation method for design cooling loads in underfloor air distribution (UFAD) systems. Energy and Buildings 43 (2-3): 517-528.

Schiavon, S., Lee, K.H., Bauman, F., and Webster, T. 2010. Influence of raised floor on zone design cooling load in commercial buildings. Energy and Buildings 42(8): 1182-1191.

Webster, T., Bauman, F., and Shi, M. 2002. Thermal stratification performance of underfloor air distribution (UFAD) systems. Proceedings, Indoor Air 2002, Monterey, CA, June 30-July 5.

Webster, T., et al. (2012). Influence of supply air temperature on underfloor air distribution (UFAD) system energy performance.

Zhao, J., Khmelenko V., Claridge D. E., (2014). Performance study of an under-floor air distribution system in an education building to identify building energy efficiency improvement opportunities. 2014 Annual Conference, Seattle, WA (SE-14-C056). ASHRAE.

Zukowski, M. 2007. A new formula for determining a minimum recommended value of inlet air velocity from UFAD system to prevent occupants from draught risk. Building and Environment 42 (1): 171-179.